A STUDY OF THE EFFECT OF ELECTRODE AND OVERLAYER FILMS ON THE ELECTRICAL PROPERTIES OF CERTAIN METAL FILMS

Thesis submitted by

E. C. JOY

in partial fulfilment of the
requirements for the Degree of
Doctor of Philosophy

SOLID STATE PHYSICS LABORATORY
DEPARTMENT OF PHYSICS
UNIVERSITY OF COCHIN

1980

DECLARATION

Certified that this thesis is based on the work done by Fr. S.C. Joy under my guidance in the Department of Physics, University of Cochin and no part of this has been presented by him for any other degree.

Dr. Joy George
(Supervising Teacher)
Professor in Industrial Physics
Department of Physics
University of Cochin

Cochin-22
March 27, 1980

SYNOPSIS

A STUDY OF THE EFFECT OF ELECTRODE AND OVERLAYER FILMS ON THE ELECTRICAL PROPERTIES OF CERTAIN METAL FILMS

The thesis consists of a study of the effect of electrode films and overlayer films on the electrical properties of certain metal films. The films have been prepared on glass substrates by thermal evaporation in a vacuum $\sim 10^{-5}$ Torr. The properties of Al films on Ag, Al, Au and Cu electrodes, Ag, Al, Au and Cu films on In electrodes, and Bi/Ag bilayer films have been studied. The influence of annealing electrodes at higher temperature on the electrical properties of metal films has also been investigated. Further, the effect of varying layer thickness in the bilayer films, both annealed at higher temperature and annealed at room temperature have been examined.

The percentage variation of resistance with time of the films is found to differ with annealed and un-annealed electrodes. In Al films the resistance is found to increase with time. The variation has been more in the case of Au, Ag and Cu electrodes while this

has not been very marked in the case of Al electrodes. In Cu films with In electrodes, the percentage variation of resistance with time was very small and was almost equal in both the films with annealed and unannealed electrodes. Al films with unannealed electrodes showed a non-uniform, rapid increase in the percentage variation, which was very large compared to that of the films with annealed electrodes. Unlike the other films, Au and Ag films with In electrodes showed a decrease in resistance with time. In these, the films with unannealed electrodes showed larger percentage variation. The role of various factors such as diffusion and alloying at the film-electrode junction, oxide formation and bubble formation have been discussed in the light of the observed variation in resistance of the films. An attempt has also been made to correlate the variation of resistance with the microscopic features seen on particular electrode-film junctions.

In Bi/Ag bilayer films, a thin overlayer of Ag (~ 50 Å) has increased the R_T/R variation with temperature, where R_T is the resistance of the film at a temperature T and R that at room temperature.

It has also increased the resistance of the film, made the TCR at room temperature more negative and shifted the resistance minimum to a higher temperature. The resistance variation with temperature has been explained on the basis of Kaidanov and Regal model.

When the total thickness of the bilayer film was kept constant and individual layer thickness varied, the resistance variation on annealing to a temperature above 160°C has been found to depend on the Ag layer thickness. With increasing Ag layer thickness, the sheet resistance of the films having more than 100 Å Ag decreased and the TCR at room temperature changed from negative to positive value. The rapid resistance rise above 100°C observed in films having 100 Å to 600 Å Ag overlayer has been explained on the basis of diffusion at the interface and aggregation of Ag film on the surface. By controlling the thickness of the layers it is possible to keep the resistance variation with temperature to a minimum. The gradual change of colour of the surface, transparency of the film, increased adhesive force etc. observed in films annealed at room temperature have been explained on the basis of reduction in crystallite size as evidenced by X-ray diffraction and the likely formation of some interphase compound.

CONTENTS

INTRODUCTION

The science and technology of thin solid films have made tremendous advances during the last couple of decades because of the demand for reliable optical, magnetic, electronic and superconducting thin film devices. With the development of new materials, improved deposition techniques and close control of the deposition parameters, thin films can now be prepared with desired and reproducible properties, and are expected to play an increasingly important role in the study of a variety of solid state phenomena of basic and practical interest.

To optimise the various properties of the films, often multiple layers have been used and the solid-solid interdiffusion of the various layers have been found to control these properties. For example, in integrated circuit technology, interdiffusion between metal layers makes strong adhesive bonding and produces necessary physical and electrical properties. Yet, inspite of these advantages, interdiffusion poses various problems. So diffusion in vacuum-deposited metal films has become an important phenomenon which

has received significant attention during these years. This study has been receiving greater momentum on account of the increasing use of thin films in electronics either as complete thin film circuits or generally as interconnections and contacts in integrated circuits.

Electromigration in thin films has also received considerable attention during the last couple of decades on account of its relevance to open circuit failure in integrated circuits, especially in aluminium stripes, even of several thousand angstroms thick. Several workers have been studying the phenomenon by following the resistivity changes and observing the formation of voids and hillocks in films.

And as such it seemed interesting to investigate the effect of interdiffusion, electromigration etc. on the electrical conduction of various metal film combinations.

One of the important methods of ensuring good electrical contacts to metal films is to deposit metal electrodes. Various good conductor materials such as the noble metals, aluminium, indium etc. are being used as electrode material. While various investigators have predeposited the electrode films,[1-5] certain others used the post deposition technique.[6-8] But only a few have done annealing of electrode films prior to evaporation.[9,10] So it is interesting and useful to know the effect of annealing

electrode on the electrical resistivity of a thin film. Therefore, in the first part of the study an investigation of the effect of electrodes, both annealed and unannealed, on the electrical resistance of thin metal films is undertaken using different film-electrode combinations of good electrically conducting materials.

Like the electrode films,[18,19] the overlayers[20-23] also modify the properties of thin films. Further, the deposition of an overlayer is a very effective method to understand the interfacial reactions taking place between two films.

Bismuth-silver bilayer has been taken for the study on account of their difference in the electrical behaviour and also due to the anomalies of the semimetal bismuth in its transport properties.[11] Bismuth films, in the polycrystalline form, are semiconducting, either n-type or p-type, and their nature can be changed from one type to another by varying the film thickness as well as the deposition parameters.[12] As the mean free path of electrons in bismuth is of the order of some microns, size effect can be observed at larger thickness even at room temperature. Since the Fermi energy of electrons is about 25 meV and the effective mass m^* along some crystal orientation is two or three orders of magnitude smaller than the free electron mass, the

deBroglie wave length may become as large as 800 Å to 1000 Å and the electronic energy states become descrete resulting in oscillations of resistivity with thickness having a period nearly equal to the de Broglie wavelength.[13] On account of these anomalies the transport properties of this semimetal have been of interest for many years.[14-17]

In the present study, thin layers of silver ($\sim$50 Å) has been deposited on bismuth films of varying thickness and the effect of this on the electrical resistance variation with temperature has been investigated. Further, the properties of bilayer bismuth silver films of constant thickness and varying individual layer thickness have been studied, annealing them at room temperature and also at higher temperatures.

CHAPTER ONE

ELECTRICAL CONDUCTION

1.1 Conduction in Bulk Metals

Conduction in bulk metals was first considered by Drude and Lorentz[24] in terms of an electron gas. The theory predicted the Wiedemann-Franz Law which connects the electrical conductivity to thermal conductivity. But when the model was used to calculate such quantities as electronic specific heat and paramagnetic susceptibility, the results had no resemblance to observed values. However the quantum mechanical approach resolved these by applying Fermi-Dirac statistics to the free electrons in a metal. According to the approach, the electrons in an atom arrange themselves in various shells around the positively charged nucleus to minimize their energy. The valence electrons in the outer shell determine the chemical properties of the metal. In a solid metal, these valence electrons lose their identification with individual atoms and form a sea of negative charge. These electrons are responsible for the electrical conductivity in a metal. Under a steady electric field E, the electron velocity V at the surface of Fermi distribution is given by

$$V = - \frac{eEl}{m} \qquad 1.1$$

where e is the electron charge, τ the relaxation time and m the mass of an electron.

The current density j is given by

$$j = \frac{ne^2\tau E}{m} \qquad 1.2$$

where n is the density of electrons.

As the relation is clearly consistent with Ohm's law, the resistivity ρ of the bulk metal

$$\rho = \frac{m}{ne^2\tau}$$

$$= \frac{mv}{ne^2\lambda} \qquad 1.3$$

λ being the electron mean free path.

As electrons obey Fermi-Dirac statistics, at 0^0K they fill all the available states upto the Fermi energy, all the states of higher energy being empty. Since the Pauli exclusion principle is applicable to electrons, by adding up all the states below the Fermi energy and equating it to the density of conduction electrons, the Fermi energy E_F can be calculated as

$$E_F = \frac{h^2}{8m}\left(\frac{3n}{\pi}\right)^{2/3} \qquad 1.4$$

where h is Planck's constant. Assuming that the Fermi surface is spherical, the velocity of an electron at the

Fermi energy is

$$v_F = \frac{h}{2m}\left(\frac{3n}{\pi}\right)^{1/3} \qquad 1.5$$

so the number of free electrons per unit volume

$$n = \frac{8\pi}{3}\left(\frac{mI}{h}\right)^3 \qquad 1.6$$

In the theory of electron scattering, it is assumed that the electrons travel freely under the influence of the applied field until they collide with something and that the electrons come away from each collision with a randomly directed velocity. The mean free path λ, of the electrons between the collisions is related to the mean time between the collisions, τ' as

$$\tau' = \frac{\lambda}{v} \qquad 1.7$$

Considering a group of electrons, let the number of electrons remaining unscattered after a small time interval dt at a time t be N. The rate of scattering $-\frac{dN}{dt}$ will be proportional to N. That is,

$$-\frac{dN}{dt} = C\,N \qquad 1.8$$

Integrating,

$$N = N_0 e^{-Ct} \qquad 1.9$$

So the interval between the collisions is

$$\tau' = \frac{1}{E_0} \int_0^{E_0} t\,dE$$

Using equations 1.8 and 1.9

$$\tau' = C \int_0^{\infty} te^{-Ct}\,dt$$

$$= \frac{1}{C}$$

So the constant of proportionality is the reciprocal of the mean time between the collisions.

Considering the time symmetry of collisions, the average electron at any point of time, will acquire a velocity

$$V_d = - \frac{eE\tau'}{m}$$

The current density

$$j = - neV_d$$

$$= \frac{ne^2E\tau'}{m} \qquad 1.10$$

Comparing 1.2 and 1.10

$$\tau = \tau'$$

So the mean free path

$$\lambda = \tau v$$

The resistivity from equations 1.3 and 1.5

$$\rho = \frac{h}{2e^2}\left(\frac{3}{\pi n^2}\right)^{1/3}\left(\frac{1}{\lambda}\right) \qquad 1.11$$

As n is independent of temperature, λ controls the temperature dependence of the electrical resistivity.

Equation 1.3 can also be written in terms of the mobility μ of electrons as

$$\rho = \frac{1}{n\mu e} \qquad 1.12$$

In a perfect and rigid lattice there will be no resistance to the flow of electrons. But at temperatures above absolute zero there will be a finite free path due to thermal vibrations of the lattice. In lowering the temperature, the increase of mean free path will be limited by lattice imperfections such as impurity atoms, dislocations, vacancies etc. This reduction in the mean free path gives an additional resistivity.

By Matthiessen's rule, the total resistivity is the sum of the resistivities due to impurities etc. (ρ_i) and that due to lattice scattering (ρ_s) which is strongly dependent on the amplitude of the thermal motions of the ions.

$$\rho = \rho_s + \rho_i \qquad 1.13$$

Since the resistance due to impurities is independent of temperature T,

$$\frac{d\rho}{dT} = \frac{d\rho_s}{dT} \qquad 1.14$$

The variation of ρ_s is dependent on the temperature. When the temperature is above the Debye temperature θ, ρ_s is proportional to the temperature T. But if the temperature is far below θ, ρ_s is proportional to T^5.

A more detailed discussion of metallic conduction is given by Wilson,[25] Kittel,[26] Dekker[27] and Slater et al.[28] and Meaden[29] has given a survey of the experimental data.

1.2 Conduction in Thin Films

In thin films, the mean free path is not only limited by thermal vibrations of the lattice and the imperfections in it as in the case of bulk metal but also restricted by the boundary surfaces. So the resistance of a film, by Matthiessen's rule, consists of ρ_s, ρ_i and a thickness-dependent part ρ_t due to the scattering of conduction electrons by the boundaries of the metal film. Therefore

$$\rho = \rho_s + \rho_i + \rho_t \qquad 1.15$$

a) Conduction behaviour

J.J. Thomson[30] was the first person who gave a reasonable treatment of the problem of conduction in thin films arising from their small thickness. He considered a film of thickness 'd' having infinite dimension in the other two direction. He assumed also that the mean free path of an electron in a bulk metal may be defined as λ and that the scattering of the electrons at the surface is diffuse.

Taking z-axis normal to the surface of the substrate, three regions can be distinguished in the figure 1.1. In the regions where θ is from 0 to θ_1 and from θ_2 to π the electrons will not be able to travel their mean free path λ due to their collision with surface boundary and in the region $\theta = \theta_1$ to θ_2 they are able to travel their mean free path. By integrating the effect of these electrons in the direction in which the field is applied, a mean free path $\bar{\lambda}$ for the film can be obtained. The result of Thomson's calculations are expressed as

$$\frac{\sigma_f}{\sigma_b} = \frac{3k}{4} + \frac{k}{2}\log\frac{1}{k} \qquad 1.16$$

where σ_f and σ_b are the conductivity of the film and that of the bulk respectively and k is the ratio of the thickness d to the bulk mean free path λ.

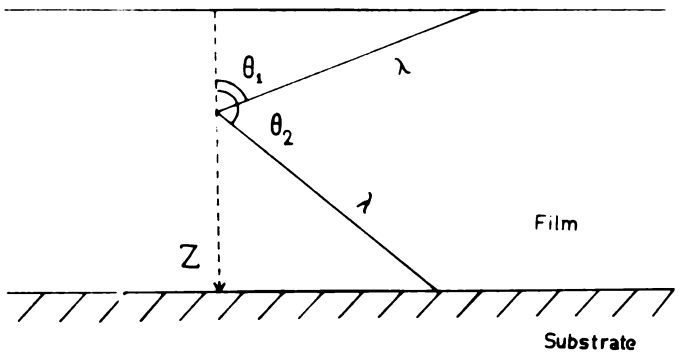

Figure 1.1 Film geometry for a single layer film.

Thomson's approach was a limited one since it was not taking into account the electron paths starting from the surface. So a more rigorous treatment was given by Fuchs[31] which was later extended by Sondheimer[32] to include other mean free path effects in metals.

In the presence of an electric field E and a magnetic field H, the Boltzmann equation for quasi-free electrons takes the form

$$-\frac{e}{m}(\vec{E} + v \times \vec{H}).\ \mathrm{grad}_v f + v.\ \mathrm{grad}_r f = \left(\frac{df}{dt}\right)_{\text{collision}} \qquad 1.17$$

where f is the non-equilibrium Fermi-Dirac distribution function of the velocity vector $\vec{v}$ and space vector $\vec{r}$ and $\left(\frac{df}{dt}\right)_{\text{collision}}$ is the change of the distribution function due to collision processes. $\left(\frac{df}{dt}\right)_{\text{collision}}$ can be determined by invoking a relaxation time τ, a time taken for the distribution f to relax to the undisturbed steady state f_0 when the electrical constraint is removed. Therefore

$$(f - f_0)_{t=t} = (f - f_0)_{t=0} e^{-t/\tau} \qquad 1.18$$

As the electric field is only in the X-direction, the acceleration due to the field in the direction is $-\frac{eE}{m}$. Since $\frac{df_0}{dt}$, the rate of change of the function in a steady state is zero, differentiation of 1.18 gives

$$\frac{\partial f}{\partial t} = -\frac{(f - f_0)_{t=t}}{\tau} \qquad 1.19$$

The left hand side of this expression can be equated to $\left(\frac{\partial f}{\partial t}\right)_{\text{collision}}$. So the Boltzmann equation, in its reduced form, can be written as

$$-\frac{eE}{m}\frac{\partial f}{\partial v_x} + v_z\frac{\partial f}{\partial z} = -\frac{(f - f_0)}{\tau} \qquad 1.20$$

To solve the equation, it is convenient to write the function f as the sum of the steady state velocity distribution f_0 and a function $f_1(\bar{v},z)$ which depends on velocity vector and position

$$f = f_0 + f_1(\bar{v},z) \qquad 1.21$$

Substituting 1.21 in 1.20,

$$\frac{\partial f_1}{\partial z} + \frac{f_1}{\tau v_z} = \frac{eE}{mv_z}\frac{\partial f_0}{\partial v_x} \qquad 1.22$$

The general solution of 1.22 is

$$f_1(v,z) = \frac{eEx}{m}\frac{\partial f_0}{\partial v_x}\left[1 + F(\bar{v})\, e^{-z/\tau v_z}\right] \qquad 1.23$$

where $F(\vec{v})$ is an arbitrary function of $\vec{v}$ determined by the boundary conditions.

Let the scattering be entirely diffuse, i.e., every free path is terminated at the surface by collision. From 1.23 it can be seen that this can be satisfied only if $F(\bar{v})$ is such that $f_1(v,0) = 0$ for all v having $v_z > 0$ and $f_1(v,d) = 0$ for all v having $v_z < 0$.

$$f_1^+(v,z) = \frac{eE_x}{m}\frac{\partial f_0}{\partial v_x}\left[1 - e^{-z/\tau v_z}\right], \quad v_z > 0 \qquad 1.24$$

and $$f_1^-(v,z) = \frac{eE_x}{m}\frac{\partial f_0}{\partial v_x}\left[1 - e^{(d-z)/\tau v_z}\right], \quad v_z < 0$$

Now the current density for a position z is given by

$$j(z) = -2e\left(\frac{m}{h}\right)^3 \iiint v_x f_1 \, dv_x dv_y dv_z \qquad 1.25$$

The total current density can be obtained by integrating equation 1.25 with respect to z. The integration can be made easy by changing into polar co-ordinates where θ is defined by

$$v_z = v\cos\theta .$$

By averaging the current density over all values of z from 0 to d, an expression can be derived for the film conductivity σ_f:

$$\sigma_f = \sigma_B\left[1 - \frac{3}{2k}\int_1^\infty \left(\frac{1}{t^3} - \frac{1}{t^5}\right)\left(1 - e^{-kt}\right)dt\right]$$

where $t = \frac{1}{\cos\theta}$, $k = d/\lambda$ and σ_B is the bulk conductivity.

Therefore

$$\frac{\sigma_f}{\sigma_B} = \left[1 - \frac{3}{2k}\int_1^\infty \left(\frac{1}{t^3} - \frac{1}{t^5}\right)\left(1 - e^{-kt}\right)dt\right] \qquad 1.26$$

Making approximations for small and large values of k,

$$\frac{\sigma_f}{\sigma_b} = 1 - \frac{3}{8k} \quad ; \quad k \gg 1 \qquad 1.27$$

$$\frac{\sigma_f}{\sigma_b} = \frac{3k}{4}\left(\log\frac{1}{k} + 0.423\right) \; ; \quad k \ll 1 \qquad 1.28$$

In the above mentioned case it was assumed that electrons are scattered diffusely. The theory, however, can be modified by assuming that some fraction p of the electrons are scattered elastically. This specular reflection will modify the conditions at the boundaries and the equations for f_1 will be modified as

$$f_1^+(v,s) = \frac{eEx}{m}\frac{\partial f_0}{\partial v_x}\left[1 - \frac{(1-p)e^{-s/\tau v_x}}{1-p\,e^{-d/\tau v_x}}\right] \; ; \; v_x > 0$$

and

$$f_1^-(v,s) = \frac{eEx}{m}\frac{\partial f_0}{\partial v_x}\left[1 - \frac{(1-p)e^{(d-s)/\tau v_x}}{1-p\,e^{d/\tau v_x}}\right] ; v_x < 0$$

By determining the current density, the ratio of the film to the bulk conductivities can be obtained as:

$$\frac{\sigma_f}{\sigma_b} = 1 - \frac{3}{2k}(1-p)\int_1^\infty \left(\frac{1}{t^3} - \frac{1}{t^5}\right)\cdot\frac{1-e^{-kt}}{1-p\,e^{-kt}}\,dt \qquad 1.29$$

Making approximations for large and small values of k,

$$\frac{\sigma_f}{\sigma_b} = 1 - \frac{3}{8k}(1-p) \qquad k > 1 \qquad 1.30$$

$$\frac{\sigma_f}{\sigma_b} = \frac{3k}{4}(1+2p)\left(\log\frac{1}{k} + 0.4228\right), \quad k \ll 1;\ p < 1 \qquad 1.31$$

In the above consideration, it has been assumed that the value of p is the same for both surfaces. But if the scattering coefficients for the two surfaces are assumed to be different values p and q, the conductivity ratio becomes

$$\frac{\sigma_f}{\sigma_b} = 1 - \frac{3}{4k}\int_1^\infty \left(\frac{1}{t^3} - \frac{1}{t^5}\right)\frac{1-e^{-kt}}{1-pqe^{-2t}}$$

$$\left[2-p-q+(p+q-2pq)\ e^{-kt}\right]dt \qquad 1.32$$

Asymptotic forms of this equation are

$$\frac{\sigma_f}{\sigma_b} = 1 - \frac{3}{8k}\left(1 - \frac{p+q}{2}\right) \quad ; \quad k \gg 1 \qquad 1.33$$

and

$$\frac{\sigma_f}{\sigma_b} = \frac{3}{4}\,\frac{(1+p)(1+q)}{1-pq}\,k\log\left(\frac{1}{k}\right) \quad ; \quad k \ll 1 \qquad 1.34$$

b) Temperature coefficient of resistance

The temperature coefficient of resistance is an important parameter, which for a bulk metal is defined as

$$\alpha_B = \frac{1}{\rho_B} \cdot \frac{d\rho_B}{dT} \qquad 1.35$$

From equation 1.14 it can be shown that

$$\alpha_B \rho_B = \alpha_0 \rho_0$$

i.e., $$\frac{\alpha_B}{\alpha_0} = \frac{\rho_0}{\rho_B} \qquad 1.36$$

In the case of thin films, by Matthiessen's rule

$$\rho_F = \rho_0 + \rho_i + \rho_t$$

Differentiating,

$$\frac{d\rho_F}{dT} = \frac{d\rho_0}{dT} + \frac{d\rho_i}{dT}$$

When the film is thick enough for boundary effects to be negligible, $\frac{d\rho_i}{dT}$ is zero. So it is possible to write

$$\alpha_f \rho_f = \alpha_0 \rho_0 = \alpha_B \rho_B$$

i.e., $$\frac{\alpha_f}{\alpha_B} = \frac{\sigma_f}{\sigma_B} \qquad 1.37$$

Therefore, when k is large

$$\left(\frac{\sigma_f}{\sigma_B}\right)_{p=0} = 1 - \frac{3}{8k} \qquad 1.38$$

$$\left(\frac{\sigma_f}{\sigma_B}\right)_{p=p} = 1 - \frac{3(1-p)}{8k} \qquad 1.39$$

$$\left(\frac{\sigma_f}{\sigma_B}\right)_{\substack{p=p \\ p=q}} = 1 - \frac{3}{8k}\left(1 - \frac{p+q}{2}\right) \qquad 1.40$$

When k is small, there is an additional term $\int_t$ which is dependent on temperature. A change in temperature will alter the mean free path in the bulk and therefore cause different electrons from a point in the film to hit the surface before they have completed the most probable length of journey. Defining a term

$$\phi(k) = k\frac{\sigma_B}{\sigma_f}$$

$$\frac{\sigma_f}{\sigma_B} = 1 - \phi(k)\frac{d\left(\frac{k}{\phi(k)}\right)}{dk}$$

For p = 0, using equation 1.26

$$\frac{\sigma_f}{\sigma_B} = \frac{1 - \frac{3}{4k}\int_1^\infty \left(\frac{1}{t^3} - \frac{1}{t^5}\right)(1 - e^{-kt})\,dt + \frac{3}{8}\int_1^\infty \left(\frac{1}{t^2} - \frac{1}{t^4}\right)e^{-kt}dt}{1 - \frac{3}{2k}\int_1^\infty \left(\frac{1}{t^3} - \frac{1}{t^5}\right)(1 - e^{-kt})\,dt}$$

Expanding and ignoring k^3 terms

$$\frac{\rho_T}{\rho_B} = \frac{6-4k + k^2\left[\log\left(\frac{1}{k}\right) + 1.5061\right]}{6\left[\log\left(\frac{1}{k}\right) + 0.4228\right]} \qquad 1.41$$

Neglecting, further, k and k^2 terms,

$$\frac{\rho_T}{\rho_B} = \frac{1}{\log\left(\frac{1}{k}\right) + 0.4228} \qquad 1.42$$

$$\approx \frac{1}{\log\left(\frac{1}{k}\right)} \qquad 1.43$$

c) Hall coefficient

When a magnetic field is applied to a conductor perpendicular to the direction of current flow, a voltage is generated in a direction at right angles to both the current and the magnetic field. If J_x is the current flowing in a particular direction x in the plane of a film due to the application of an electric field along the direction, H_z is the magnetic field applied at right angles to this direction and E_y is the field generated at right angles to both J_x and H_z directions, the Hall coefficient R_H is defined as

$$R_H = \frac{E_y}{J_x \cdot H_z} \qquad 1.44$$

For a metal it can be shown that

$$R_H = \frac{1}{ne} \qquad 1.45$$

From measurements of R_H and ρ_B it is possible to determine the mobility μ and the number of electrons per unit volume n using the relation

$$\rho = \frac{1}{ne\mu}$$

d) Magnetoresistance

When a metal is placed in a magnetic field its electrical resistance is found to increase. This problem of the effect of a magnetic field on the resistance of a thin film was first treated in detail by Sondheimer.[33] This magnetoresistance effect depends on the binding of electrons in the lattice in a complicated way.

A magnetic field H makes the electrons move in helical orbits. For an electron the radius of this orbit

$$r = \frac{mv\sigma}{He} \qquad 1.46$$

where mv is the momentum of the electrons. The change in the electron paths, especially the scattering by the specimen boundaries makes changes in the resistance.

The change depends on the relative configuration of the specimen, electric current and magnetic field.

The magnetoresistance effect is observable only when $r > \lambda > d$. Since larger values of mean free path values λ are obtainable at low temperatures the magnetoresistance studies are normally made on thicker single crystal films at liquid helium temperature.

Magnetoresistance of bulk metals are often analysed in terms of Kohler's rule

$$\rho_H - \rho_0 = \rho_0 f\left(\frac{H}{\rho_0}\right) \qquad 1.47$$

where ρ_H and ρ_0 are the resistivities at H and zero magnetic fields and f is a universal function.

i) Longitudinal magnetoresistance

The resistance depends on two parameters $\beta \left(= \frac{d}{r}\right)$ and $\gamma \left(= \frac{d}{\lambda}\right)$. The resistance decreases steadily as β increases. As β tends to infinity, the resistance tends to the bulk value.

ii) Transverse magnetoresistance

According to Sondheimer's[33] theory, when the magnetic field is perpendicular to the film surface, the magnetoresistance is an oscillatory function of the field

strength. The resistance increases initially with β and reaches the first maximum when β is of the order of 1. The subsequent maxima occur at 7, 13 etc. The amplitude of the oscillation decreases rapidly and the oscillation itself dies out when γ is very large.

When the field is parallel to the film surface, MacDonald and Sarginson[34], assuming that the Hall field across the film thickness was constant, obtained a rather complicated expression for the magnetoresistance. According to their theory the resistivity passes through a single maximum and then decreases to the bulk value.

e) Influence of heat treatment

It has been found that the electrical resistivity of thick films ($d \gg \lambda$) is higher than the bulk value. This excess value can be accounted for the scattering of electrons by structural defects and impurities present in the film.

During deposition of films, many structural defects such as dislocations, stacking faults, interstitials etc. are frozen in them. The contribution to resistivity from dislocations and stacking faults is not very significant. Greater contribution comes from vacancies. An important contribution arises from grain

boundaries in films. If the grain size is smaller than the electron mean free path, internal diffuse scattering at the grain boundaries will increase the resistance significantly.

A mild heat treatment may anneal out some of these defects which should lead to a corresponding decrease in film resistivity. In films deposited at low temperatures, annealing causes a irreversible resistance decrease. Upto 70°K the annealing mechanism consists of a rearrangement of microcrystals within displacement spikes or the annihilation of Frenkel defects. Above 100°K there begin the migration of interstitials, grain growth etc. But above 140°K, this continuing irreversible decrease due to annealing is superimposed by the normal increase of resistance in metals. So there may be a resistance minimum in resistance Vs. temperature curve. The temperature corresponding to the resistance minimum occurs at the Debye temperature of the metal.

A theory of resistivity changes occuring in thin films on account of the annealing out of defects has been given by Vand.[35] He assumed that the distortions in films are the "combined type", i.e., vacancies and interstitials in close proximity. According to him, a

characteristic energy E is required to combine these and thus to make them cancel one another. This energy can vary from zero to the self-diffusion activation energy. But the energy required to bring about their migration to one another is assumed to be negligible. Let r(E) be the resistivity contributed by one distortion per unit volume and N(E)ΔE be the number of distortions per unit volume. The total contribution by imperfections is

$$\rho_i = \int_{-\infty}^{\infty} r(E)\, N(E)\, dE \qquad 1.48$$

The value of ρ_i may change with time on annealing. The distribution function of the "energy spectrum" of the distortions will be of the form

$$F_o(E) = r(E)N(E)$$

Vand has shown that

$$F_o(E) = -\frac{1}{kU}\frac{d\rho}{dT} \qquad 1.49$$

where $\frac{d\rho}{dT}$ is the slope of the resistance Vs. temperature curve on heating the film at a uniform rate, k is the Boltzmann's constant and

$$U = \frac{u(u+2)}{u+1} \qquad 1.50$$

where $u + \log u = \log 4\pi t\nu_{max}$ 1.51

n being the number of atoms that can initiate a defect ν_{max}, the Debye cut off frequency for the lattice; and t, the time required to reach the particular temperature at which $d\rho/dT$ is measured. By substituting the values of $d\rho/dT$ measured for successive values of temperature from the resistance Vs. temperature curve and corrected for the temperature coefficient of resistivity in equation 1.49, the distribution function $F_o(E)$ can be obtained.

The lattice-distortion spectrum for different deposition rates shows that defects are fewer in films prepared at lower deposition rates.

Hoffman et al.[36] have suggested another explanation to account for the decay of resistance on annealing. According to their theory the vacancies which are present in the film in numbers that exceed their equilibrium value coalesce into larger groups until they finally organise into sheets and collapse to form dislocation rings.

In films of certain metals annealing instead of decreasing their resistance, may increase it. Such behaviour can be seen in films of bismuth, gallium and antimony if heated at low temperatures.[37] These type of metals have lower electrical resistivity in the liquid

state. The amorphous state in films of these metals can be regarded analogous to supercooled liquid. So the films have the lowest resistance in the amorphous state. On annealing, the amorphous structure changes to normal structure via metastable phases with the consequent resistivity changes.

Annealing studies also reveal the influence of structural defects on electron transport. On annealing partially continuous films deposited at low temperatures, grain growth occurs due to the surface diffusion of islands and the aggregation of the physically touching islands. Borel's[38] study shows the occurence of such phenomenon in silver films. This growth of crystallites on annealing produces changes in the size and the separation of islands and causes rapid changes in the electrical conductivity.

It is also to be noted that the natural aging and annealing behaviour of films deposited at ambient temperature depends on the deposition conditions.[39] The effect of annealing also depends on the substrate. The resistance decrease is larger for substrates with smaller grain size and high adsorption energy.

Several workers have investigated the properties of annealed films on amorphous substrates. Hunos[40] and

Lucas[21] have shown that it is possible to obtain values close to bulk resistivity for annealed Au films.

Annealing of a film may increase its resistivity due to agglomeration and oxidation.

At lower temperature, the film particles condensed on the substrate have lower mobility and remain on the substrate more or less where the particle lands. Therefore a continuous film is formed on the substrate. But on annealing, the mobility of the particles increases and they coalesce into larger discontinuous islands. This process is known as agglomeration. Agglomeration occurs rather suddenly and attended by sharp increase of resistance. The mobility of the smaller islands on the substrate and the number of islands with sufficient energy to move are determined by a thermally activated process.

On heat treatment, resistance of many thin films may increase on account of oxidation. The increase in the resistance of a film is found to be considerably greater than that which can be accounted from the reduced thickness of the conductive portion of the film resulting from the oxidation of the surface. Basseches[41] has suggested that the oxidation is occuring along the grain boundaries of the film. The oxidation of the grain

boundaries can occur either as a result of oxygen diffusing in from the surface or from trapped oxygen diffusing internally.

1.3 Conduction in Bi-layer Films

As in the case of single layer metallic films size effect, i.e., decrease in conductivity with decreasing specimen thickness can be expected in double-layer films.

Considering a double-layer film having a base layer of thickness a and bulk mean free path λ_1 superimposed by a layer of thickness b and bulk mean free path λ_2, as in Fig.1.2, Lucas[42] proposed a model for size effect in specular double-layer films. Taking the z-axis normal to the substrate surface and its origin at the substrate he assumed that the conduction electrons reflect specularly at $z = 0$ and at $z = a + b$. Further he made the assumptions that (i) within the bulk metal electron - phonon collisions are diffuse, (ii) no additional scattering occurs at the interface boundary $z = a$ and (iii) the films are continuous and of infinite extent in X and Y directions with smooth parallel surfaces and interface.

According to the model, equation 1.22 can be written as

$$f = f_0 + f_{1,2}(v,z) \qquad 1.52$$

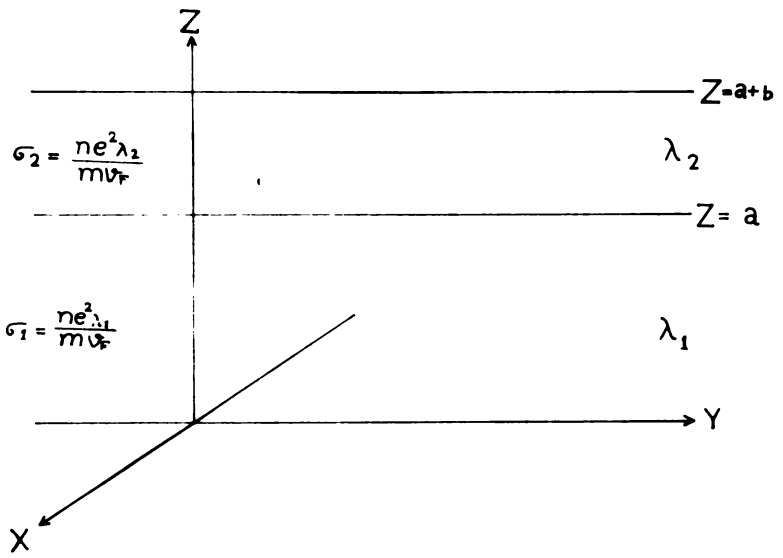

Figure 1.2 Film geometry for a double layer film.

where f_1, $0 \leqslant z \leqslant a$

and f_2, $a \leqslant z \leqslant a + b$

The Boltzmann equation is written as

$$\frac{\partial f_{1,2}}{\partial z} + \frac{\partial f_{1,2}}{\tau_{1,2} v_z} = \frac{eE}{mv_z} \frac{\partial f_0}{\partial v_x} \qquad 1.53$$

The general solution is

$$f_{1,2}(v,z) = \frac{\tau_{1,2} eE}{m} \frac{\partial f_0}{\partial v_x} \left[1 + F_{1,2}(v) \exp \frac{-z}{\tau_{1,2} v_z} \right], \qquad 1.54$$

where $\tau_{1,2}$ are the relaxation times of the conduction electrons in each layer and $F_{1,2}(v)$ are arbitrary functions to be determined from the boundary conditions $z = 0$, $z = a$ and $z = a + b$.

Defining the distribution functions

$$f^+_{1,2}(v,z) = f_{1,2}(v_x, v_y, v_z; z) \quad , v_z > 0 \qquad 1.55a$$

$$f^-_{1,2}(v,z) = f_{1,2}(v_x, v_y, -v_z; a+b-z), \; v_z < 0 \qquad 1.55b$$

the general solution 1.54 becomes

$$f^+_{1,2}(v,z) = \tau_{1,2} \frac{eE}{m} \frac{\partial f_0}{\partial v_x} \left[1 + g^+_{1,2}(v) \exp \frac{-z}{\tau_{1,2} v_z} \right], \qquad 1.56a$$

$$f^-_{1,2}(v,z) = \tau_{1,2} \frac{eE}{m} \frac{\partial f_0}{\partial v_x} \left[1 + h^-_{1,2}(v) \exp \frac{z+b-z}{\tau_{1,2} v_z} \right], \qquad 1.56b$$

where $g^+_{1,2}(v)$ and $h^-_{1,2}(v)$ replace $F_{1,2}(v)$, and

$$h^-_{1,2}(v) = h_{1,2}(v_x, v_y, -v_z)$$

Since the scattering is specular, the continuity condition at $z = 0$ is

$$f_1^+(v,0) = f_1^-(-v,0) \qquad 1.57$$

At $z = a + b$

$$f_2^-(v,a+b) = f_2^+(-v,a+b) \qquad 1.58$$

and at $z = a$,

$$f_1^+(v,a) = f_2^+(v,a) \qquad 1.59a$$

$$f_1^-(v,a) = f_2^-(v,a) \qquad 1.59b$$

Expanding equations 1.57 and 1.58 and simplifying,

$$g_1^+(v) = h_1^+(v)\ e^{(-a-b)/\tau_1 v_z} \qquad 1.60a$$

$$h_2^+(v) = g_2^+(v)\ e^{(-a-b)/\tau_2 v_z} \qquad 1.60b$$

Solving 1.59 and 1.60

$$h_1^+(v) = \left[\frac{\exp\ \frac{b}{\tau_1 v_z}}{1 - \exp\left(\frac{-2a}{\tau_1 v_z} - \frac{2b}{\tau_2 v_z}\right)}\right]\left(1 - \frac{\tau_2}{\tau_1}\right)\left(1 - \exp\frac{-2b}{\tau_2 v_z}\right), \qquad 1.61a$$

$$g_2^+(v) = \left[\frac{\exp\ \frac{a}{\tau_2 v_z}}{1 - \exp\left(\frac{-2a}{\tau_1 v_z} - \frac{2b}{\tau_2 v_z}\right)}\right]\left(1 - \frac{\tau_1}{\tau_2}\right)\left(1 - \exp\frac{-2a}{\tau_1 v_z}\right), \qquad 1.61b$$

Now the distribution functions may be obtained. The current density J can be obtained by substituting the

value of f(V,s) in 1.25. The ratio of the average conductivity of the film to the bulk conductivity of the first layer

$$\frac{\sigma_f}{\sigma_1(B)} = \frac{a}{a+b}\,\frac{\sigma_{1(f)}}{\sigma_{1(B)}} + \frac{b}{a+b}\,\frac{\sigma_{2(f)}}{\sigma_{2(B)}} \qquad 1.62$$

with resort to polar coordinates,

$$\frac{\sigma_f}{\sigma_{1(B)}} = \frac{1}{a+b}\left[a+b.\,\frac{\tau_2}{\tau_1} + \frac{3}{4}\left(\lambda_2-\lambda_1\right)\left(1-\frac{\tau_2}{\tau_1}\right)\right]$$

$$\left[\int_0^{\pi/2} \frac{\cos\theta\,\sin^3\theta\,(1-A^2)\,(1-B^2)}{1-A^2B^2}\,d\theta\right] \qquad 1.63$$

where $A = e^{-a/\lambda_1\cos\theta}$ and $B = e^{-b/\lambda_2\cos\theta}$

Assuming that the Fermi velocity in the first layer is same as that in the second layer, writing $k_1 = \frac{a}{\lambda_1}$ and $k_2 = \frac{b}{\lambda_2}$ and changing the variable of integration from θ to $\cos\theta = T$,

$$\frac{\sigma_f}{\sigma_{1(B)}} = \frac{1}{k_1\lambda_1+k_2\lambda_2}\left[k_1\lambda_1 + \frac{k_1\lambda_2^2}{\lambda_1} + \frac{3}{4\lambda_1}\left(\lambda_1-\lambda_2\right)^2\right.$$

$$\left.\int_0^1 F(T)\,dT\right] \qquad 1.64$$

where $F(T) = (T^3 - T)\left[\frac{(1-x^2)(1-y^2)}{1-x^2y^2}\right]$

$$x = e^{-k_1/T} \quad \text{and} \quad y = e^{-k_2/T}$$

When $a \gg b$, $\lambda_1 \gg \lambda_2$ and $k_2 \gg k_1$

$$\frac{\sigma_2}{\sigma_{1(B)}} = 1 - \frac{3}{4}\frac{\lambda_1}{a}\int_0^1 (T-T^3)\,(1-e^{-2k_1/T})\,dT \qquad 1.65$$

This is identical with the Fuch's equation for a film with diffuse scattering at both surfaces.

According to the theoretical analysis, a size effect can be expected in thin films formed of two or more layers of isotropic bulk conductors. Experimental investigations of Lucas[43] and Chopra and Randlett[20] have shown that an addition of a few angstroms of overlayers increases the resistance of a film under certain conditions.

Lucas[21] attributed the reason for the resistivity increase in "specular" films (e.g. Au film) to artificial roughening of the upper surface at the addition of a surface layer of the same material. But Chopra and Randlett[20] question this assumption on the ground that deposition of the same material should increase the surface smoothness rather than reduce it. According to

them the changes are also dependent and are as a result of an enhanced surface scattering rather than a change in the specularity parameter. The surface potential for the conduction electrons is modified at the interface and this modification influences the scattering of electrons and thus influences the effective number of electrons and their mobility near the surface. An increase or decrease in the amount of surface scattering may result depending on the nature of the change at the interface.

CHAPTER TWO

DIFFUSION IN THIN FILMS

The problem of diffusion in thin films was brought to light in 1935 when DuMond and Youtz[44] observed interdiffusion in layered thin films of gold and copper at low temperatures. They deposited many layers of gold and copper to produce an artificial grating to determine X-ray wavelengths. But, to their surprise, they observed that the gratings, after two or three days, have lost their ability to diffract X-rays due to interdiffusion of the materials. After a detailed study of these unstable gratings they pointed out two fundamental aspects of interdiffusion, namely,

i) the diffusion in the solid phase is a rapid process over small distances even at room temperatures and

ii) the diffusion of gold through copper in thin film gratings is faster by many orders of magnitude than that in their bulk form.

The study on the problem of interdiffusion in thin films has gained momentum during the past decades and has received greater attention ever since the publication of Weaver's[45] review on interdiffusion in 1971.

Diffusion in thin films differ from that in bulk specimens. According to Nicolet[46] bulk diffusion is associated with a larger activation energy and so a crossover from one process to the other occur as the temperature changes. This crossover temperature which is called the Tammann temperature is at one half or two third of the melting temperature in degrees Kelvin of a solid. Below this temperature, atomic diffusion is controlled by grain boundaries and other defects in the material and above this temperature by regular bulk process.

According to Balluffi and Blakely[47] the main reasons for the special characteristics of thin film diffusion are:

1) Thin films diffuse at low temperatures because of their poor thermal stability.

2) In thin films all volume elements are in close proximity to either a free surface or an interphase boundary.

3) They contain high densities of short circuit paths like grain boundaries and dislocations.

4) Large biaxial stresses are often present in the plane of the film.

5) As a result of special fabrication conditions there may be high concentrations of uncontrolled impurities in the film.

6) There may be disordered and meta-stable structure in the film.

7) Diffusion occurs over short distances under the influence of large concentration of electrostatic potential or concentration gradients.

8) Chemical gradients and low temperatures may affect the possible maintenance of local equilibrium at phase boundaries during multiphase diffusion.

As Tu and Lau[48] have pointed out thin film interdiffusion is very sensitive to the microstructure. Cook and Hillard,[49] and Kirsch et al.[50] have already shown that the rate of interdiffusion between two epitaxial single crystal films is quite different from that between two similar but fine-grained films. To some extent the microstructure of the films affects also the driving force and direction of the reaction.

Diffusion process in layered films may become complicated and not uniform on account of enhanced diffusion due to large defect densities and also on account of the possible formation of oxides, pores and ordered phases.[51]

2.1 Short-circuit Diffusion along Grain Boundaries and Dislocations

Diffusion through grain boundaries and dislocation is the dominant transport mechanism in thin films.[47] Thin films may contain dislocation densities of the order of $10^{10} - 10^{11}$ cm^{-2} and have grains of size smaller than 100 Å.[52,53] These defects and grain boundaries offer themselves as paths which enhance atomic mobility in metals[54,55] and also in non-metals.[56,57] Since diffusion through these short circuits requires lower activation energy than that for lattice diffusion, atoms diffuse rapidly through these paths even at room temperature.

Harrison[58] classified the kinetics of short-circuit diffusion into three categories which he termed as A, B and C types. In A-type of kinetics there may be extensive lattice diffusion which causes overlapping of diffusion levels both in adjoining grains and in their boundaries. In B-type kinetics, each boundary is

assumed to be isolated and the flux at large distances from the boundary approaches zero. In C-type, atomic transport is considered to occur only within the boundaries. The B-type kinetics has been observed by Usman et al.[59] during the diffusion of Cu into Ni. Fu and Rosenberg[60] have noticed a kinetics very close to the C-type in the diffusion of Pd atoms along the boundaries of polycrystalline Ag films. According to Gupta,[61-64] the high density of structural defects makes it possible to observe in thin films any of these three types of kinetics if appropriate annealing conditions are given.

The grain structure and the annealing conditions are two important factors which control diffusion kinetics in thin films.

Various investigators have shown the influence of grain size in the diffusion phenomenon in thin films. Campisano et al.[65] studied thin film couples of copper and lead deposited sequentially onto inert substrates. The copper film was of average grain size ~ 100 Å and the polycrystalline film of lead was ~ 2000 Å. Although the materials are immiscible in their bulk solid phases and do not form compounds, after annealing under a flow

of pure argon they found that lead had penetrated through the copper film. But the presence of copper in the lead film was found to be below the level of detection. Then they prepared a polycrystalline copper substrate and preannealed at 800°C for several hours in order to have copper grain size $\sim$ 30 μm. Lead film was deposited on this and annealed. On analysis, copper was found in the lead film while in copper the presence of lead was below the level of detection. The experiment clearly demonstrate the motion of materials, in thin films, from the layer having larger number of grains into layers having lesser number. Baglin and d'Heurle's[66] study of Cr/Cu film couples and Harris et al.'s[67] investigation of Ti/Mo/Au metallisation system confirm this behaviour.

Annealing at higher temperatures makes changes in the grain size of film materials and, hence, modifies the rate of diffusion. Films of higher melting point metals usually have grains of smaller size.[68] But, on annealing, these smaller grains grow faster and, as a consequence, their ability to permeate through the adjacent film in contact decreases. This increase in grain size and the consequent reduction in the diffusion rate have been observed in film pairs of Cu/Pb,[65] Cr/Cu and Bi/Cu.[66]

As grain size of films controls the diffusion phenomena, the grain boundary diffusion in thin film couples depends also on the method of film preparation. Sputtered films have larger grains than that of evaporated films. So sputtered films show lower values of diffusion rate. Such behaviour has been observed by Nemadovic et al.[69] in Au-Ni thin film couples.

Interfacial compound formation is a factor which affects the grain boundary diffusion significantly. In certain combinations like Cu-Au and Si-W the formation of interfacial compound has been found to slow down the mass transport.[70,71] An oxide layer at the interface has also found to impede the diffusion.

During diffusion annealing grain growth or recrystallisation may occur in bimetallic diffusion couples. This process can change the structure of the diffusion path and alter the morphology of the diffusion interface.

In thin film fabrication, solutes may be incorporated to improve adhesion to the substrate, to prevent corrosion, to reduce electromigration or to improve some other specific properties.[72] The presence of these solutes may influence the grain boundary

diffusion. While there may not be any observable effects in certain cases, in other cases there may be an increase or reduction of diffusion. The same solute may also exhibit different effect in changing the short circuit diffusion.[73]

In multiphase short circuit diffusion, complex diffusion zones may be produced. In such cases the intermediate phases do not form as thin layers of uniform thickness parallel to the plane of the thin film diffusion sandwich. But, instead, rapid diffusion occurs at the grain boundaries and the new phases form and grow preferentially in the grain boundary region. Tisone and Drobek[74] observed such multiphase diffusion in Pt-Ti thin film specimen.

2.2 Effects due to Nearby Surfaces or Interfaces

Every volume element in a thin film diffusion couple is in close proximity to a free surface or a phase boundary. This proximity may have a strong influence on the diffusion.

Studies of equilibrium charge configurations associated with dislocations,[75] grain boundaries[76] and free surfaces give good evidence to support the existence of defect space charges. Significant electrostatic

potential gradients may also be developed across thin films under non-equilibrium conditions. Such conditions may exist during the formation of oxides at free surfaces.[77] The potential gradients may originate from the difference in mobilities of the diffusing metal and oxygen ions.

Under special circumstances other effects due to nearby surfaces may occur. For example, the concentration profile of ^{110}Ag deposited on flat surfaces of GaAs, after annealing, was found to depend on whether the GaAs surface was (111) or $(\bar{1}\bar{1}\bar{1})$. Dzhafarov and Kulikov[78] attributed the behaviour to the difference in the nature of the interaction of Ag with the Ga and As surfaces.

2.3 Effect of Stresses

Large biaxial stresses of the order of $10^{9} - 10^{11}$ dynes cm^{-2} are usually found in thin films.[79-81] Such a high value of stress should be expected to have great effect in thin film diffusion.

Biaxial stresses have considerable effect in the process of short circuit diffusion in thin films. The grain boundary and dislocation diffusion occurs by a defect mechanism. But the defect concentration and their

jump frequencies in the short circuits are affected by the axial stresses.

Stresses may have influence on diffusion of materials in thin film couples where multiphase formation occurs. In bulk specimens it has already been observed that the stress may have influence not only on the diffusion rate in each phase, but also on the chemical composition of the phases at the interphase boundaries.[82,83] According to Balluffi and Blakely[47] this effect of biaxial stress should be very small in thin films.

Biaxial stress may produce fissures, pores, spalling etc. in multiphase diffusion zones and thus affect markedly the diffusion conditions in the films. Many intermediate phases are observed to be formed in diffusion zones characterised by considerable hardness and brittleness.[84] The partial molar volumes in many of these phases vary from those of other phases present in the zone. This may produce large stress in the zone. Blisters, spalls etc. produced by this stress may introduce fresh diffusion circuits and create short circuits along internal surfaces. Observations of blistering in certain oxide films[85,86] has been recorded by Dearnaley and Hartley.[84]

2.4 Effect of Impurities

In thin films there may be large concentration of impurities which may have considerable effect in the diffusion process. The impurities may be incorporated during the fabrication and thereby exert an effect on the subsequent diffusion. This is called "bulk impurity effect". Impurities may also be diffused into the film from the environment, i.e., from the atmosphere, or the specimen surface or substrate. This "near-surface" effect may alter the diffusion in the nearby specimen volume. As all volume elements are close to the surface, the "near surface" effects are important in thin films. Concrete cases of impurity effect on diffusion have been given by several investigaters.[56,87-90]

2.5 Disordered or Metastable Structures

Thin films may often possess non-equilibrium structures. They may have disordered or even amorphous structures. In certain cases they may possess non-equilibrium metastable polymorphs that have crystal structures different from the equilibrium structure. Hasegawa[91] observed difference in the diffusion behaviour of Cu in GaAs samples prepared by various methods and interpreted the difference on the basis of the variation in defect concentrations. Weaver and Brown[92] attributed

the rapid initial diffusion in Ag-Al thin film couples to a high initial concentration of vacancies. Tisone and Lau[93] observed considerable difference in the inter-diffusion behaviour of Au-b.c.c. Ta and Au-βTa film couples. Their behaviour was attributed to the difference in crystal structure and microstructure. Francombe et al.[94] have noticed the presence of metastable f.c.c. Au rich phase during the early stages of diffusion in Au-Al films.

In cases of multiphase diffusion, there may be cases where certain equilibrium phases missing. In some cases certain phases may appear or disappear at a later stage of diffusion. Difficulty in nucleation may cause the late appearance of certain phases, which in turn may disturb the diffusion fluxes in the diffusion zone and cause the disappearance of an already existing phase. Various investigators[45,74,95-98] give evidence for these phenomena in many thin film couples.

In a metal-semiconductor interface there may be a glassy metallic interfacial phase of some 10 to 20 Å thick as reported by Phillips.[99] This glassy phase is similar to a liquid metal. Therefore there is a tendency of semiconductor atoms and impurities to diffuse into the interfacial region.

2.6 Other Effects

In thin films there may be a "gradient energy" due to the compositional gradient. Such compositional gradients are often present during the diffusion anneal of thin films. The gradient energy has considerable influence on thin film diffusion kinetics when the diffusion distance is less than 30 Å.

In semiconductor and ionic crystal films, electrostatic fields associated with space charge regions near film surfaces may lead to nonlinear diffusion behaviour.

2.7 Theories of Interdiffusion

There are no detailed theories appropriate for massive interdiffusion in thin films. But considering various metal systems, expressions for diffusivities in single crystal film pairs have been obtained. These values are of importance in interpreting the more complex behaviour of practical polycrystalline films.

Metal systems can, in general, be divided into miscible and compound forming systems. The miscible systems may be fully-miscible or partially-miscible.

A. Miscible systems

a) Miscible single-crystal films

In a simple diffusion couple with a planar interface, heat treatment at a temperature T leads to planar interdiffusion at the interface between the films of metals A and B. At time t = 0, the concentration Vs. distance graph would be discontinuous at the interface. After a finite time t = t, there would be a continuous variation of concentration. In a finite specimen with the metals in equal proportion, the concentration would eventually become uniform at C = 0.5. If the diffusion coefficients D_A and D_B of the two metals A and B respectively are equal, the case would be as in figure 2.1.

The diffusion coefficients in the couples are not, in general, equal. In this case the concentration Vs. distance diagram would be as in Fig.2.2 where more material has diffused from one side of the interface than from the other. There is an effective displacement of the original interface. The results may be expressed in terms of a single inter-diffusion coefficient if the displacements are measured with respect to the Matano interface ($x' = 0$) defined as the plane across which the net flow is zero. The mutual diffusivity $D_{AB}(x)$ shows

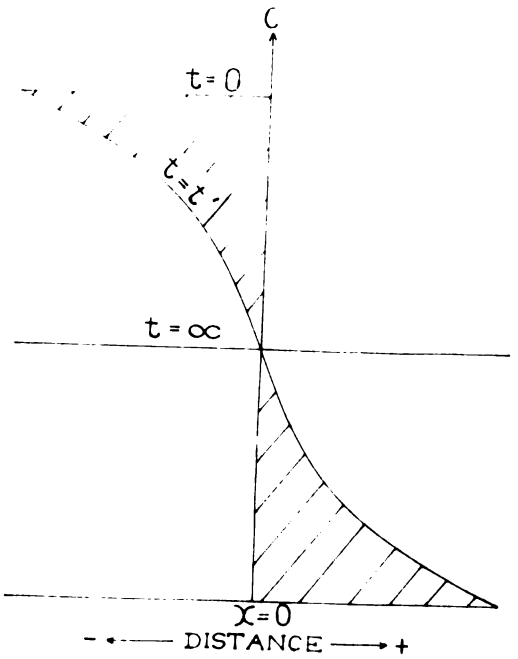

Figure 2.1 Concentration Vs. distance in a simple miscible diffusion couple having the same diffusion coefficients.

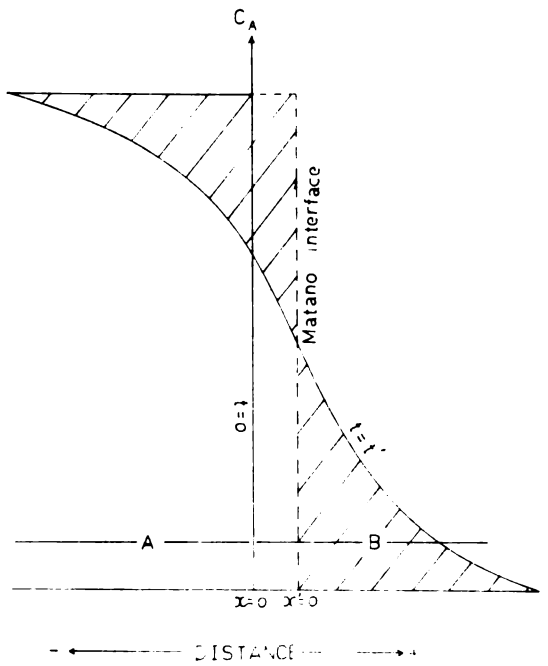

Figure 2.2 Concentration Vs. distance in a miscible diffusion couple having unequal diffusion coefficients.

the progress of A atoms at a depth x from the original interface, where the host matrix A and B have a concentration $C_A(x)$ and $C_B(x)$ respectively. The interdiffusion coefficient relative to the individual coefficients is given by

$$D_{AB}(x) = D_A C_B(x) + D_B C_A(x) \qquad 2.1$$

By Fick's second law, the time rate of change of concentration C of a constituent

$$\frac{\partial C(x,t)}{\partial t} = \frac{\partial}{\partial x}\left(D \frac{\partial C(x,t)}{\partial x} \right) \qquad 2.2$$

In the case of concentration dependent $\bar{D}(x)$, the equation cannot be reduced further. But by measuring distances x' relative to the Matano interface, the equation can be simplified.

Translating to the Matano interface the condition

$$\int_{C_A(x')=0}^{C_0} x' dC_A = \int_{0}^{C_A(x')=0} (-x') dC_A \qquad 2.3$$

is satisfied.

Boltzmann showed that a solution is possible if the two independent variables t and x are replaced by a single variable λ given by $\lambda = x/\sqrt{t}$

Equation 2.2 may now be written as

$$-\frac{\lambda}{2}\frac{\partial C}{\partial \lambda} = \frac{\partial}{\partial \lambda}\left(\bar{D}\frac{\partial C}{\partial \lambda}\right)$$

Integrating with respect to λ and choosing a particular time $t = t_1$, this becomes

$$\bar{D}_{(C=C_1)} = \frac{1}{2t_1}\left(\frac{dx'}{dC}\right)_{C=C_1}\int_{C=C_1}^{C=0} x'\,dC \qquad 2.4$$

where $\int_{C=0}^{C=C_0} x'\,dC = 0$

The equation gives a means to obtain $\bar{D}$ from a measurement of C Vs. depth in a diffused sample. Using values of $\bar{D}$ at different concentrations in equation 2.1, the unique values of the individual diffusivities D_A and D_B can be determined. Repeating the process at various temperatures, Arrhenius plots for D_A and D_B can be made. From these, activation energies Q_A and Q_B can be obtained.

b) Partially miscible single crystal films

In many miscible systems where no intermetallic compounds are formed, the solubility of the metals, each in the other, is limited. In such diffusion couples, there will always be a discontinuity in the concentration Vs. distance curve as in figure 2.3. The interface

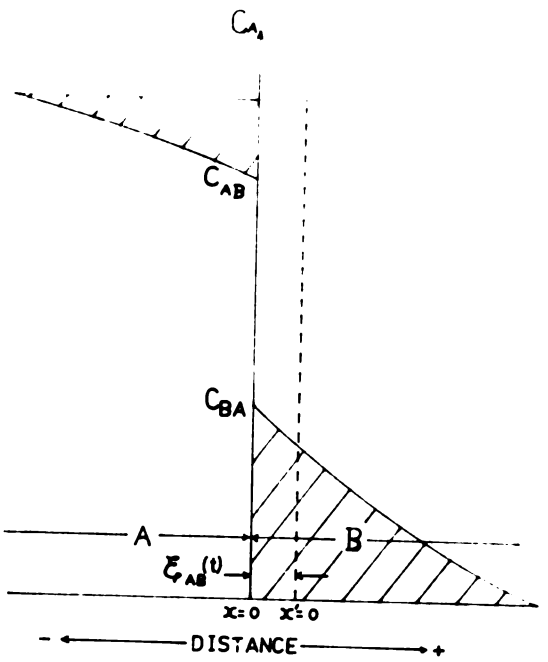

Figure 2.3 Concentration Vs. distance in a partially miscible diffusion couple where no intermetallic compounds are formed.

concentrations are limited by C_{AB} and C_{BA}.

According to Kidson,[100] the displacement of the Matano interface ξ_{AB} after diffusion for a time t is

$$\xi_{AB} = 2\left(\frac{\bar{D}_{BA}K_{BA} - \bar{D}_{AB}K_{AB}}{C_{AB} - C_{BA}}\right)t^{\frac{1}{2}} \qquad 2.5$$

where $K_{AB} = \left(\frac{dC}{d\lambda}\right)_{AB}$ and $\bar{D}_{BA}$ is the interdiffusion coefficient at the same point on the B side of the physical interface.

The system can be treated just as in the case of miscible systems. In this case the displacement of the interface shows a parabolic time dependence, but the direction of the movement depends on the relative magnitude of the diffusion coefficients in the terminal phases.

e) Polycrystalline films

Experimental study of diffusion of polycrystalline couples show that diffusion in polycrystalline film couples is different from that in single crystal film couples. In polycrystalline Ag-Au couples,[50] Au diffuses out through the Ag film to the surface and Ag similarly diffuses through the Au film. But no such interdiffusion is evident in single crystal couples. Diffusion in the polycrystalline films, as pointed out in section 2.2, is dominated by the short circuiting effect of defects and grain boundaries.

To understand the mechanism of the low-temperature diffusivity between polycrystalline films, the Whipple[101] model is usually taken as the starting point. At low temperatures, a rapid grain boundary diffusion coefficient D_b and a slower lattice diffusion coefficient D_l are assumed. Then the shape and magnitude of the diffusion profiles depend on the magnitudes of D_b, D_l and the density of grain boundaries. One of the important features of the diffusion profiles is the presence of zero concentration gradients after each annealing cycle. From this it can be assumed that grain boundary diffusion is extremely fast compared to the lattice diffusion to the interior of the grains. Another feature of the diffusion profile is the large concentration level of the 'plateaus'. It appears from this that most of the impurity diffuse into the grain interior. Therefore the model must assume that transport into the interior of the grains is aided by a diffusion enhancement mechanism such as a high concentration of vacancies, dislocations or the motion of grain boundaries. The Whipple model, therefore, can be applied in the case of polycrystalline couples by replacing the lattice diffusivity D_l by a defect-enhanced lattice diffusivity D_l'. When $D_b \gg D_l$, the model simplifies to give the concentration

$$C = C_1 + C_2$$

Where C_1 is the concentration due to diffusion at the interface and C_2 is that due to sideways diffusion from the grain boundaries.

Assuming that the grain sizes are uniform, L x L, in the plane of the film, the average concentration is given by

$$\bar{C} = \frac{2}{L}\int_0^{L/2} C_1 dx + \frac{4}{L}\int_0^{L/2} C_2 dx \qquad 2.6$$

If $L \gg 4\left(D_1' t\right)^{\frac{1}{2}}$ and C_0 is the composition at $y = 0$, the integration after applying the values of C_1 and C_2 gives

$$\frac{\bar{C}}{C_0} = \frac{8\left(D_1' t\right)^{\frac{1}{2}}}{L\pi^{\frac{1}{2}}} + \operatorname{erfc}\left(\frac{y}{2\left(D_1' t\right)^{\frac{1}{2}}}\right)\left\{1 - \frac{8\left(D_1' t\right)^{\frac{1}{2}}}{L\pi^{\frac{1}{2}}}\right\} \qquad 2.7$$

From the first term it can be seen that there is a $t^{\frac{1}{2}}$ dependence in the beginning which slowly levels off with annealing time. The second term is appreciable only near the interface.

B. Compound forming systems

a) Single crystal films

The most complex case of diffusion in metal systems is that in which two metals form one or more intermetallic

compounds. A typical case where there is a single intermetallic compound β existing between films of metals A and B when heated to a temperature T is as in figure 2.4. There are discontinuities in the concentration gradient at the interfaces between the intermetallic compound and the terminal phases.

The width of the β phase, as derived by Kidson,[100] after a time t

$$W_\beta = \xi_{\beta B} - \xi_{A\beta}$$

$$= 2\left[\left(\frac{(DK)_{B\beta} - (DK)_{\beta B}}{C_{\beta B} - C_{B\beta}}\right) - \left(\frac{(DK)_{\beta A} - (DK)_{A\beta}}{C_{A\beta} - C_{\beta A}}\right)\right]\sqrt{t}$$

$$W_\beta = B_\beta\, t^{\frac{1}{2}} \qquad 2.8$$

When there are several compound phases, the width of a layer of a phase j in a system made up of N phases,

$$W_j = \xi_{j,j+1} - \xi_{j-1,j}$$

$$= 2\left[\left(\frac{(DK)_{j+1,j} - (DK)_{j,j+1}}{C_{j,j+1} - C_{j+1,j}}\right) - \left(\frac{(DK)_{j,j-1} - (DK)_{j-1,j}}{C_{j-1,j} - C_{j,j-1}}\right)\right] t^{\frac{1}{2}}$$

$$= B_j\, t^{\frac{1}{2}} \qquad 2.9$$

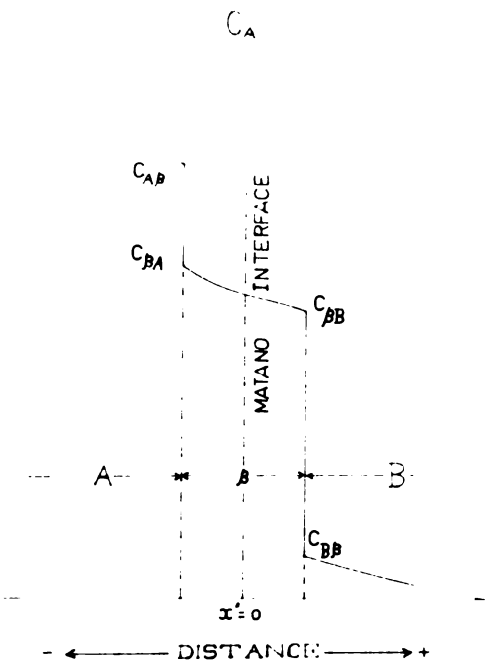

Figure 2.4 Concentration Vs. distance in a compound forming diffusion couple where a single intermetallic compound β is formed.

The relative widths of the layers of adjoining phases will depend in a complex way on the miscibility gaps and the diffusivities of the migrating atoms in each phase.

In these systems the chemical diffusion coefficient $\bar{D}$ is related to the individual diffusion coefficients D_1 and D_2 by the relation

$$\bar{D} = C_1 D_2 + C_2 D_1$$

where C_1 and C_2 are atomic fractions. The driving force in the diffusion process is the chemical potential gradient. In certain cases, the chemical potential gradient may be in the opposite direction to the concentration gradient and produce "uphill" diffusion. But this does not occur in the case of two pure metals.

b) Polycrystalline films

The formation of a new compound by diffusion may be described by the above mentioned diffusion models taking into account the possibility of diffusion through grain boundaries and then into the grains. Baird[102] has shown that the application in this case is similar to that for two metals forming a solid solution and the quantity of the new phase formed will be proportional to $t^{1/n}$ where $2 < n < 4$.

The compound formation occurs by the migration of atoms to suitable interface locations. The atoms are captured there and bonded into the new compound lattice. In certain cases the rate of migration may be faster than the bonding rate. This may lead to a concentration profile consisting of a series of plateaus. The diffusion process then becomes reaction controlled. In this case the growth rate of the new phase will be proportional to time t.

Therefore, from the phase growth dependence on time, a reaction-limited process can be distinguished from a grain boundary assisted process. As Nicolet[46] has pointed out a square root of time growth ($\propto t^{\frac{1}{2}}$) is typical of a growth process limited by atomic transport across a newly formed compound layer and a linear growth with time ($\propto t$) is typical of a growth process which is limited by an interfacial reaction. All the reaction rates are thermally activated with activation energy varying substantially and in an orderly way.

2.8 Characterisation

Most of the characterisation studies have dealt with the identity and kinetics of compound formation and profiles of interdiffusing species. Since the 1970s the study became relevant on account of the importance of thin

film reactions in technological applications. Various direct and indirect methods have been used to characterise the diffusion and the reactions occuring at the interface of thin film couples. But no single method has been found sufficient to analyze a diffusion process completely. Therefore the problem has to be approached with several different experimental techniques.

a) Direct methods

There have been two direct approaches to the problem of determining the in-depth atomic composition of thin films. One approach is the particle energy loss technique and the other is sputter sectioning.

(i) Particle energy loss techniques

The techniques utilize a beam of energetic particles and measures their energy loss on their inward and/or outward trajectories to obtain a measure of the depth at which the scattering or reaction took place. Rutherford backscattering spectrometry utilises this technique.

In a Rutherford backscattering spectrometer, energetic ion beams in the range of a few hundred keV to several MeV are produced in the accelerator and analysed, magnetically or electrostatically, to give an energetically

well defined beam of particles. These ions are passed through collimating aperture to the target chamber and the backscattered particles are detected with an energy analyser. Though the backscattering has the ability to determine quantitatively the compositional depth profiles, it can neither identify the high mass species nor detect low levels of light-mass impurities in heavier mass substrates.

(ii) Sputter sectioning

In this method, a sample is sectioned by sputtering with a beam of high energy particles and the newly exposed surface or the sputtered species examined. While the sputtered surface is analysed in Auger electron spectrometry (AES), the sputtered species detection method is used in secondary ion mass spectrometry (SIMS).

The best method to obtain depth information is to make use of more than one analytic method. As Mayer and Poate[103] have pointed out this approach has been followed by several investigators in combining backscattering with AES or SIMS.

b) Indirect techniques

As many properties of thin films depend sensitively on the amount of interdiffusion or reaction, these properties have been studied to determine the changes occuring in thin film couples.

(i) X-ray diffraction

X-rays have been used in a more convenient way to examine the structure of films and the interdiffusion and reactions in two-layer films. The powder technique in conjunction with diffractometers is widely used in thin film work. Various designs of diffractometers like the Bragg-Brentano diffractometer, the Seemann-Bohlin X-ray diffractometer etc. have been used by investigators in determining the structure of films and the interfacial reactions.[49,95,104-118]

(ii) Electron diffraction

Many investigators like Tisone and Drobeck,[74] Herl and Rieder,[119] Howard et al.[120] made use of the electron diffraction technique in the study of diffusion in thin film couples.

(iii) Resistance measurement

Since the resistance of a thin metal film reflects to a remarkable degree the microstructure of the film,[121] the variation of resistance in films demonstrates the changes occuring in them. Even before 1960, resistance measurement technique was used to investigate the alloying phenomenon in thin films.[122] Belser has observed increase of

resistance with diffusion and alloying in thin film couples.[121] While there is a progressive increase of resistance in miscible systems, sharp increases have been noticed at clearly defined temperatures in phase forming systems. Due to the remarkable dependence of resistivity on microstructure, resistance measurement has been widely used by investigators,[23,123,128] to study the structural changes occuring in metal films, aggregation of one of the metals in layered films, and diffusion and interfacial alloying or phase formation in bilayer films.

(iv) Optical methods

Measurement of optical constants has also been made use of to measure the rate of diffusion through films. Coleman and Yeagly[129] measured the reflectivity of Zn surface on annealing a Cu-Zn double layer film at constant temperature. Schopper[130] investigated Au-Pb system by measuring the reflectivity of Au.

(v) Other methods

Various other methods like "scratch test" of measuring film adhesion,[131] photoemission spectrometry[132] etc. have also been used by many workers. Implanted noble gas atoms of Ar and Xe have also been used as diffusion markers to investigate the relative movement of the interfacial layers in thin film couples.[107]

2.9 Diffusion Barriers

Diffusion between film materials at the film-electrode junctions and that in the layered films is a serious problem encountered in many technological devices. Usually diffusion barriers are used in these devices to reduce the interdiffusion.

An ideal diffusion barrier should have the following qualities:

(a) the transport rate of the materials of two layers A and B across the barrier level should be small.

(b) the loss rate of the barrier into A and B also should be small.

(c) the barrier should be thermodynamically stable against A and B.

(d) there should be strong adhesion of the barrier with A and B.

(e) the specific contact resistance of the barrier to A and B should also be small.

(f) the barrier should be resistant to mechanical and thermal stresses.

(g) the barrier should also have high thermal and electrical conductivity.

All these conditions are not usually found in a barrier. Therefore in selecting a barrier a compromise is required.

Metal layers, in general, have a polycrystalline form. So if they are used as barrier layers, diffusion may take place through the grain boundaries at elevated temperatures. So these "elemental barriers" are to be treated as non-barriers.

The single crystal films, however, have been found to be efficient barriers at least in low temperature regions. Tu and Rosenberg[60] have found that a 300 Å single crystal silver layer was impermeable to gold and lead even after annealing for 48 hrs. at 200°C. Similarly Kirsch et al.[50] have observed no detectable diffusion in Au/Ag single crystal film couple after annealing at 150°C for 40 minutes. Even though the single crystal film barriers are rather efficient, they are extremely difficult to construct. So these barriers are not of much help in practical applications.

Another method of reducing interdiffusion is to form an interfacial layer of an alloy or a compound. Certain intermetallic layers have been found to be effective diffusion barriers.[120,133,134] Oxide layers are very efficient diffusion barriers[135] and, hence, are used extensively.

CHAPTER THREE

ELECTROMIGRATION IN THIN FILMS

3.1 Introduction

An electric field generally induces a migration of atoms towards the anode or cathode. This electromigration in bulk metals has been reviewed by several authors.[136-138] Electromigration in thin films has received considerable interest on account of its relevance to open-circuit failure in integrated circuits. A couple of decades ago, a high rate of failure was traced in integrated circuits where aluminium stripes were deposited as connecting leads. Though these stripes were of several thousand angstroms thick and were well heat sunk to keep the temperature below 200°C, the devices went open on passage of current. Electromigration of aluminium through grain boundaries was then detected as the principal cause of the failure. Intensive study of this phenomenon in thin films was then taken up by several workers, first by following the resistivity changes and then observing the formation of voids and hillocks. Work done in this field has been reviewed by d'Heurle and Rosenberg.[139]

3.2 Mechanism of Electromigration

When an electric current flows through a metal two forces act on the metal ions: an electrostatic force which is opposite to the direction of the electron flow exerted by the applied field and a drag force in the direction of the electron flow resulting from a continuous transfer of momentum from the conducting electrons to the ions. On account of these two opposing forces, the thermally activated ions move in the direction of the predominant force. The ion drift velocity, by the modified Nernst - Einstein expression, as given by Ho and Huntington[140] is

$$V = DEe_s^*/kT \qquad 3.1$$

where D is the self diffusion coefficient, E the electric field, k Boltzmann constant, e_s^* the effective charge which is the difference between the charge due to electron-ion interaction and the charge associated with an unscreened ion.

Applying Ohm's law, equation 3.1 can be written as

$$\frac{V}{J} = D\rho e_s^*/kT \qquad 3.2$$

where ρ is the resistivity and J the current density.

The temperature dependence of the diffusion coefficient is given by

$$D = D_0 \, e^{-\Delta H/kT}$$

where ΔH is the activation energy.

Substituting in equation 3.2,

$$\frac{V}{J} = \left(D_0 \, es^*/k\right)\left(\rho/T\right) e^{-\Delta H/kT}, \qquad 3.3$$

Assuming that ρ/T and es^* are independent of temperature

$$\frac{V}{J} = A \, e^{-\Delta H/kT}, \qquad 3.4$$

where A is a constant.

From equation 3.4 it can be seen that V is proportional to J at a given temperature and that V and D have the same temperature dependence.

Therefore,

$$\frac{V}{D} = \frac{AJ}{D_0} \qquad 3.5$$

The activation energy can be determined from a log D versus $\frac{1}{T}$ plot. The values of V and D are obtained from the concentration profiles.

The linear dependence of V on J (equation 3.4) has been found to be true for relatively low current

densities of the order of 10^4 A cm^{-2}. But there has been no experimental verification of this linear relationship at very high current densities greater than 10^6 A cm^{-2}

In theoretical treatments[141] it has been customary to consider separately the force arising from the electric field and that arising from the electron current. The former direct force includes the force ZeE due to the external field E acting on the ion of valence Z and any local screening of E by the static polarisation of the electron cloud surrounding the ion. The later force which is termed electron wind arises from the momentum transfer of the electrons to the impurity. So introducing the concept of Z^*, the effective charge number, the force

$$F = Z^* |e| E = \left(Z^*_{el} + Z^*_{wd} \right) |e| E \qquad 3.6$$

According to Kumar and Serbello[142] this separation is artificial. Using the linear response theory, they have obtained a response function for the force exerted on an impurity in the presence of an electric field. With this force response function it is possible to calculate the driving force even in cases which are difficult to treat with other theories. Schaich[143,144] has also shown that the linear-response theory yields results consistent with previous works.

From the fundamental equation for electron transport it can be shown that the volume of a material 'q' carried by electromigration during a time t

$$q = n\,l\,\delta\left(D/kT\right) Z^{*} E\rho t \qquad 3.7$$

where n, l and δ are the number, length and width of the grain boundaries.

3.3 Direction of Electromigration

D'Heurle and Gangulee[145] have observed electron transport from the negative to the positive end of the conductors in Cu-Al and Cu-Be alloy film samples. Their observation is found to be in agreement with the results of Huntington and Grone[146] in the case of Au thin films and that of Revits and Totta[147] in the study of lattice diffusion of Cu. But this is in contradiction to the reports of Hummel and Breitling,[148] and Klotsman et al.[149] that electromigration occurs from the positive to the negative end in the grain boundaries of Cu, Ag and Au. D'Heurle and Gangulee have also observed that the transport of residual Al in solution in Cu-Al samples occurs from the negative to the positive end.

Kammochi and Hirano[150] have pointed out the contradiction in the direction of electromigration in thin films and in bulk specimens of aluminium. Blech and Meieran,[151] and Rosenberg[152] have found that in thin films of Al the ions

move towards the anode through the grain boundaries. But Pieri et al.[153] have found that the grain boundary migrates towards the anode in bulk specimen of Al in a temperature range 440°- 600°C.

The sign of the mass transport for grain boundary electromigration, therefore, in noble metals appears to be a serious problem. The suggestions of Klotsman[154] and others, as indicated by Huntington,[141] for the sign reversal in Z^* for grain boundary transport in Ag may, mutatis mutandis, be used to understand the problem upto a certain extent.

According to Klotsman, the changes in the electron-ion ratio in the grain boundary would expand the Fermi surface locally within its Brillouin zones which may transform it into a hole conductor. Another consideration is the symmetry of the surface which is lower than that in bulk crystals. The electron wave functions reflected from such surfaces are susceptible to extra Bragg reflections. For every electron scattering which is caused by a defect moving in the interface region, the surface may pick up a pseudo-momentum $\hbar K_s$, where K_s is a surface translational vector. The K_s value may be large enough to overbalance the electron momentum exchange and thus to cause a hole wind. Another

explanation is based on the high resistivity of the grain boundary region.[155] No clear cut explanation has been given to the problem and hence it remains as an open question.

3.4 Preventive Measures

Various preventive measures have been tried to reduce the unwanted electromigration in electrical devices and thus to improve their life time. Single crystal stripes have shown considerable increase in the life time. But the production of such stripes in a commercial level is not practical. Alloying of aluminium seems to be a simple and efficient remedy for the problem. Alloying aluminium with 1 wt. % of copper appears to make a 70-fold increase in life time. The impurity appears to act as an obstacle in the short circuit path and thus decrease the mobility. For effective blocking it seems that the impurity must have a somewhat different size than the solvent. The copper impurity, although moves very slowly, works well in aluminium.

CHAPTER FOUR

THIN FILM PREPARATION

There are a number of references [156-161] which give in detail the various methods of thin film preparation. The methods can in general, be divided into physical methods and chemical methods. While the chemical methods depend on a specific chemical reaction or on thermal effects, the physical methods cover deposition techniques which depend on the ejection of material from a source.

4.1 Chemical Methods

a) Electrolytic deposition

In this method the metallic ions in the electrolyte migrate toward the cathode under the influence of an applied electric field and deposit on the substrate. The deposition is governed by the laws of electrolysis. The type of film growth can vary from single crystal to unoriented deposits of very fine grain size and disordered structures.

b) Electroless deposition

It has been found possible to obtain films directly from solutions. Here the electrolytic action

is achieved without an external potential by a chemical-reduction process. The growth rate of the film depends on the temperature of the solution. Therefore, it is necessary to control the temperature fairly closely to obtain controlled growth conditions.

c) Anodic oxidation

An oxide film can be grown by anodic polarisation of a large number of metals in a suitable aqueous solution. The process involves the migration of oxygen ions to the anode surface through a medium. The growth rate of an anodic film depends on the current density and the temperature of the electrolyte. Anodisation may be carried out at constant current, constant voltage or by a sequence of constant current and constant voltage.

d) Chemical vapour deposition

Chemical vapour deposition method is widely used for obtaining films, especially single crystal films. In this method a volatile compound of a substance is first vaporised. The vapour is then thermally decomposed or made to react with other gases, vapours or liquids so as to yield the non-volatile reaction product.

To obtain the non-volatile reaction products, the CVD technique employs various types of reactions.

(i) Disproportionation

An equation of the type

$$A + AB_2 \rightleftharpoons 2AB$$

is typical of this reaction where the left hand side occur at low temperatures and the right hand side at high temperatures. So, if a gas of AB in equilibrium at high temperature is passed into a low temperature zone, disproportionation will occur and a deposit of A will be obtained.

(ii) Polymerisation

Polymer films may be prepared from monomer vapours. The process can be accomplished at higher temperatures by the use of electron beam, ultraviolet irradiation, or glow discharge. By replacing some or all of the carbon atoms in organic polymers with Si, P, N etc., inorganic polymers may be produced.

(iii) Reduction, oxidation, nitriding

This is usually undertaken using a halide of the required metal or metal oxide. The two possible reactions are of the form

$$2\,AX + H_2O \xrightarrow{\text{(steam)}} AO + 2\,HX$$

$$2\,AX + H_2 \longrightarrow A + 2\,HX$$

where X stands for halogens.

Metals, semiconductors and oxides may be deposited using this technique, applying either hydrogen or steam onto hot substrates.

(iv) Decomposition

The process can be represented by

$$AB \longrightarrow A + B.$$

The decomposition can be effected by heat (pyrolysis) or by the use of either ultraviolet or infra-red radiation.

e) Other Methods

(i) Langmuir Blodgett technique

The technique is used for producing monolayer films of fatty acids.

(ii) Chemical spray method

In this process, thiourea, selenourea and thioacetamide is made to interact with salt solutions of heavy metals to form precipitates of II-VI compounds when heated at a suitable value.

4.2 Physical Methods

The two physical methods of thin film deposition are sputtering and evaporation.

A. Sputtering

The ejection of atoms from the surface of a target material by bombardment with energetic particles is called sputtering. The ejected atoms can be condensed onto a substrate to form a thin film. Various types of systems have been employed for sputtering deposition of films.

(i) Glow discharge

In a glow discharge system, the glow discharge between two electrodes gives the energetic ions that are needed for the ejection of atoms.

(ii) Bias sputtering

In this system, the substrate may be left floating. If a negative potential is applied to the substrate, the film will be subjected to steady ion-bombardment throughout its growth which cleans the film of adsorbed gases.

(iii) Assymetric sputtering

An assymetric ac is applied between the cathode and the substrate so that more material is deposited in one half cycle than is removed by reverse sputtering in the other half cycle. The ion-bombardment

removes not only the adsorbed gases but also the initial oxide layers.

(iv) Ion plating

This system is a combination of evaporation from a heated wire and use of a discharge.

(v) Getter sputtering

In this system, a secondary enclosure within the main vacuum system is employed. The gettering action of the sputtered material in the inner chamber reduces the reactive gas content in the enclosure.

(vi) Triode sputtering

In this, a secondary electron gun is used to increase the concentration of ionising electrons. This makes the sputtering possible at lower pressures.

(vii) R.F. sputtering

By using a r.f. field, enhanced ionisation can be achieved. So it is possible to sputter at lower pressures.

(viii) Ion-beam sputtering

In this system sputtered films can be prepared even at pressures below 10^{-3} Torr. Ions can be produced

in a high pressure chamber and can be extracted into a differentially pumped vacuum chamber for sputtering.

(ix) Reactive sputtering

Films of oxides, nitrides etc. of the target metal can be prepared in this system by introducing a mixture of the inert sputtering gas and a small quantity of the reactant in gas form.

B. Evaporation

The deposition by thermal evaporation method is simple and very convenient and, hence, is at present most widely used. A vast number of materials can be evaporated in vacuum and caused to condense on cooled substrates to yield thin solid films.

a) Evaporation theory

In 1913 Langmuir[162] showed that the Herts-Knudsen equation, derived by Knudsen for the evaporation of a liquid can be applied to the evaporation from free solid surfaces. According to him the rate of free evaporation of vapour atoms from a clean surface of unit area in vacuum

$$m_e = 5.83 \times 10^{-2} \quad p_e \left(\frac{M}{T}\right)^{\frac{1}{2}} \text{ g cm}^{-2}\text{s}^{-1} \qquad 4.1$$

where p_e is the equilibrium vapour pressure, in Torr, of the evaporant under saturated vapour conditions at temperature T and M is the molecular weight of the vapour species.

The evaporation rate may also be expressed as

$$N_e = 3.513 \times 10^{22} \; p_e \left(\frac{1}{MT}\right)^{\frac{1}{2}} \text{ molecules } cm^{-2}s^{-1} \qquad 4.2$$

The rate of deposition of this vapour on a substrate depends on the source geometry, its position relative to the substrate and the condensation coefficient. Taking an ideal case of deposition from a clean and uniformly emitting point source onto a plane receiver, the rate of deposition, by Knudsen's cosine law, varies as $\cos \theta / r^2$,

where r is the radial distance of the receiver from the source and θ is the angle between the radial vector and the normal to the receiver direction.

b) Vapour sources

Thermal evaporation of materials may be achieved directly or indirectly by a variety of methods.

(i) Resistive heating

The simplest method of evaporating materials is heating with resistance-heated wires and foils of

various types made of refractory metals such as W, Mo, Ta etc. The materials can be heated indirectly in crucibles of quartz, graphite, alumina, zirconia etc. The indirect heating may be from below with the crucible sitting in a metal heater, from inside with the crucible built around the heater windings, or from on top using a radiant heater.

(ii) Arc evaporation

Materials may be evaporated by striking an arc between two electrodes. The method makes use of a standard dc arc-welding generator connected to the electrodes. This type of heating may be used to evaporate refractory materials.

(iii) Laser evaporation

A material can be evaporated from its surface by keeping a laser source outside the vacuum chamber and focusing a laser beam onto the surface of the material.

(iv) R F heating

RF heating may be supplied directly to the material or indirectly from the crucible.

(v) Electron-bombardment heating

In this method, heating is done by electron bombardment of the materials. The source is capable of evaporating any material at rates ranging from fractions of an angstrom to microns per second. There are various types of electron guns suitable for the purpose.

(vi) Other methods

Gunther's method of three temperature technique[164] using two separate sources is a satisfactory method for preparing alloys and compounds. Flash evaporation is another method used for rapid evaporation of a multicomponent alloy or compound. This is usually done by continuously dropping fine particles of the material into a hot evaporator. The powder may be fed into the heater by agitating the feed chute mechanically, ultrasonically or electronically.[159]

CHAPTER FIVE

GROWTH PROCESS OF THIN FILMS

Thin films are generally prepared by the condensation of atoms from vapour phase onto a substrate. The condensation process begins as three-dimensional nuclei and these nuclei grow into continuous film by diffusion controlled processes. The structure and properties of films depend on the growth process of the films.

5.1 Film Nucleation

The vapour molecules impinging on the substrate can either adsorb and stick permanently to the substrate, can adsorb and re-evaporate in a finite time, or can immediately bounce off the substrate. The impinging atoms lose their velocity normal to the surface and then physically adsorbed. They may move over the surface by jumping from one potential well to the other on account of thermal activation energy from the surface or their own kinetic energy parallel to the surface. These atoms may interact with other adatoms on the surface to form a stable cluster with the release of the heat of condensation. If they are not adsorbed, they re-evaporate into

the vapour phase. Therefore condensation is the net result of an equilibrium between the adsorption and the desorption process. If this steady state is attained and a critical beam density is obtained, atom pairs are formed on the surface, which, in turn, act as condensation centres for other atoms.

a) Theories of nucleation

(i) Capillarity theory

Pound and others[165,166] extended the classical capillarity theory for homogeneous nucleation from the vapour phase by Volmer and Weber[167] and Becker and Doering[168] to the particular shapes of clusters in a thin film.

In this theory, if supersaturation is sufficiently high in the vapour phase, clusters are formed by collisions of adatoms on the substrate surface. They develop with an increase in free energy until a critical size is reached. Above this size the growth continues with a decrease in free energy. The radius of the critical nucleus r^* is given by

$$r^* = -\frac{2\sigma_{cv}}{\Delta G_v} \qquad 5.1$$

where σ_{cv} is the condensate-vapour interfacial free

energy and ΔG_v is the Gibb's free energy difference. The critical value of total free energy can be shown to be

$$\Delta G^* = \frac{16}{3} \pi \frac{\sigma_{sv}^3}{\Delta G_v^2} \phi(\theta) \qquad 5.2$$

where $\phi(\theta) = \frac{1}{4}(2 - 3\cos\theta + \cos^3\theta)$, θ, being the contact angle of the critical nucleus. The nucleation rate I is proportional to the product of the concentration N^* of the critical nuclei and the rate Γ at which molecules join the critical nuclei by diffusion process. Here

$$N^* = N_0 \, e^{(-\Delta G^*/kT)}$$

where N_0 is the density of adsorption sites.

The diffusion process yields

$$\Gamma \approx N_1 \, a_0 \, \nu' \, e^{(-Q_d/kT)} \qquad 5.3$$

where a_0 is the separation between adsorption sites ν' is the frequency, Q_d is the activation energy for surface diffusion and N_1 is the density of adatoms.

This density

$$N_1 \approx \frac{R}{\nu} \, e^{(Q_{des}/kT)} \qquad 5.4$$

R, being the rate of incidence of single atoms from the vapour and Q_{des}, the energy of desorption of single atoms from the substrate.

The nucleation rate, from the theory, is

$$I = \frac{4\pi \sigma_{gv}}{\Delta\theta_v} \sin\theta \; Ra_o N_o \; e^{(Q_{des}-Q_d-\Delta\theta^*)/kT} \qquad 5.5$$

From the exponential dependence on $\Delta\theta^*$, it can be seen that the nucleation rate is very sensitive to changes in supersaturation. Further, the effective supersaturation rapidly varies with the change of substrate-temperature. The nucleation rate depends also on the impingement flux R.

(ii) Atomistic theory

Rhodin and Walton[169,170] have pointed out that the applicability of the capillarity model and the use of bulk thermodynamical quantities for small clusters are questionable. This difficulty may be overcome if the nucleation process could be treated by writing the partition functions and potential energies for the reacting species and products.

Treating the nucleation clusters as macromolecules, Walton and Rhodin considered the energies and bonds of nucleation. According to the theory, at low substrate temperatures or very high super-saturations, the critical nucleus may be a single atom which forms a

pair with another to form a stable cluster having one bond per atom. At higher temperatures this may not be a stable cluster. So the next stable cluster may be the one having a minimum of two bonds per atom.

The nucleation rate, according to the theory, is proportional to $N^* T$. Assuming that the vibrational partition functions as unity, the nucleation rate of critical nuclei with n^* atoms

$$I = R\, a_o^2\, N_o \left(\frac{R}{\nu N_o} \right)^{n^*} e^{\left[(n^*+1)\, Q_{des} - Q_d + E_n^* \right]/kT} \qquad 5.6$$

where E_n^* is the energy required to dissociate the n-adatom critical cluster into n single atoms adsorbed on the surface.

The atomistic theory also shows that the nucleation rate has a very sensitive dependence on supersaturation ($e^{E_n^*}$ dependence) and depends on the impingement rate R.

b) Remarks

The two theories are almost identical. The capillarity theory predicts correctly the dependency of nucleus size and nucleation rate on substrate temperature, impingement flux and the nature of the substrate. But it

may not always give quantitative information about the size of the critical nucleus. The atomistic theory puts its emphasis on very small critical nuclei. So this theory is the best to describe the condensation of materials of large free energy of condensation or condensation at very high supersaturation where the critical nucleus is small. The capillarity theory is suitable to describe the condensation of materials of low free energy of formation or at low supersaturations where the critical nucleus is large.

Nucleation theory states that there will be a barrier to the condensation of a permanent deposit. If there is a nucleation barrier, the film, in the initial stages of growth, will show an island structure. If the barrier is large, the film would consist of a few large aggregates. They are large because their minimum possible stable size is large and are few because the frequency of nucleation is small. The film will be discontinuous upto a relatively high film thickness. But a film formed under small nucleation barrier would be of many, but small aggregates and would become continuous at relatively low thickness. Therefore, while high nucleation barrier films give a coarse-grained film, low-nucleation barrier films give a finer-grained film.

The size of the critical nucleus is also dependent on the boiling point of the film material, the binding energy of the adsorbed atom to the substrate, the substrate temperature and the deposition rate. For high boiling point materials, the nuclei are stable even if they are very small. But for low-boiling point metals, nuclei become stable only when they become relatively large. The rate of formation of critical nuclei depends on the ability of adsorbed atoms to diffuse and collide with each other. If the binding between adsorbed atom and substrate is strong, the critical nucleus will be smaller and the nucleation frequency will be higher. Since the size of the critical nucleus is dependent on temperature, an increase in the substrate temperature at constant deposition rate will increase the size of the critical nucleus. Further, at higher temperatures, island structure will persist to a higher average film thickness. An increase of the deposition rate results in increased rate of nuclei formation and smaller islands.

5.2 Film Growth

It is aimed here to examine the stages of film formation consequent to the nucleation and the formation of three dimensional islands, i.e., the stages of the growth and intergrowth of islands to form a continuous

film. Based on the electron microscopic observations of the growth of films, Pashley et al.[171] have distinguished the characteristic growth stages, namely the island stage, the coalescence of islands, the channel formation and the formation of the continuous film.

In the island stage, the randomly distributed three dimensional nuclei grow to form observable islands. The growth of these islands is diffusion controlled. Adatoms and subcritical clusters diffuse over the substrate and are captured by stable islands.

As islands increase their size the larger ones appear to grow by coalescence of the smaller ones. This stage is known as the coalescence stage. During this stage there is a considerable transfer of mass between the islands by diffusion. This movement takes place in a fraction of a second and the density of islands decreases considerably.

When the islands grow during deposition, their completely rounded shape begins to change. The islands become elongated and join to form a continuous network structure. The process is a very rapid one initially, but slows down at the formation of the network. The network contains a large number of empty channels.

As deposition continues, secondary nucleations occur in the channels and are incorporated to the bulk as they grow and touch the sides of the channel. Slowly the empty channels are filled and the film becomes continuous but having many small irregular holes. Now secondary nucleations take place in these holes. These nuclei grow and coalesce with the main film. The process of nuclei formation and coalescence with the main film continues until the holes are filled in.

The kinetics of each stage may vary markedly depending on the deposition parameters. However, a liquid-like behaviour is manifested by the deposit until the complete film is formed. During the growth recrystallisation, grain growth, orientation changes etc. occur as a result of coalescence. Therefore the coalescence phenomena have profound effect on the structure and properties of the resultant film.

5.3 Factors Affecting the Film Growth and Film Properties

The growth and structure of evaporated films are strongly dependent on several factors like nature of the substrate, contamination and the parameters of the deposition process.

a) Substrate

The mobility of adatoms on the substrate surface is usually decreased and film adhesion increased with increase of the binding force between the substrate and the evaporant atom. The increase of the binding force also increases the density of nuclei formation which affects the coalescence process and the size and structure of islands during their growth stage. Difference in the expansion coefficients of the substrate material and the film will produce stresses in the film whenever the temperature of the film changes from its temperature at the time of deposition.

b) Substrate temperature

An increase in the substrate temperature increases the mobility of condensed atoms on the surface and the probability of desorption of evaporant atoms from the substrate. Therefore the crystalline structure of the film may be changed.

Heating the substrate in vacuum have the additional effect of cleaning its surface.

c) Source temperature

The emission rate of radiant energy from the surface of an evaporation source is proportional to T^4

where T is the temperature in ^{0}K. Since the evaporation rate is a steeper function of temperature than T^4, the evaporating efficiency of the source increases with increasing temperature. An increase in the evaporation rate will increase the nucleation rate and hence, the structure of the film.

d) Melting point of the deposit

It has been shown by Levinstein[172] that the size and orientation of crystals in evaporated films can be related to their melting points. Films of low melting point metals have larger crystals which may be preferentially oriented to the substrate. But films of high melting point metals consist of smaller crystals having no specific orientations.

e) Adsorption of residual gases

The presence of residual gases in the vacuum chamber during film deposition may affect the structure and purity of the film. Stahl[173] has shown the oxidation of several metals during their film formation in a vacuum of the order of 10^{-5}Torr. Oxidation may occur during the transit from source to the substrate or during the process of condensation. If the rate of evaporation is slow, the

possibility of combining with gas molecules impinging on the substrate to form oxides will be high. Similarly trapping of gases and vapours in the film will also be high. Therefore, a faster growth of film makes it more pure.

f) Angle of incidence of the evaporant

The angle of incidence of the impinging beam of vapour atoms can affect the structure of the evaporated film. At oblique impingement, as the velocity component of the migrating atoms on the surface is high, the mobility of these atoms are high. So greater agglomeration occurs. With increasing size of islands, the self-shadowing becomes pronounced and columnar growth in the direction of the incident vapour occurs. The reason for this is that the vapour atoms are unable to penetrate the interstices between the nuclei growing on the substrate surface. So condensation is confined to the peaks of the prominent grains and in a direction which tends towards the vapour beam.

g) Electrostatic effect

Chopra[174] has shown that an electric field in the plane of the substrate can induce coalescence at an early stage and thus make the film electrically conductive

at a smaller average thickness. Films prepared within an applied field are of lower electrical resistance. With increase of the field the resistivity decreases to a value which is very close to the bulk value. This phenomenon is more marked at higher substrate temperatures.

Electron irradiation of substrates produces coalescence of islands at an early stage and affects the further growth. This may be due to the increased nucleation density or a combination of nucleation and electrostatic effects.

CHAPTER SIX

EXPERIMENTAL DETAILS

6.1 Vacuum Equipment

The films for the investigation have been prepared in a 'Hindhivac' vacuum coating unit capable of producing a vacuum better than 10^{-5} Torr. The coating unit consists of a cabinet upon which the work chamber rests. The cabinet contains the vacuum pumping system together with all the electrical components necessary for the film deposition process. The layout of the unit is as in figure 6.1.

a) Pumping system

The pumping system consists of an oil diffusion pump backed by a rotary pump. There is a hand operated water-cooled baffle valve which serves to isolate the work-chamber from the pumping system and makes it possible to let air into the chamber without switching off the pumping system. There is an isolation valve which is situated between the diffusion pump and the rotary pump. This valve makes it possible to keep the diffusion pump under vacuum when this backing valve and the baffle valve are closed and allows the diffusion pump to remain at

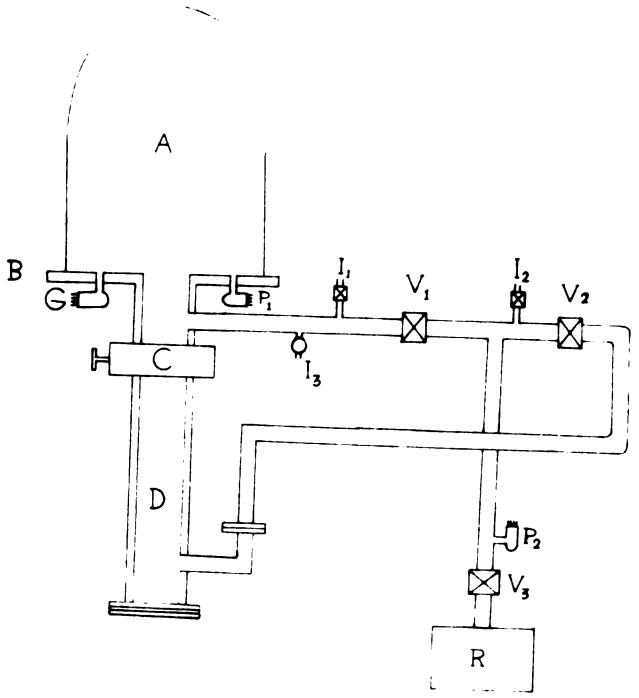

Figure 6.1 Layout of the vacuum coating unit. A, Vacuum chamber; B, Base plate; C, High vacuum valve; D, Diffusion pump; R, Rotary pump; G, Penning gauge; P_1 and P_2, Pirani gauge heads; V_1, Roughing valve; V_2, Backing valve; I_1, Bell jar air admittance valve; I_2, Fore pump air admittance valve; I_3, Needle valve for gas inlet.

operating temperature when the work chamber is being roughed. There is another isolation valve, called roughing valve, in the roughing line in between the work chamber and the rotary pump. When high vacuum pumping is in progress, this valve is closed and the backing valve is opened to allow the rotary pump to back the diffusion pump. The diffusion pump is protected from water failure by a water flow switch which cuts off the electrical supply to the pump heater when the water flow rate falls below the required value.

The system also contains two air admittance valves, to admit air one into the rotary pump and the other into the chamber, and a fine control needle valve to admit a controlled amount of gas or air into the chamber when required.

A neoprene tubing is included in the roughing line to reduce the transfer of vibrations from the rotary pump to the other parts of the system. All the couplings are made leak proof by demountable screw seals which compress neoprene O-rings of proper size.

b) Work chamber

The work chamber consists of a 12 inch diameter bell jar resting on a base plate. A neoprene

L gasket attached to the bell jar makes seal with the base plate. The weight of the bell jar supplies sufficient compression on the gasket to make a seal at the start of evacuation and the compression increases with the increase of vacuum in the chamber.

The base plate has provisions to accommodate various electrical feed throughs, gauge heads, thermocouples etc. The main electrical feed-throughs consist of two low-tension, heavy current teflon-insulated metal leads, a high tension teflon-insulated metal lead and multi-filament feedthroughs for substrate heater, electrical measurements etc. Gauge heads, both Penning and Pirani, are attached to the base plate through proper demountable adapters. A source shutter which can be operated by an external lever is also attached to the base plate through a Wilson seal.

The work chamber is equipped with a work-holder mounted on a tripod and positioned above the base plate. The supports for filaments or boats are attached to the LT lead-ins and to the earth points. The dc high tension discharge cleaning unit in the chamber consists of a shielded annular ring of super

pure aluminium supported by the tripod. There is also a baffle plate within the tripod just above the base plate. Provision is also made in the chamber to adjust the distance between the source and the substrate. The lay-out in the work chamber is as in figure 6.2. Whenever a single source is used, it is usually positioned vertically below the centre of the workholder. When two sources are required, they are fixed side by side at the centre with a screen in between them. A LT electrode selector switch makes consecutive evaporation possible.

c) Measurement of vacuum

Pressure in the range 1 to 10^{-3}Torr is indicated by a Pirani gauge having two heads, one attached to the roughing line and the other to the base plate. A selector switch makes the measurement of pressure at the required gauge head possible. Higher vacuum in the chamber can be measured with a Penning gauge capable of measuring upto 10^{-6}Torr.

d) Ultimate pressure

There are various factors like leakage from outside, outgassing from the inner walls of the chamber and of the sealing materials, and presence of water vapour and light gases which determine the ultimate

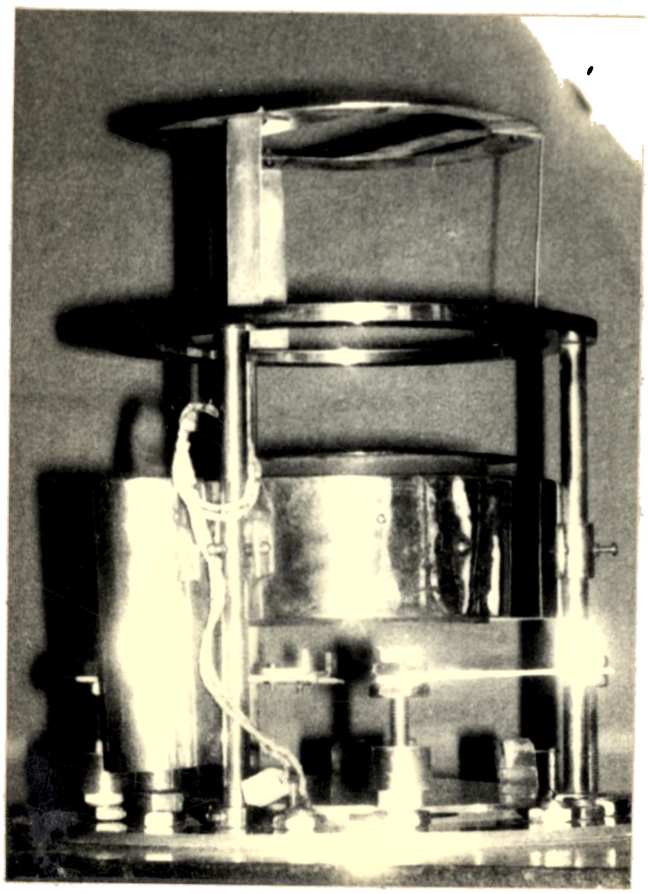

Figure 6.2 Layout in the work chamber.

pressure in the chamber. In an air tight system the rise of pressure due to leakage from outside is small. The outgassing rate in the system has been found to decrease to a certain extent after keeping it in vacuum for several hours. The presence of a moisture trap like P_2O_5 trap decreases the water vapour content considerably. Therefore, a P_2O_5 trap has been kept in contact with the work chamber and the chamber has been kept in vacuum for several hours before the operation of the diffusion pump. This process has been found to improve the pumping speed of the system and to produce higher ultimate vacuum.

6.2 Film Deposition

a) Evaporant materials

As purity is an important factor which affects the properties of films, high purity materials have been used in the study. Good electrical conducting metals aluminium (99.999 %), copper (electrolytically prepared), gold (22 caret), indium (better than 99.95 %) and silver (99.999 %) and a semimetal bismuth (99.999 %) have been used for the investigation.

b) Evaporation sources

For the evaporation of materials a source is required in a vacuum system to support the evaporant and to supply the heat of vaporisation. The operating temperature for any particular material is estimated on the basis that a vapour pressure of 10^{-2}Torr must be established to produce useful condensation rates. So the sources have to maintain the charge at a temperature sufficiently high to produce the desired vapour pressure. In order to avoid the contamination of the deposits, the vapour sources should also have negligible vapour pressure and dissociation pressure at operating temperatures. Further, the materials should be available in the desired shape and amenable to different forms of heating. Considering all these requirements, the refractory metals are found to be the suitable ones.

Taking into account the melting point of the metals evaporated, the temperature at which their vapour pressure reached 10^{-2}Torr, the wetting and reactions of the metals with different source materials, tungsten filaments were selected for the evaporation of aluminium and molybdenum boats for all other metals. The molybdenum boats were made from foils of length 4 cm, breadth 0.6 cm

and thickness 0.001 cm. A small dimple was made at the centre of the foil by pressing in order to keep the charge required for evaporation.

c) Substrate

Glass is an excellent substrate material for thin metal films and can be cleaned to a higher degree than is possible with most other substrates. Glass substrates also possess high electrical insulation property. So optically plane microscope glass slides of size 7.5 cm x 2.5 cm x 0.12 cm were used as substrates. Microscope cover glass slides were also used as thinner substrates.

d) Substrate cleaning

Cleanliness of the substrate surface has definite and decisive influence on the growth and adhesion of films. Contaminants which are found frequently on substrates are dust, lint, finger prints, oil etc. Various cleaning procedures have been given in the literature.[157,158,175-178]

The cleaning process requires the breaking of bonds between contaminent molecules and that between the contaminents and the substrate. This may be done by chemical means as in solvent cleaning or by

supplying sufficient energy to the contaminents by heating or by glow discharge. For solvent cleaning various solutions of acids, alkalies and organic solvents are used. To increase the rate of contaminent removal heating and ultrasonic agitation of the solvent are generally employed.

After trying several chemical methods initially, a cleaning method was finally adopted in which chemical, ultrasonic and ion bombardment cleanings have been combined. The glass substrates were scrubbed several times with fine cotton in a strong teepol solution. They were then cleaned with distilled water and treated with iso-propyl alcohol and acetone until the majority of contaminents have been removed as tested by the absence of breath figures. Then they were cleaned ultrasonically in distilled water. The substrates were then dried in a gentle blow of hot air. They were then subjected to uniform heating at a temperature of the order of 150°C and removed straight to the work chamber where they were subjected to ion-bombardment. This ion bombardment cleaning, besides removing impurities, makes many beneficial changes on the substrate surface such as modification of glass surfaces through the addition of oxygen and enhanced nucleation during subsequent film deposition.[17]

e) Film preparation

Two different procedures were adopted in the preparation of the samples depending on whether they are film-electrode combination or bilayers.

(i) Electrode-specimen film combination

Only good electrically conducting materials were used in the preparation of electrode-film combinations. To prepare the films, two well-cleaned glass substrates were placed on the work holder together with proper masks. The masks were of equal size and covered a length of 4 cm. in the middle of the substrate leaving the two ends exposed for the deposition of the electrode film. Another substrate, partially covered with a mask, was also placed along with the others in order to determine the thickness of the film. The material for the electrode film, an amount sufficient to produce a thickness of the order of 3000 $\mathring{A}$, was loaded on the evaporant source and evaporated to completion in a vacuum better than 10^{-5} Torr.

One of the film was then removed from the chamber, placed in an evacuated desiccator and kept at room temperature. Silicagel was used in the desiccator to avoid the effect of moisture on the film.

The other film was kept in a vacuum system, evacuated to a pressure less than 10^{-4}Torr and heated gradually to a temperature of the order of 150°C by radiation heating. The film was annealed at this temperature for one hour and then cooled slowly to the room temperature.

The two electrode films, both annealed and unannealed, were taken out and placed symmetrically together with two identical masks, on the workholder of the coating unit. The masks exposed a rectangular surface of length 5 cm. and width 0.5 cm. at the centre of the substrate. After evacuating the chamber the specimen film was deposited in a vacuum better than 10^{-5}Torr. The films were then taken out for electrical measurement.

While gold, silver, copper and aluminium were used for the electrode films of aluminium specimen film, indium was used as the electrode film of gold, silver, copper and aluminium specimen films. The thickness of the specimen films were adjusted to be $\sim$ 1200 Å in the case of aluminium, $\sim$ 1150 Å for gold, $\sim$ 850 Å for silver and $\sim$ 1150 Å for copper.

(ii) Bismuth-silver bilayer films

The bilayer films of the semimetal bismuth and the good conductor metal silver were prepared by evaporating the materials from two sources kept side by side and separated from each other by a screen. The evaporation is done sequentially in the same pump down without much delay between the two evaporations. The thickness of the individual layer in the bilayer film varied in two different ways:

1) the thickness of the bismuth underlayer varied from 1000 Å to 2000 Å keeping the thickness of the silver overlayer at a constant value of the order of 50 Å.

2) keeping the total thickness of the bilayer film a constant ($\sim$ 1000 Å), the thickness of the silver overlayer varied upto 900 Å.

Bismuth films of thickness ranging from 1000 Å to 2000 Å were also prepared to compare the properties of the films with those having a silver overlayer of thickness $\sim$ 50 Å.

To ensure uniform film thickness, the source to the substrate distance was kept fairly large ($\sim$ 27 cm).

6.3 Film Thickness

a) Control of film thickness

Considering the thickness distribution given by Holland,[154] thickness t of a deposit from a small plane source is given by the equation

$$t = \frac{m \cos\theta \cos\beta}{\pi \rho r^2} \qquad 6.1$$

where m is the total mass of material evaporated, θ is the angle between the normal to the plane source and the line between the source and the receiving surface, β is the angle between the normal to the surface and the line between the source and the receiving surface, r is the distance of the surface from the source and ρ is the density of the deposit.

Assuming that the density of the film is same as that of the bulk and the vapour is incident normally on the plane surface which is parallel to the small plane source (i.e., $\theta = \beta = 0$), the thickness

$$t = \frac{m}{\pi \rho r^2} \qquad 6.2$$

By knowing the density of the material and the distance r, the amount of material m required for a particular thickness can be calculated.

On the basis of the equation 6.2 the amount of material required for a particular value of 't' was weighed with a Kerey semimicrobalance and evaporated from the source to completion. Thus the thickness of the film was approximately controlled.

b) Thickness measurement

Film thickness was measured using multiple beam interferometry of Tolansky.[180] The method of the Fizeau fringes of equal thickness and, in certain cases, the fringes of equal chromatic order (FECO) were used for the purpose.

(i) Fizeau fringes of equal thickness

To produce the fringes, a uniform, opaque and high reflectivity coating is required on the surface having a sharp step between the substrate surface and the film surface. The Fizeau interferometer can be formed by placing a semisilvered reference plate called Fizeau plate on top of the step at a small angle to the substrate surface and the reflecting surfaces facing

each other. By illuminating the interferometer with a collimated monochromatic light, the fringe system can be viewed in a microscope. The arrangement is as in figure 6.3a and the fringes produced are as in 6.3b.

The distance between two successive dark fringes corresponds to $\lambda/2$, λ being the wavelength of the monochromatic light. At the step the fringe system is displaced by an amount d as shown in figure 6.3b and the displacement is proportional to the film thickness t. The film thickness t is given by

$$t = \frac{d}{D} \cdot \frac{\lambda}{2} \qquad 6.3$$

where D is the fringe spacing.

(ii) Fringes of equal chromatic order

The arrangement to produce fringes of equal chromatic order is similar to that of Fizeau fringes. The monochromatic source is replaced by a white source and the reflected light is focused on the entrance slit of a spectroscope. The fringes can then be observed in the spectroscope. The schematic diagram of the interferometer and the appearance of fringes are as in figure 6.4.

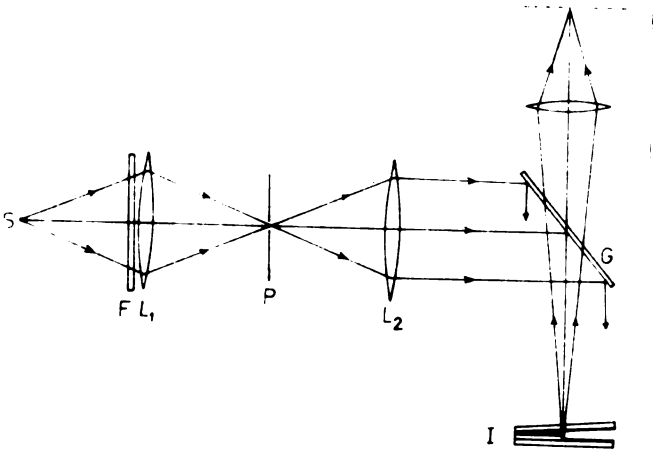

(a)

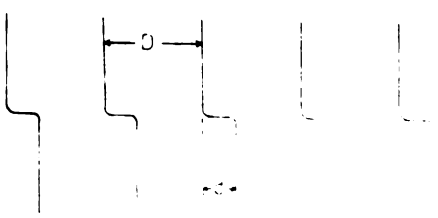

Figure 6.3a. Interferometer arrangement for Fizeau fringes of equal thickness S, source; F, Filter; L_2, collimating lens; P, Pinhole; G, Semisilvered glass plate; I, Interferometer; H, Image plane.

b. Fringes produced by the interferometer D, Fringe spacing; d, Fringe shift.

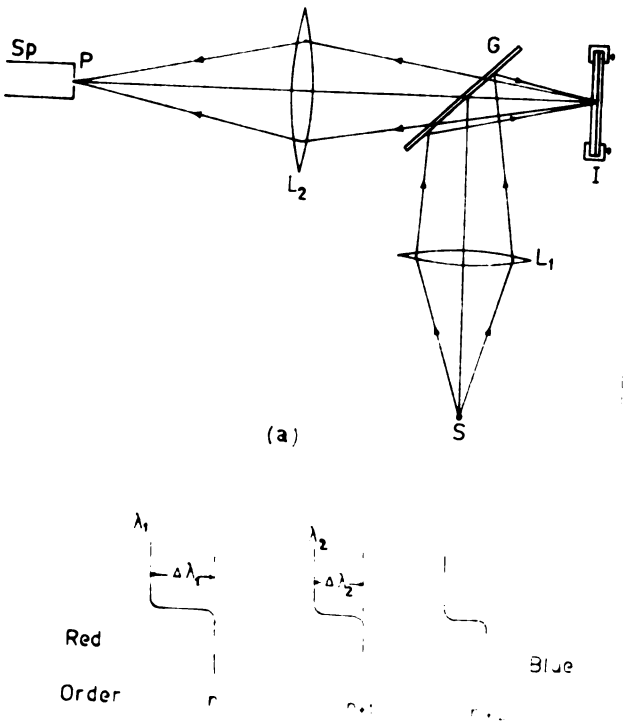

Figure 6.4 a. Interferometer arrangement for fringes of equal chromatic order. S, Source; L_1, Condensing lens; L_2, Projection lens; G, Glass plate; I, Interference plates; Sp, Spectroscope; P, Slit of the spectroscope.

b. Fringes of equal chromatic order.

Considering two fringes corresponding to λ_1 and λ_2 having a fringe shift $\Delta\lambda$, as shown in figure 6.4b, the thickness of the film t is given by

$$t = \frac{\lambda_2}{2} \quad \frac{\Delta\lambda}{\lambda_1 - \lambda_2} \qquad 6.4$$

λ_1, λ_2 and $\Delta\lambda$ can be measured with the spectroscope and t can be calculated.

To determine the thickness of a film, the substrate having the film with a step was placed on the work holder and a thick uniform silver layer was deposited on it. The thickness of the film was then measured using a Fizeau or a FECO interferometer. Filtered mercury green light was used as the monochromatic beam in the Fizeau arrangement.

In measuring thickness of the films the difference between the calculated value from equation 6.2 and the measured value by using an interferometer was found to be less than ten percent.

6.4 Resistance Measurement

In the present investigation, the resistance of the film-electrode combination was very small compared to

that of the bismuth-silver bilayer film. So two different methods were used for the resistance measurement in the two cases. In the later case a direct measurement of resistance was done while in the former case an indirect determination of resistance from the potential and current measurement was used.

a) Film-electrode combination

The resistance of the films having annealed or unannealed electrodes was determined by measuring the potential across the film and that across a standard 10 ohm resistance. After attaching pressure contacts made of copper to the electrode films as in figure 6.5a, the specimen film, a standard 10 ohm oil-immersed resistance and an adjustable resistance were connected in series to a stabilised DC power supply. To measure the potential across the film and the standard resistance, necessary connections were also given to the proper terminals of an OSAW vernier potentiometer of accuracy 10^{-7} volt div.$^{-1}$ as shown in figure 6.5b.

Two films, one having annealed electrodes and the other having unannealed electrodes, were transferred to a thick walled desiccator and kept side by

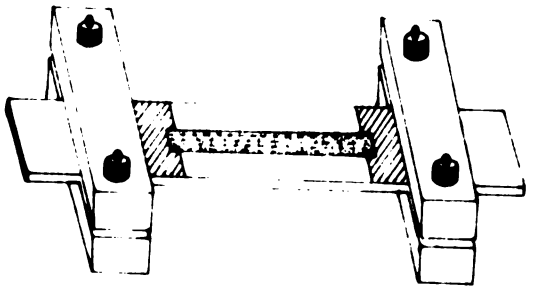

(a)

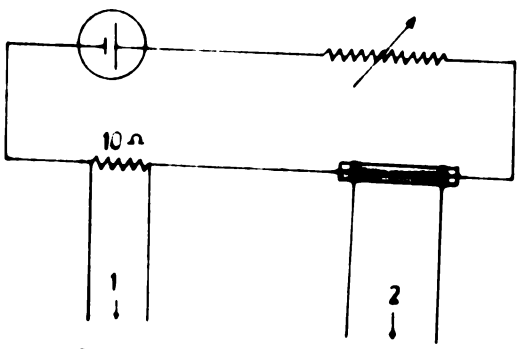

(b)

Figure 6.5 a. Schematic diagram of film-electrode combination with pressure contacts.

b. Circuit for electrical resistance measurement.

side. Contact with the atmosphere was given only through a small hole of 3 mm. diameter. This arrangement was giving the films a controlled and constant contact with atmosphere. The arrangement also prevented sudden temperature changes in the film environment.

Resistance measurements of the films were made at intervals of time and continued for more than 360 hours. The percentage variation of resistance of the films was then related to time.

b) Bilayer films

U-shaped pressure contacts were attached to the films in such a way that the effective length of the films remained to be 3 cm. Resistance of the films were measured using a Marconi Universal Bridge Model TF 2700. Either the DC supply or the 1 kilocycle oscillator of the Bridge was used for the measurement.

Resistance of the films were measured at various temperatures ranging from room temperature to about 180°C, keeping them in a vacuum of the order of 10^{-4} Torr.

6.5 Heat Treatment

The electrode films and the bismuth-silver bilayers were given heat treatment in a vacuum of the

order of 10^{-4}Torr. The heating was done by radiation heating from filament heaters pressed in between copper plates (size 15 cm x 15 cm x 0.5 cm). The samples were kept at a distance of 1 to 2 cm. below the heater and heated radiantly through the back of the substrate, the temperature being controlled with a temperature controller.

A chromel-alumel thermocouple was used to measure the temperature of the film. The thermocouple wires were taken into the chamber through vacuum seals and the junction was pressed onto the glass substrate surface, as near to the film as possible.

The potential difference was measured with a voltage recorder of accuracy 0.2 millivolt cm^{-1}. By knowing the room temperature and the potential difference, the temperature of the specimen was determined from the standard potential-temperature chart.

After making necessary electrical connections and attaching the thermocouple to the substrate, the films were placed in the annealing chamber below the heater. After evacuating the chamber to a pressure of the order of 10^{-5}Torr, the films were heated by

passing electric current through the heater. The current was controlled by a variac. The temperature of the film was determined from the potential of the thermocouple read from the voltage recorder.

In the case of electrode films, the films were annealed at a temperature of the order of 150°C for about one hour. They were then cooled to room temperature before taking them out of the chamber.

In bilayer films having a constant silver layer thickness $\sim$ 50 Å, a film, after attaching contacts and electrical connections for resistance measurement, was placed in the chamber and the chamber evacuated. The film was then slowly heated to 160°C and annealed for more than one hour above that temperature. After cooling to room temperature, its resistance was measured. Then slowly heating the film, its resistance was again measured at intervals of 10°C rise in temperature till the temperature reached above 160°C.

The same process of heating and measurement of resistance was done in the case of pure bismuth films.

After evacuating the chamber the resistance of the double layer films having $\sim$ 1000 Å bilayer

thickness and varying individual layer thickness was measured. The film was then heated and its resistance measured at intervals of 10°C till the temperature reached above 150°C. The film was kept at that temperature for more than one hour and then slowly cooled to room temperature determining its resistance during the cooling process.

6.6 Bilayer Films - Annealed at Room Temperature

Bismuth-silver bilayer films of varying layer thickness have been prepared and kept at room temperature for several days. The silver layer thickness varied from 50 Å to 900 Å. The films were kept in atmosphere or in desiccators and their surface features observed at intervals of time. The general nature of the variation of resistance of these films with time was also studied.

6.7 Surface Features

Surface features of the films have been studied under reflected light using a Karl Zeiss metallurgical microscope provided with microphotograph attachments. The electrode-film combinations were examined after completing all electrical measurements. The bilayer films were examined before and after subjecting them to

heat treatment. The surface features of the double layer films were also examined at various stages of their room temperature annealing.

6.8 X-ray Diffraction

Structure of the bilayer films were studied by X-ray diffraction technique using a 90 mm diameter Debye-Scherrer camera. Filtered Cu K_α radiations produced at 20KV and 10 milliamperes filament current were used for the study.

Specimens on thin cover glass slides were used for the study of films in the as-deposited form. X-rays were allowed to fall on the surface of these samples at normal incidence. Film material scraped from the substrate and filled in thin-walled cellophane tubes was also used for the diffraction study.

A 10 to 11 hour exposure time was found to be sufficient to obtain a good powder photograph of the specimen. Weak lines due to Cu K_β were also found along with the K_α lines.

CHAPTER SEVEN

RESULTS AND DISCUSSION

7.1 Results

The present investigation mainly consists of the effect of electrode films on the electrical conductivity of metal films and the influence of silver overlayers on the conductivity of bismuth films.

A. Electrode-film combinations

Only films of good electrical conductor materials were used for the study. Aluminium films were deposited onto glass substrates having annealed and unannealed gold, silver, aluminium or copper electrodes. Similarly films of gold, silver, copper and aluminium were deposited on electrodes of indium. In all the cases the percentage variation in resistance with time for various film-electrode combinations were determined and the films with annealed electrodes were compared with those having unannealed electrodes. In most of the cases the films with annealed electrodes showed a marked difference from those with unannealed electrodes.

a) Aluminium films with gold electrodes

Figure 7.1 shows the percentage variation in resistance of aluminium films with gold electrodes as a function of time. The films with annealed and unannealed electrodes showed a gradual increase in resistance with time. The rate of increase in films with annealed electrodes was very large compared to that in films with unannealed electrodes. In 200 hours the resistance of films with annealed electrodes increased more than 90 percent of its original value. But, by that time, the films with unannealed electrodes showed only a very small increase—of the order of 5 percent.

Microscopic observations also revealed difference at the film-electrode junction. Films with annealed electrodes showed microdiscontinuities as in figure 7.2 on the surface of the overlapping junction at the positive end. But films with unannealed electrodes did not show any such distinguishable features.

b) Aluminium films with silver electrodes

The percentage variation of resistance with time of two identical aluminium films, one with annealed electrodes and the other with unannealed electrodes

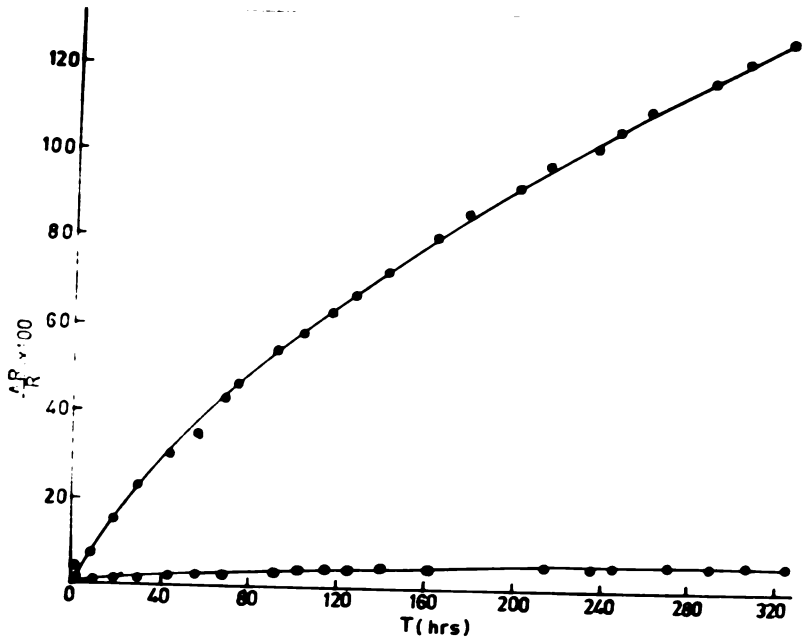

Figure 7.1 $\frac{\Delta R}{R}$ x 100 Vs. time - Al film with Au electrodes. O, Unannealed electrodes; ●, annealed electrodes.

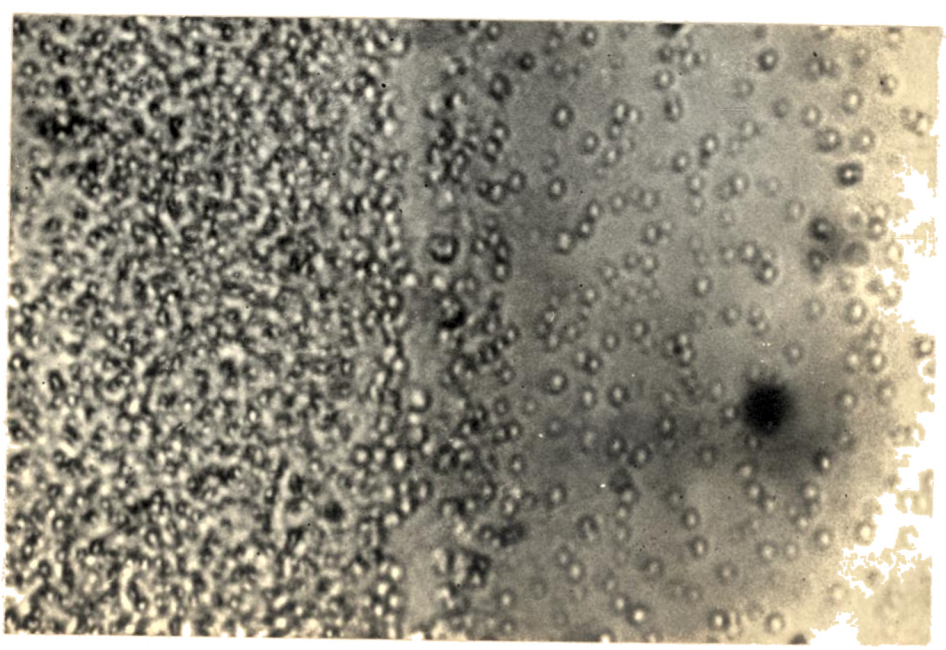

Figure 7.2 Microdiscontinuities at an annealed Au electrode-Al film junction. The overlapping region is at the left (1800 x).

were as in figure 7.3. As in the case of aluminium films with gold electrodes, films with annealed silver electrodes showed greater variation of resistance with time. However, the variation in the case of films with silver electrodes is only about 48 percent after 200 hours. In films with unannealed electrodes the variation was only around 8 percent, a little more than that observed in films with unannealed gold electrodes.

Surface features in these films were also similar to that in films with gold electrodes. Micro-discontinuities were observed at the positive end of the film-electrode junction of the films with annealed electrodes.

c) Aluminium films with aluminium electrodes

Aluminium films with annealed aluminium electrodes and those with unannealed electrodes showed similar resistance variation with time as in figure 7.4. In both the cases the resistance variation was found to be very small. After 200 hours the resistance variation was found to be only about 5 percent in the case of films with unannealed electrodes and about 4 percent in films with annealed electrodes. However, the films with

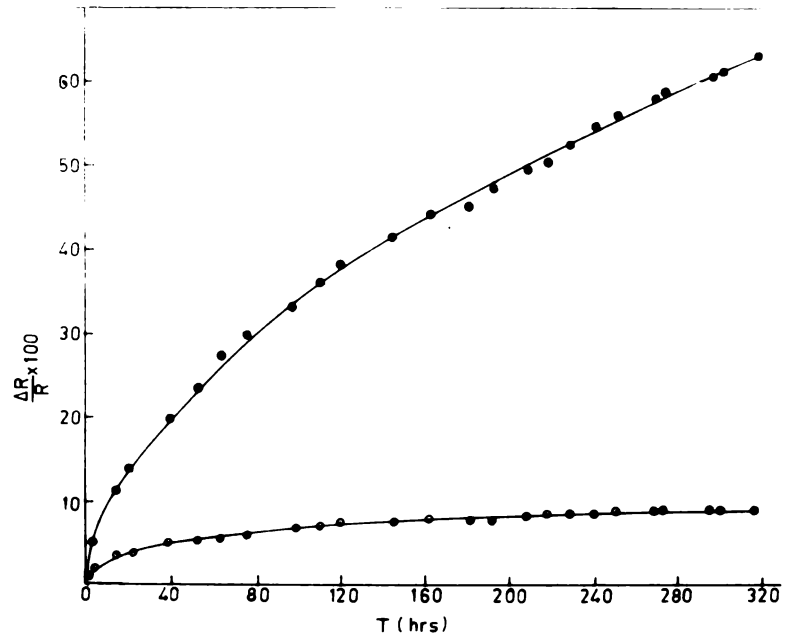

Figure 7.3 $\frac{\Delta R}{R}$ x 100 Vs. time—Al film with [illegible] electrodes. ○, Unannealed electrodes; ●, annealed electrodes.

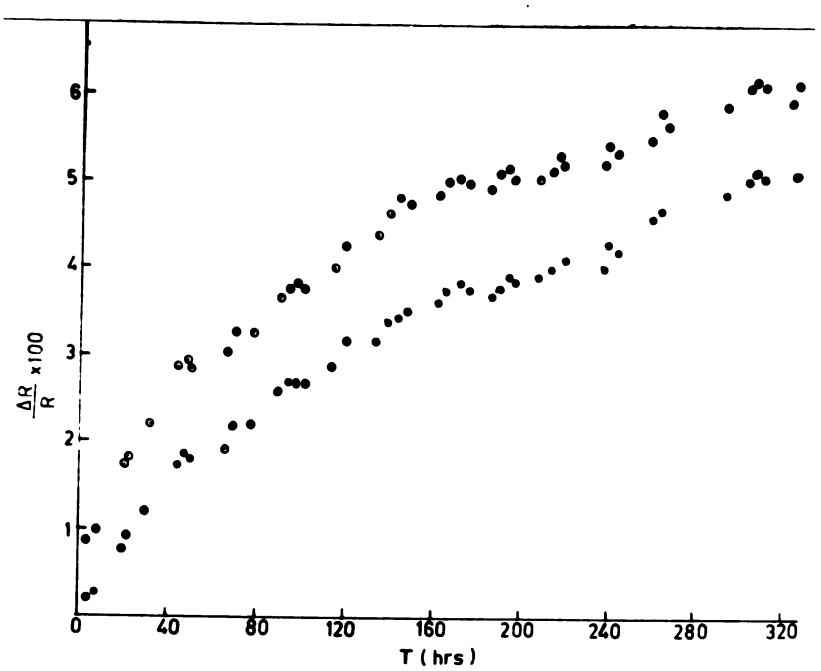

Figure 7.4 $\frac{\Delta R}{R}$ x 100 Vs. time—Al film with Al electrodes. ○, Unannealed electrodes; ●, annealed electrodes.

unannealed electrodes showed a larger increase of resistance for the first few hours as can be seen from figure 7.4. But afterwards both the curves appear to be almost parallel. Instead of a smooth, continuous change the films showed fluctuations in the resistance variation with time.

Microscopic observations revealed no noticeable change in the film-electrode junctions of these films.

d) Aluminium films with copper electrodes

The variation of resistance in aluminium films with copper electrodes is entirely different from that observed in aluminium films with gold or silver electrodes. While in the case of gold and silver electrodes the films with annealed electrodes showed greater percentage variation of resistance, in copper electrodes the films with unannealed electrodes showed larger increase of resistance with time. A few hours after the deposition, the resistance of these films with unannealed electrodes began to increase rapidly as shown in figure 7.5. Within 50 hours the resistance increased more than 600 percent, whereas the increase in films with annealed electrodes remained to be very small, about 15 percent.

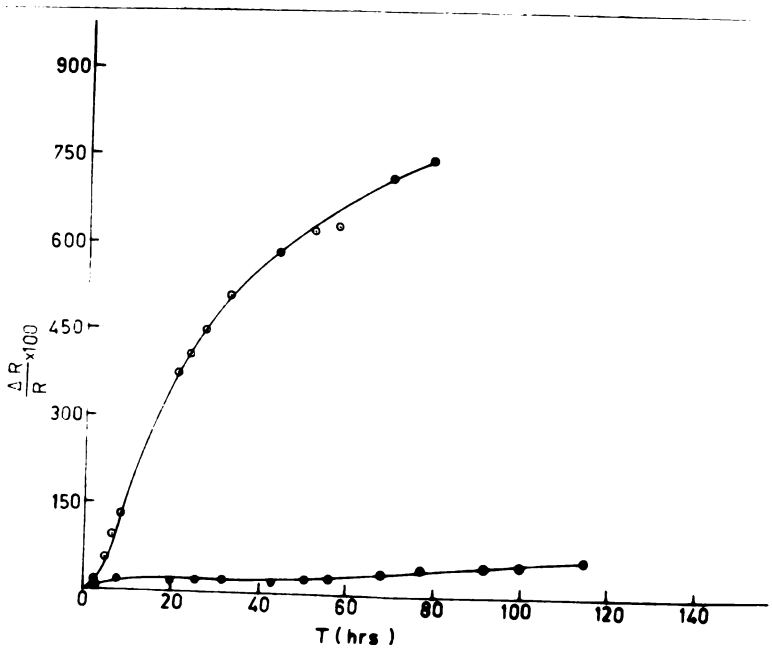

Figure 7.5 $\frac{\Delta R}{R}$ x 100 Vs. time--Al film with Cu electrodes.
O, Unannealed electrodes:, ●, annealed electrodes.

In films with unannealed copper electrodes microscopic examination revealed the presence of striations in the overlapping region at the positive end of the film (figure 7.6). These striations were parallel to the direction of the applied electric field, along the length of the aluminium film.

e) Gold films with indium electrodes

Resistance of gold films with annealed and unannealed electrodes decreased with increase of time. Their percentage variation with time was as in figure 7.7. The rate of variation was more in films with unannealed electrodes. While films with annealed electrodes had about 4 percent variation after 100 hours, films with unannealed electrodes had about 6 percent decrease.

Microscopic observations revealed that the films with annealed electrodes had a sharper electrode - film junction compared to those with unannealed electrodes (figure 7.8).

f) Silver films with indium electrodes

Like gold films, silver films also showed a decrease of resistance with time. As shown in figure 7.9, the resistance variation of silver films was large

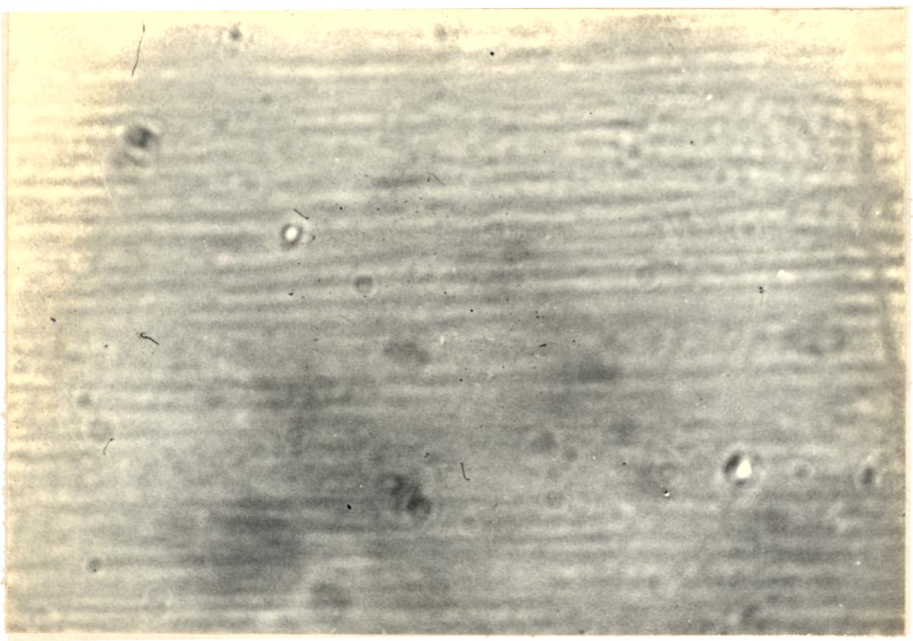

Figure 7.6 Striations on an unannealed Cu electrode-film junction (1800 x).

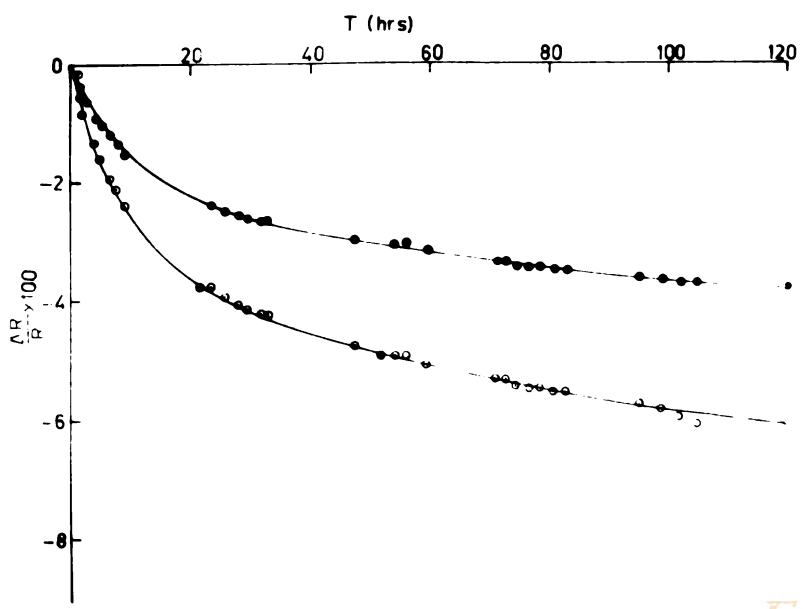

Figure 7.7 $\frac{\Delta R}{R}$ x 100 Vs. time—Au film with In electrodes. O, Unannealed electrodes; ●, annealed electrodes.

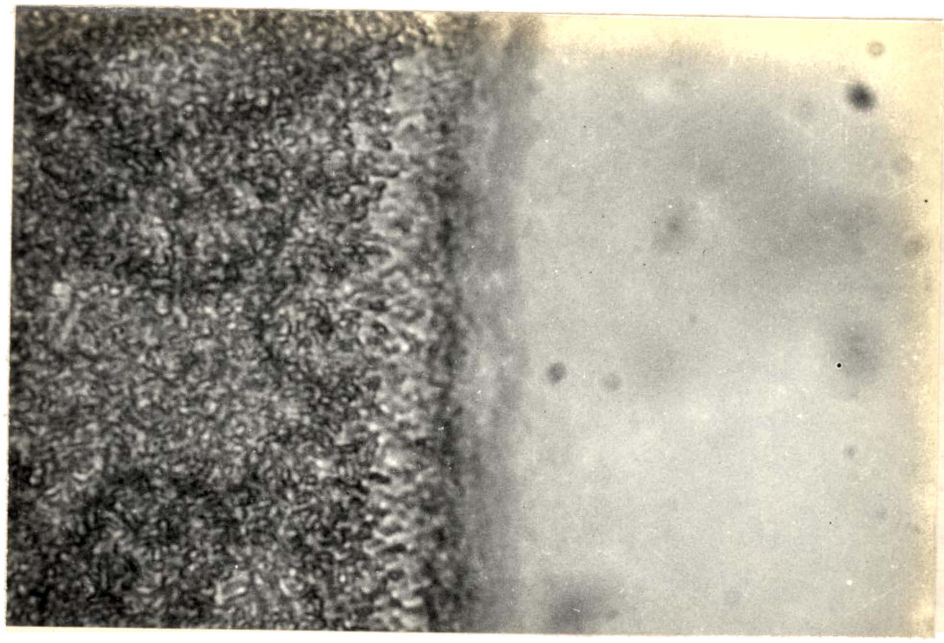

Figure 7.8 Sharp electrode-film junction--Au film with annealed In electrodes. Electrode region at the left (1800 x).

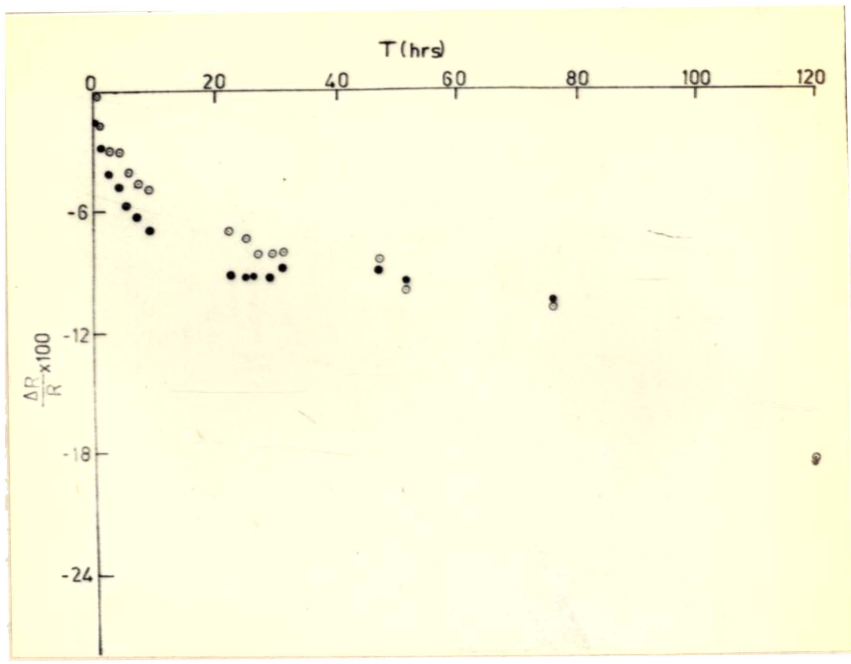

Figure 7.9 $\frac{\Delta R}{R}$ x 100 Vs. time--Ag film with In electrodes. O, Unannealed electrodes; ●, annealed electrodes.

compared to that of gold films. After the initial difference in the variation for the first few hours, the resistance variation of the films with annealed and that of films with unannealed electrodes tend to equalise, as can be seen from the figure.

As in the case of gold films with indium electrodes, silver films also showed a rather sharp electrode-film junction. In films with unannealed electrodes, there was a cluster formation close to the negative electrode-film junction and separated from the electrode edge (figure 7-10). The density of this cluster decreased gradually to either side of it along the length of the film.

g) Copper films with indium electrodes

Unlike gold and silver films, copper films with indium electrodes showed an increase in the percentage variation of resistance with time (figure 7.11). But this increase in films with annealed and unannealed electrodes was very small. After the initial increase and the following decrease, their resistance slowly increased in an oscillatory manner. The resistance variation was almost equal in both the cases.

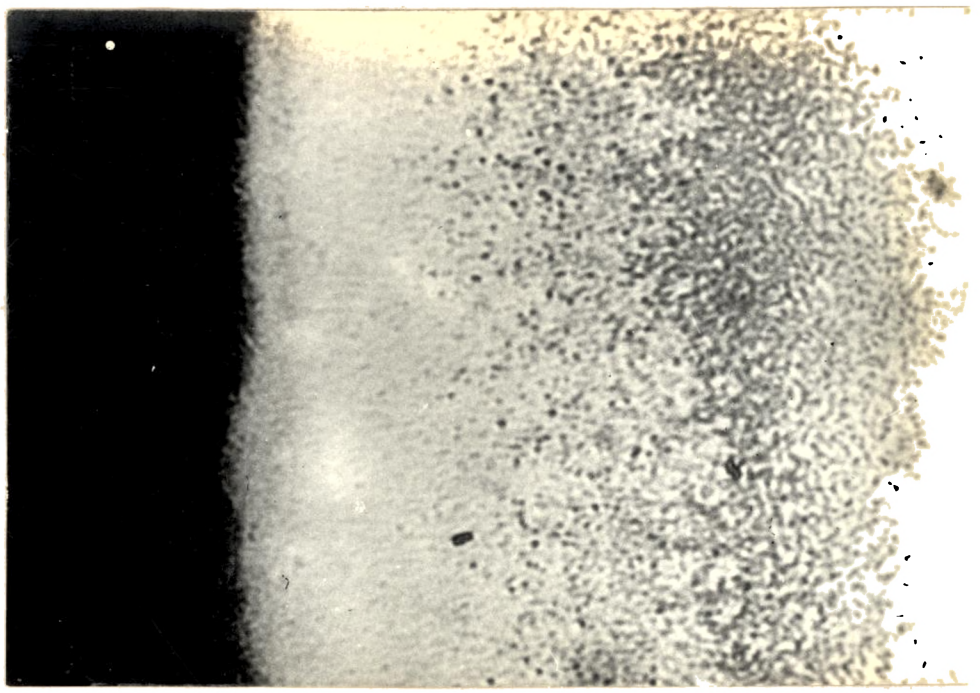

Figure 7.10 Cluster formation in Ag film near the negative film-electrode junction (unannealed). Electrode region at the left (1800 x).

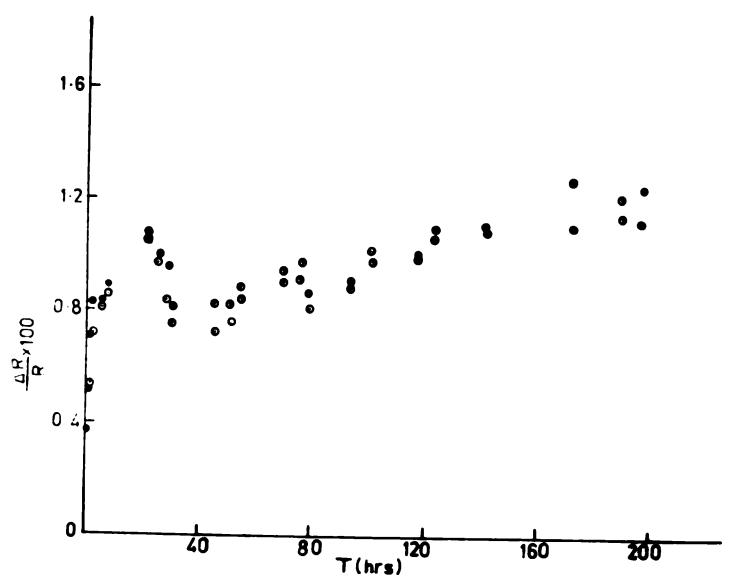

Figure 7.11 $\frac{\Delta R}{R}$ x 100 Vs. time--Cu film with In electrodes. O, Unannealed electrodes; ●, annealed electrodes.

The film-electrode junction of copper films was different from that of gold and silver films. In copper films the junction was rather spread out irrespective of whether the electrodes were annealed or not (figure 7.12).

h) Aluminium films with indium electrodes

The percentage variation of resistance in aluminium films with indium electrodes was as in figure 7.13. In these films there was an appreciable increase in resistance. The films with unannealed electrodes had a smaller initial resistance compared to those with annealed electrodes. But their resistance increased non-uniformly to very high values. Within 160 hours their resistance had gone as high as greater than 1100 percent. But the increase of resistance in films with annealed electrodes was gradual and uniform. In these films the increase was only of the order of 50 percent after 160 hours.

B. Bilayer films

B.1 Bismuth films having very thin ($\sim$ 50 Å) overlayer film of silver

In this part of the study, the effect of a silver overlayer of thickness about 50 Å on the resistance of bismuth films has been investigated and in each

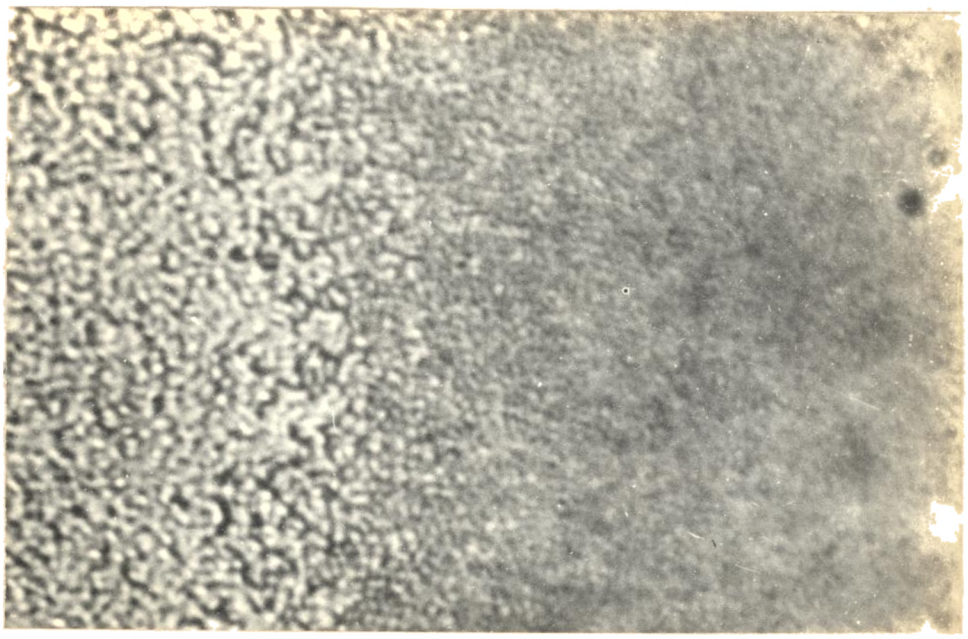

Figure 7.12 Spread out electrode film junction—Cu film with In electrodes. Electrode region at the left (1800 x).

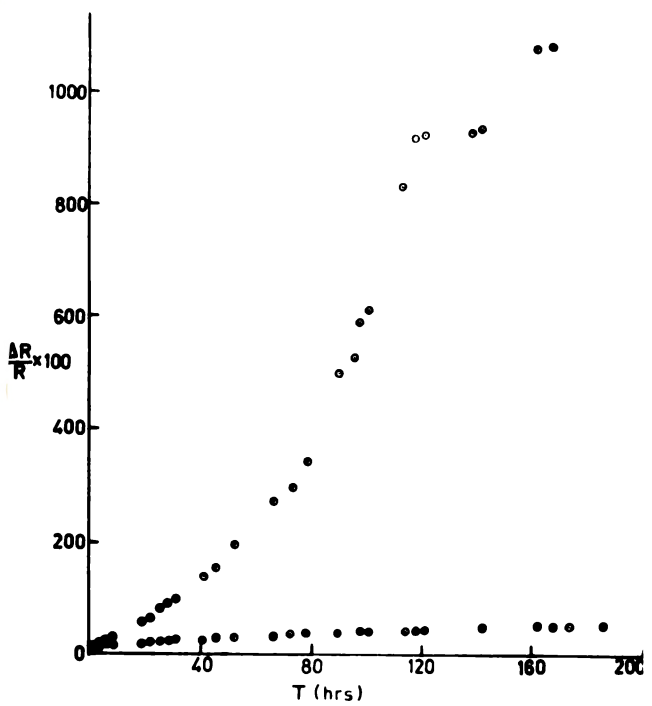

Figure 7.13 $\frac{\Delta R}{R}$ x 100 Vs. time—Al film with In electrodes. O, Unannealed electrodes; ●, annealed electrodes.

case the $R_{T/R}$, where R_T is the resistance of a film at a temperature T and R that at room temperature, was related to the temperature of the film. This $R_{T/R}$ variation with T has been compared with that of pure bismuth films of the same dimensions.

The resistance of bismuth films with an overlayer of silver was more than that of a pure bismuth film of the same bismuth layer thickness and surface area. The variation of room temperature sheet resistance with thickness of films was as shown in figure 7.14.

In bismuth films it has been observed by several investigators that they have a resistance minimum at a particular temperature and an increase in their resistance with further heating and cooling.[181-185] Like pure bismuth films, bismuth films of thickness varying from 1000 Å to 2000 Å having a thin silver overlayer showed a resistance minimum at a particular temperature and an increase of resistance with further heating and cooling.

The variation of $R_{T/R}$ with temperature for films of thickness $\sim$1000 Å, $\sim$1500 Å and $\sim$ 2000 Å having silver overlayers in comparison to pure bismuth films of same thickness were as in figures 7-15, 7-16 and 7-17 respectively. In all the cases the resistance

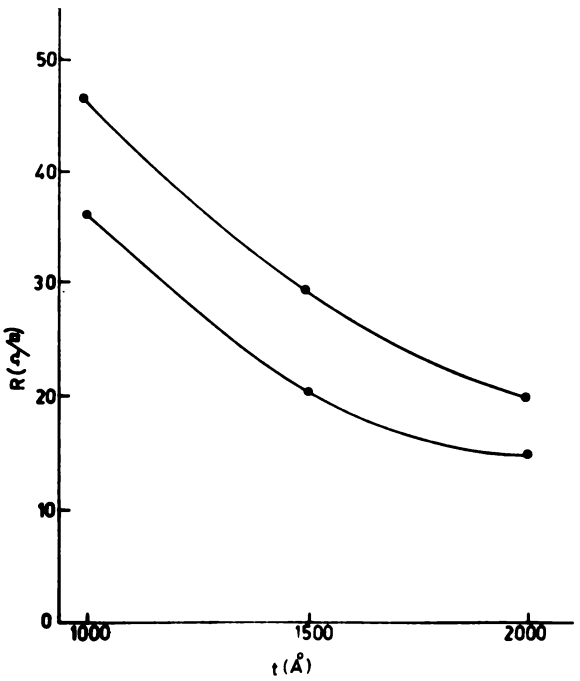

Figure 7.14 Room temperature sheet resistance Vs. thickness. ●, bismuth film; ○, bi-layer film.

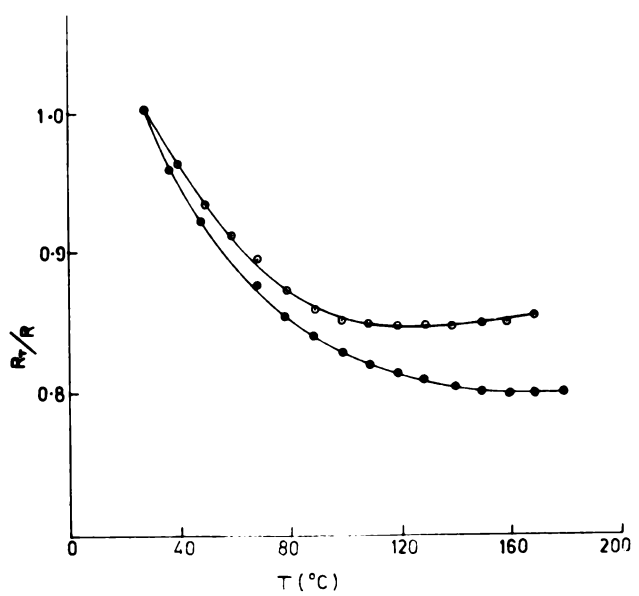

Figure 7.15 $R_{T/R}$ Vs. T — Bi thickness ~ 1000 Å. ○, Bi film; ●, bilayer film.

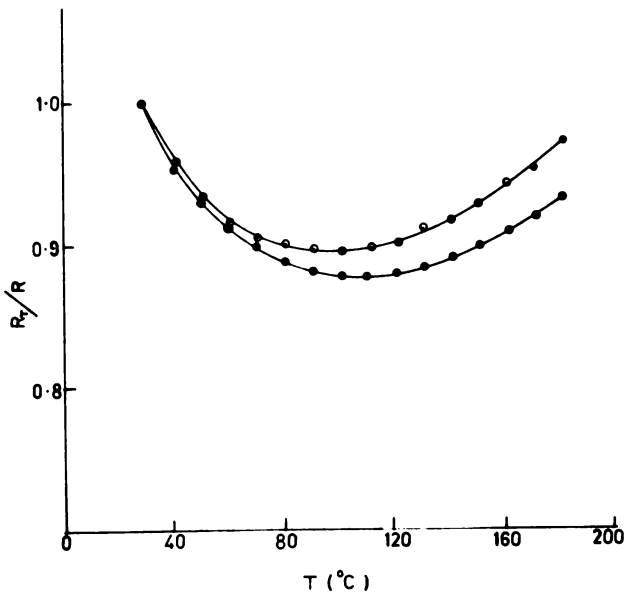

Figure 7.16 $R_{T/R}$ Vs. T — Bi thickness ~ 1500 Å.
O, Bi film; ●, bilayer film.

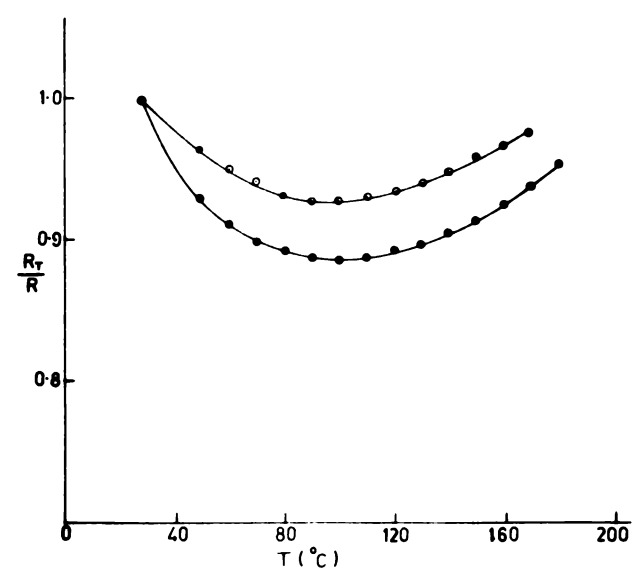

Figure 7.17 $R_{T/R}$ Vs. T — Bi thickness ~ 2000 Å.
O, Bi film; ●, bilayer film.

ratio for a particular temperature was found to be less in the case of bilayer films. The $R_{T/R}$ variation was also found to decrease with increase of thickness, as in the case of pure bismuth films. In addition to these, a shift of the resistance minimum to a higher temperature in samples with a silver overlayer was observed, even though the bismuth layer thickness remained the same. (Table 7-1). The temperature coefficient of resistance of the films were also changed as given in Table 7.2.

The films were found to be of n type by the hot probe method. X-ray diffraction studies revealed that the films were polycrystalline having no preferred orientations.

B.2 Bilayer films of varying layer thickness

a) Films annealed at higher temperature

(i) Resistance variation

As already mentioned in section 6.2 (e)(ii) the total thickness of the bilayer was kept constant ($\sim$ 1000 Å) and the silver overlayer thickness varied from zero to 900 Å. Their resistance was measured at various temperatures during both heating and cooling

Table 7-1

Temperature corresponding to the resistance minimum of films with different thickness

Thickness (Å)	$T_{minimum}$	
	Bi film (°C)	Bi film with ~50 Å Ag overlayer (°C)
1000	135	160
1500	100	110
2000	95	100

Table 7-2

Temperature coefficient of resistance at room temperature for different bismuth film thickness—with and without silver overlayer

Thickness (Å)	Bismuth film (ppm/°C)	Bi film with a ~50 Å silver overlayer (ppm/°C)
1000	-2424	-3137
1500	-2842	-3009
2000	-1474	-2732

under vacuum. The variation of resistance with temperature of the specimens, in the order of increasing overlayer thickness was as in figures 7.18 to 7.27. The resistance value and the variation of resistance were dependent on the silver overlayer thickness. The value of the initial resistance of the bilayer films was found to decrease with increasing silver layer thickness.

The resistance of pure bismuth films and that of films with 50 Å silver overlayer decreased irreversibly with rise of temperature. After annealing at a temperature above 160°C, their resistance was found to vary reversibly with temperature showing a resistance minimum (figures 7.18 and 7.19).

The resistance of bilayer films having silver layer thickness $\sim$ 100 Å, on heating, decreased first, reached a minimum around 100°C and then increased with a steep rise around 120°C. After this rise the resistance decreased to a steady value during annealing above 160°C. On cooling the resistance increased with decrease of temperature. The general nature of the resistance variation remained the same in films having silver layer thickness upto 200 Å. However, as the thickness of this

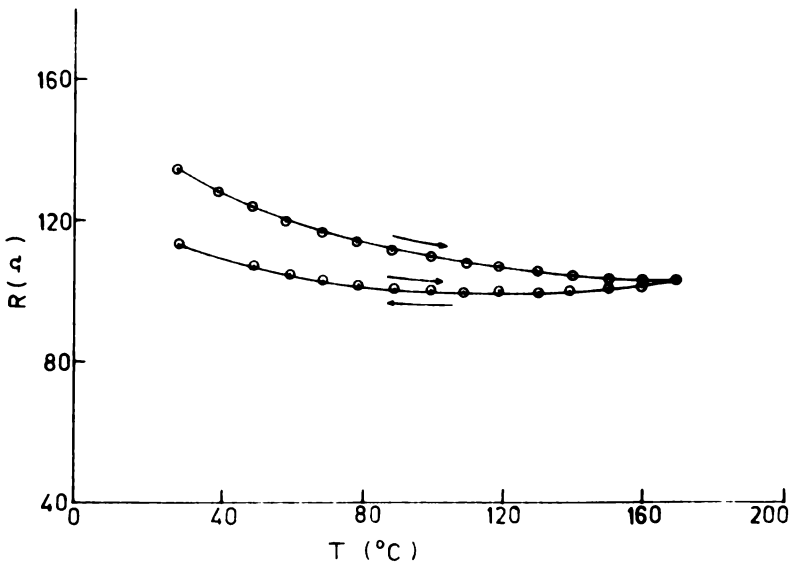

Figure 7.18 Resistance Vs. temperature (Bi ~ 1000 Å).

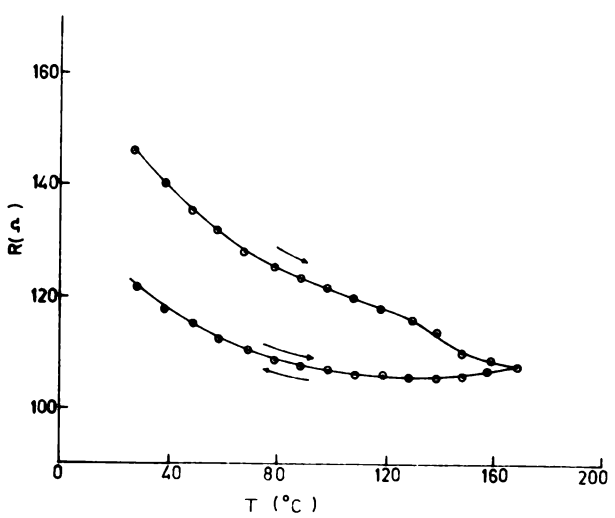

Figure 7.19 Resistance Vs. temperature
(Bi ~ 950 Å, Ag ~ 50 Å).

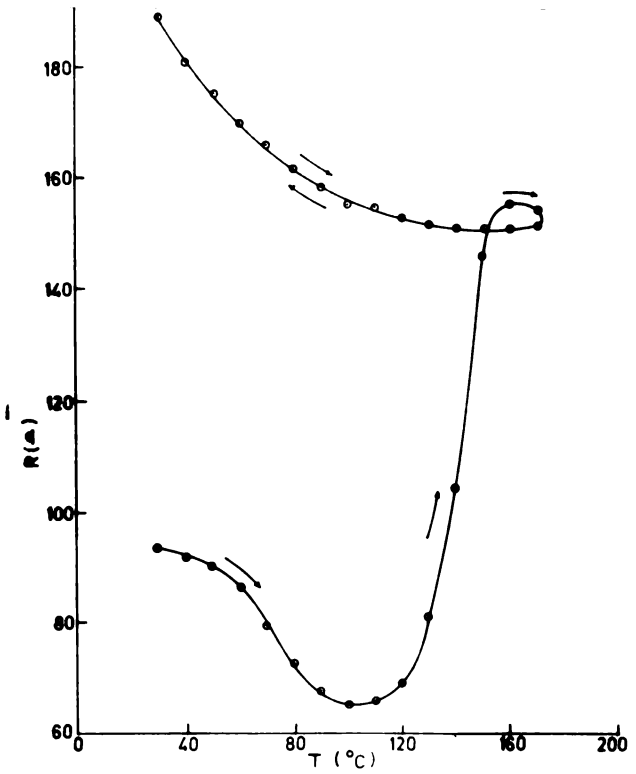

Figure 7.20 Resistance Vs. temperature (Bi ~ 900 Å, Ag ~ 100 Å)

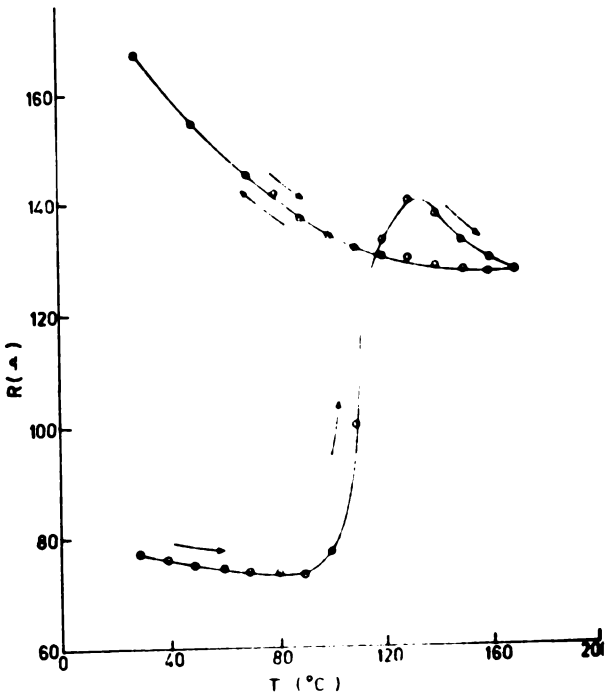

Figure 7.21 Resistance Vs. temperature (Bi ~ 850 Å, Ag ~ 150 Å).

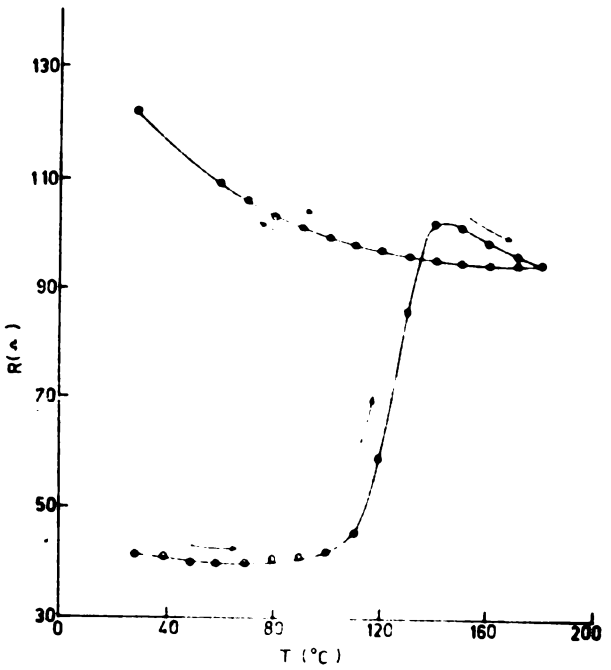

Figure 7.22 Resistance Vs. temperature
(Bi ~ 800 Å, Ag ~ 200 Å)

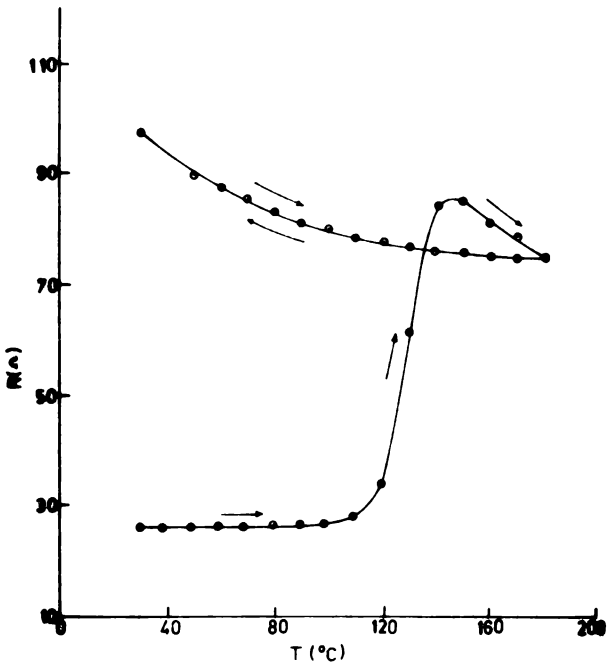

Figure 7.23 Resistance Vs. temperature (Bi $\sim$ 700 Å, Ag $\sim$ 300 Å).

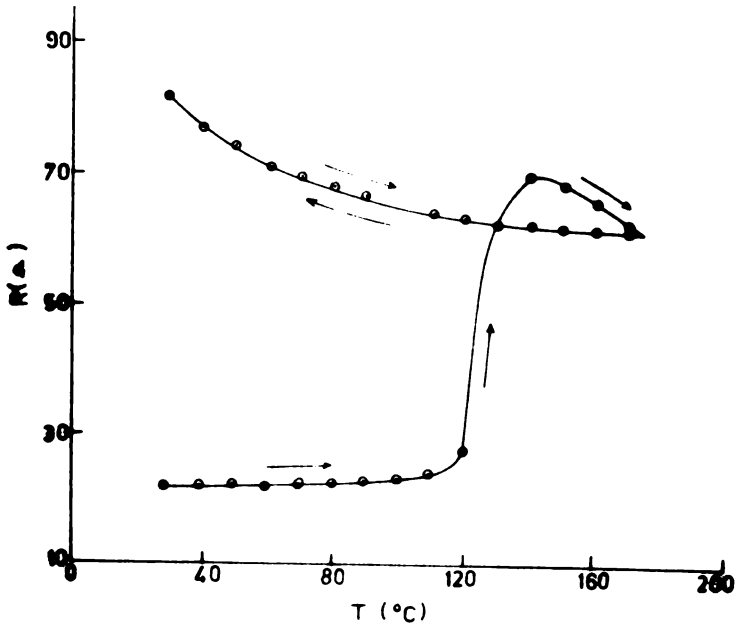

Figure 7.24 Resistance Vs. temperature
(Bi ~ 600 Å, Ag ~ [illegible] Å)

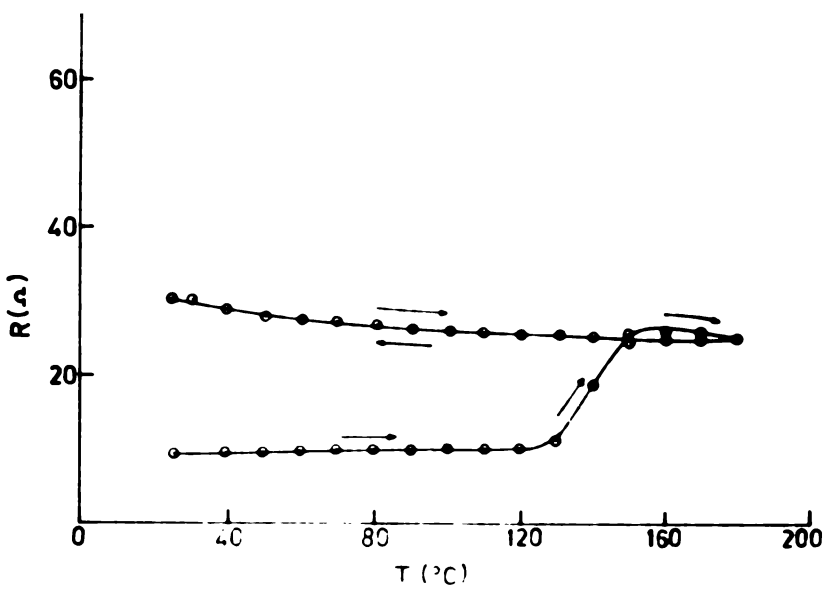

Figure 7.25 Resistance Vs. temperature
(Bi ~ 500 Å, Ag ~ 500 Å).

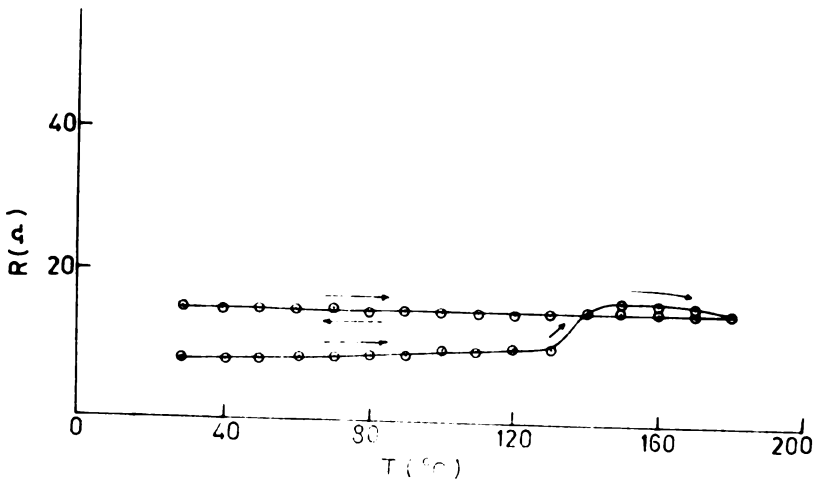

Figure 7.26 Resistance Vs. temperature (Bi ~ 400 Å, Ag ~ 600 Å).

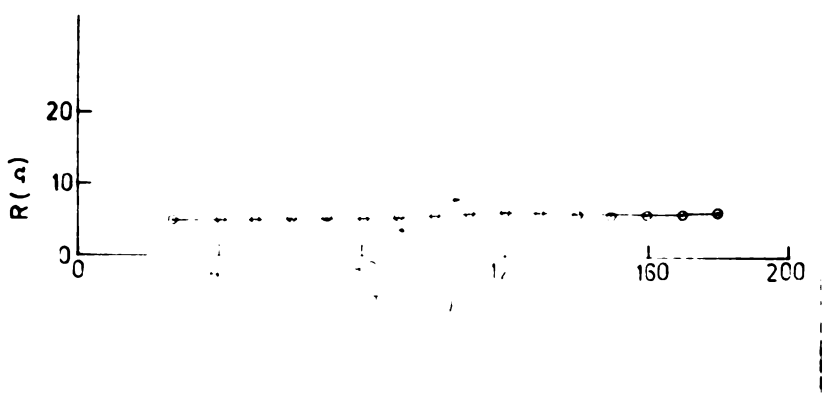

Figure 7.27 Resistance Vs. temperature (Bi ~ 300 Å, Ag ~ 700 Å).

layer increased, the temperature corresponding to the resistance minimum shifted to lower temperatures. The difference between the resistance minimum and the maximum also decreased with increasing silver layer thickness.

The decreasing tendency of resistance at the early stages of heating was found to disappear with increasing silver layer thickness. For a film with 300 Å silver overlayer, the resistance slowly increased from the very beginning followed by the steep increase and the final slow decrease. With increasing silver layer thickness the magnitude of the resistance variation also decreased.

On cooling after the first heating and annealing for one hour above 160°C, the resistance of the films having less than 600 Å thick silver layer increased. On further heating and cooling, the resistance of the films followed the same cooling curve. The slope of this cooling curve also decreased with increasing silver layer thickness. For a film with 600 Å silver layer, the resistance after the first heating remained almost steady during further heatings and coolings as can be seen in figure 7.26.

When the silver layer thickness was above 700 Å, the resistance increased with rise of temperature, although the increasing rate was very small. The nature of the curve during cooling was almost the same as that on heating.

The variation of the room temperature sheet resistance of the films with silver layer thickness, before and after heat treatment, was as in figure 7.28. The temperature coefficient of resistance at room temperature with varying silver layer thickness was as given in Table 7-3. The TCR values showed a sharp difference between the films having a 50 Å overlayer and those having a 100 Å overlayer. As the thickness of the silver layer increased, the TCR at room temperature slowly changed from a negative to a positive value.

On annealing identical samples at different constant temperatures, the time taken to reach the maximum value of resistance was found to decrease with rise of temperature. For example, while a film having 200 Å silver layer took several hours to reach the maximum value at 100°C, it has taken only about two hours at 120°C and few minutes at 140°C.

Table 7-3

Temperature coefficient of resistance at room temperature for different silver layer thickness

Ag layer thickness (Å)	TCR at room temperature	
	First heating (ppm/°C)	Further heatings (ppm/°C)
0	-4050	-2150
50	-3580	-2100
100	-1680	-4220
150	-1180	-3800
200	- 770	-3740
300	+ 190	-3220
400	+ 410	-3080
500	+ 500	-2760
600	+ 630	- 170
700	+ 750	+ 885
800	+ 790	+1020
900	+1020	+1060

(ii) Surface features

Freshly prepared samples having thinner overlayers had no special surface features when examined under the microscope. But these films annealed at 160°C and exposed to hydrogen sulfide atmosphere for fifteen minutes were found to have dispersed dark regions on the surface (figure 7.29). But these features were absent in unannealed films exposed to hydrogen sulfide (figure 7.30).

(iii) X-ray diffraction

The bilayer films, in the as deposited form, produced continuous rings in the Debye-Scherrer pattern indicating their polycrystalline nature.

Films having 200 Å silver overlayer, whether annealed at various higher temperatures or unannealed, produced identical Debye-Scherrer powder pattern (figures 7.31 to 7.34).

b) Films annealed at room temperature

(i) General

On keeping the films in atmosphere for several days, the colour of the surface was found to change gradually. The metallic colour of the surface slowly

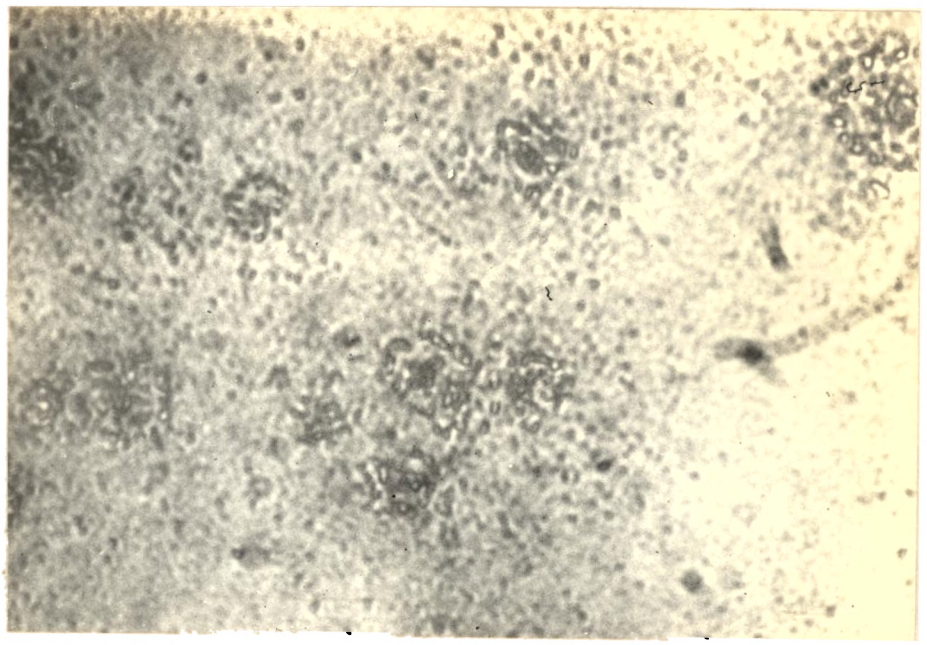

Figure 7.29 Surface features of unannealed bilayer film (Ag $\sim$ 200 Å) exposed to H_2S atmosphere (1800x).

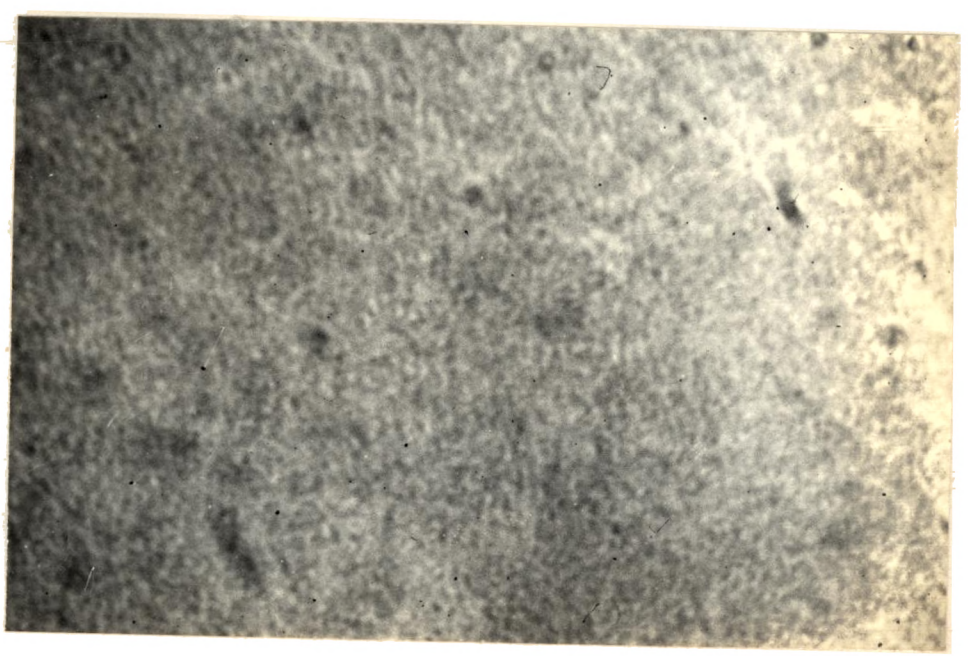

Figure 7.30 Surface features of annealed bilayer film (Ag $\sim$ 200 Å) exposed to H_2S atmosphere (1800x).

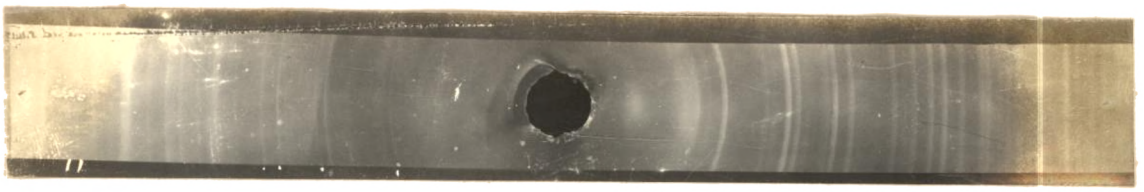

Figure 7.31 Debye-Scherrer pattern of unannealed bilayer film material.

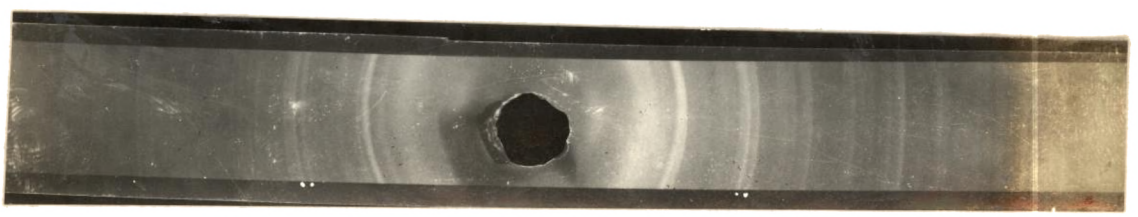

Figure 7.32 Debye-Scherrer pattern of bilayer film material - annealed at 80°C.

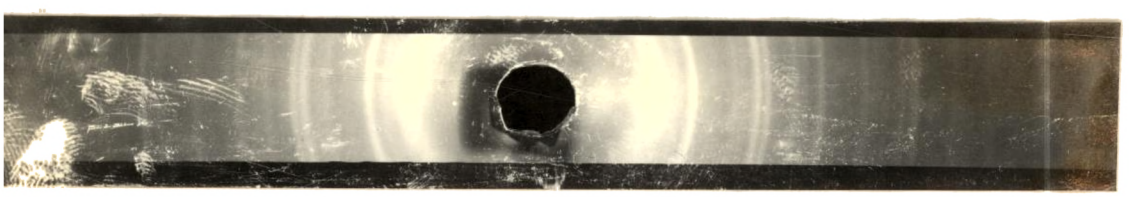

Figure 7.33 Debye-Scherrer pattern of bilayer film material - annealed at 120°C.

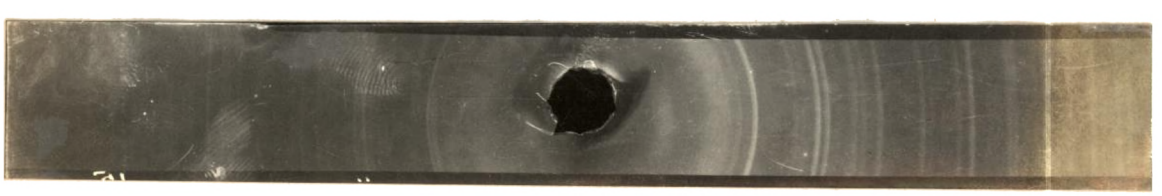

Figure 7.34 Debye-Scherrer pattern of bilayer film material - annealed at 160°C.

changed into pink and finally became light blue. This colour change occured either on the free surface or on the surface close to the substrate depending on the thickness of the silver overlayer. The films which were normally opaque immediately after their deposition slowly became semitransparent together with the change in colour. This colour change was not found in those regions where there was no overlapping of the two layers (figure 7.35). The changes were not found to happen also in samples annealed at higher temperatures.

The nature of the surface features observed on films having various layer thicknesses was as in Table 7-4. Pure bismuth films remained opaque and no colour change was seen on the surface except a light brown colour due to the oxide formation on the free surface. In films having 50 Å to 100 Å thick silver layers, the colour change was observed on the free surface and in films having more than 300 Å thick silver layer the change was found at the substrate side. In films with 200 Å silver layer, the colour change was more uniform throughout and the transparency was maximum.

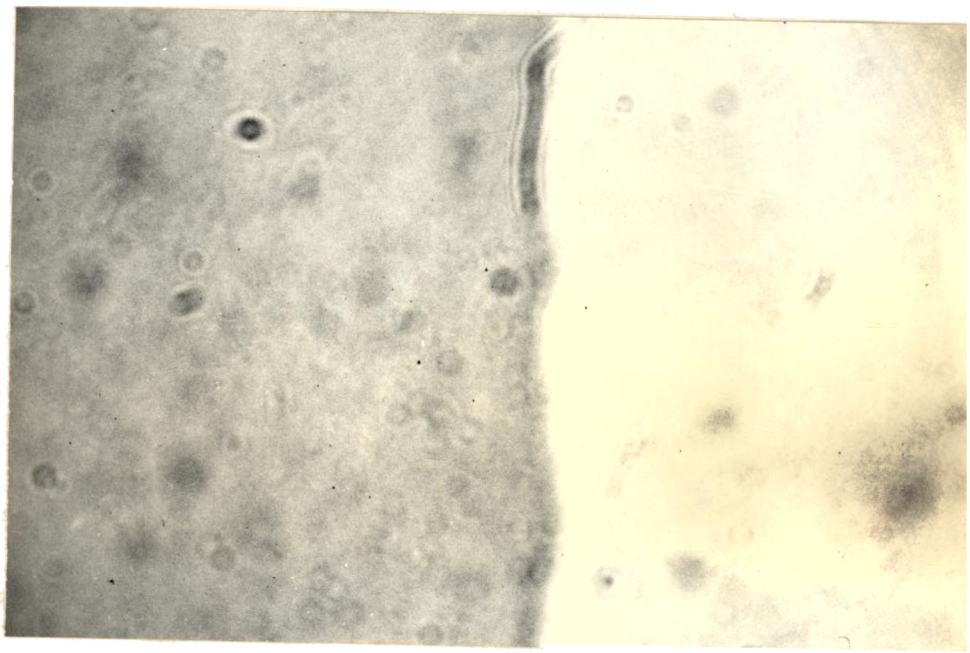

Figure 7.35 Bi film with overlapping of Ag at the left (144 x).

Table 7-4

Changes observed on the film surfaces in relation to the layer thickness

Thickness of layers (in Å)		Colour		Nature of the film
Bismuth	Silver	Glass surface	Free surface	
1000	—	Bi metal colour	light brown	Opaque
950	50	,,	light blue	Slightly transparent
900	100	,,	,,	,,
850	150	Light blue	light pink	Semi transparent
800	200	,,	,,	Maximum semi-transparency
700	300	,,	Ag white	Semi transparent
600	400	,,	,,	,,
500	500	Light blue with tinges of pink colour	,,	,,
400	600	light pink	,,	Transparency decreases
300	700	faint yellow	,,	Slightly transparent
200	800	,,	,,	Very little transparency
100	900	Traces of yellow colour	,,	,,

(2) Films having 200 Å silver layer

Due to the special features of 200 Å silver layered films, their properties were examined further.

(i) Variation of resistance with time

The variation of resistance with time was as in figure 7.36. Their resistance increased with time. After the initial steep increase, the rate of increase was found to decrease.

(ii) Surface features

Freshly prepared films were opaque having no special surface features. After a few days a 'flower-like' formation began to appear on the films. The number and the size of these features increased with time. Figures 7.37 to 7.41 show the various stages in the growth of the flower-like formation and their spreading.

(iii) Adhesion

No quantitative measurement of the adhesion of the film to the substrate was made in the study. But a qualitative measurement by scratch test revealed that films which have already become semitransparent,

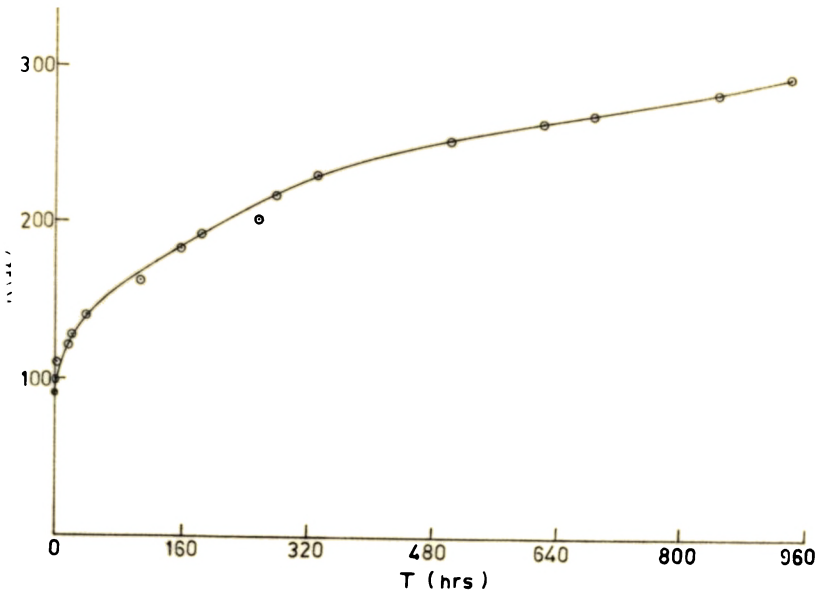

Figure 7.36 Resistance Vs. time of bilayer film (Bi ~ 800 Å, Ag ~ 200 Å) annealed at room temperature.

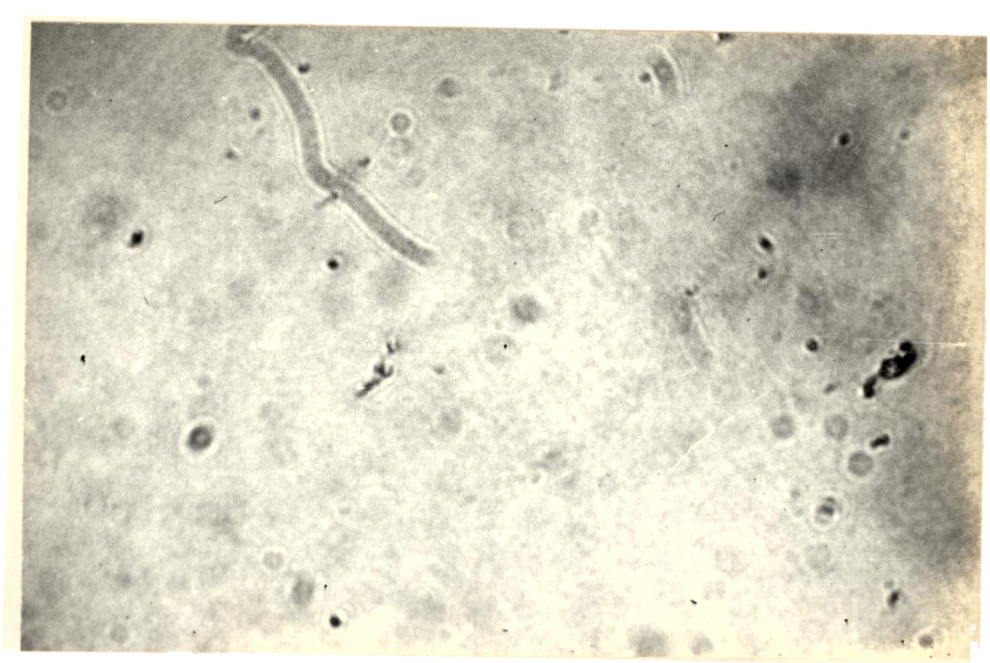

Figure 7.37 Surface features on room temperature annealed bilayer film, immediately after preparation (360 x).

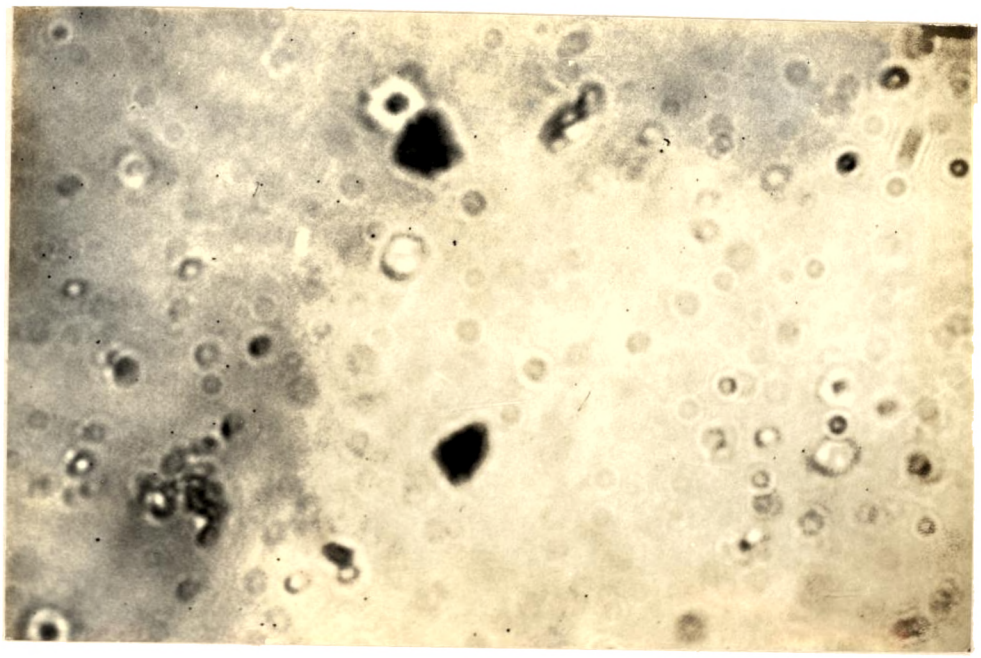

Figure 7.38 Surface features on room temperature annealed bilayer film, after 4 days (360 x).

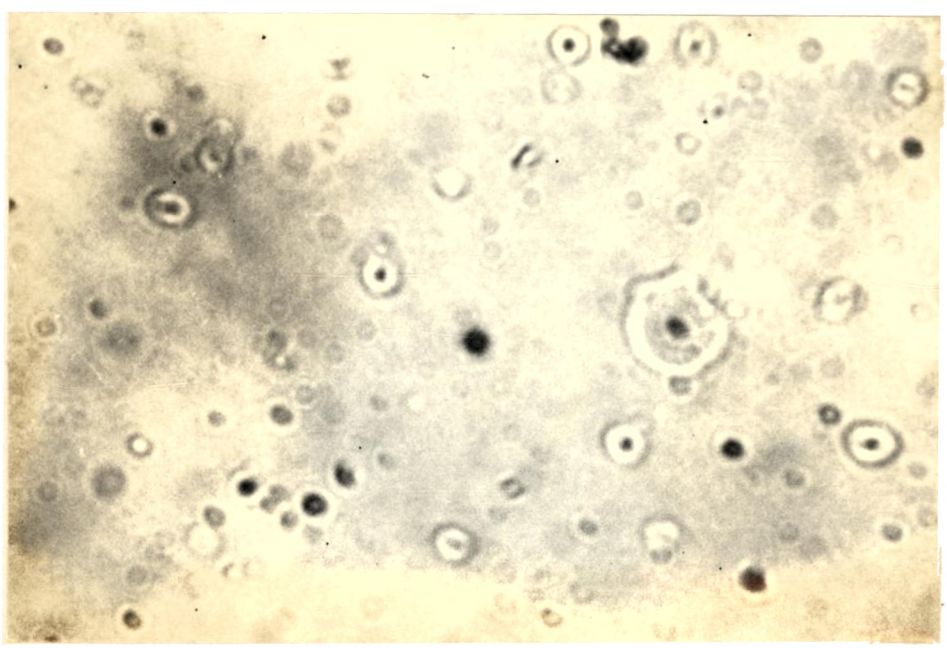

Figure 7.39 Surface features on room temperature annealed bilayer film, after 8 days (360 x).

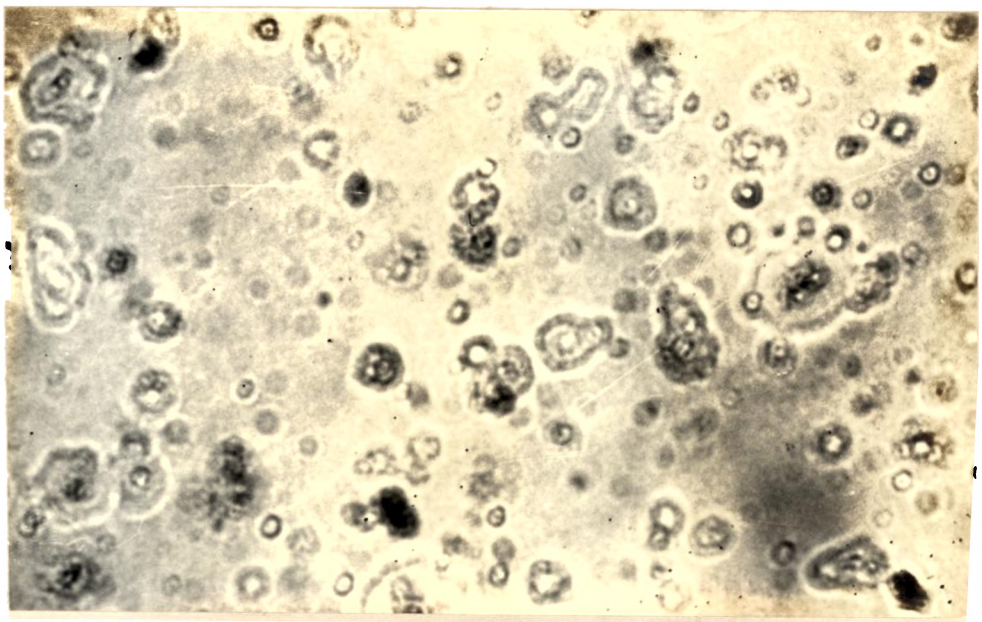

Figure 7.40 Surface features on room temperature annealed bilayer film, after 16 days (360 x).

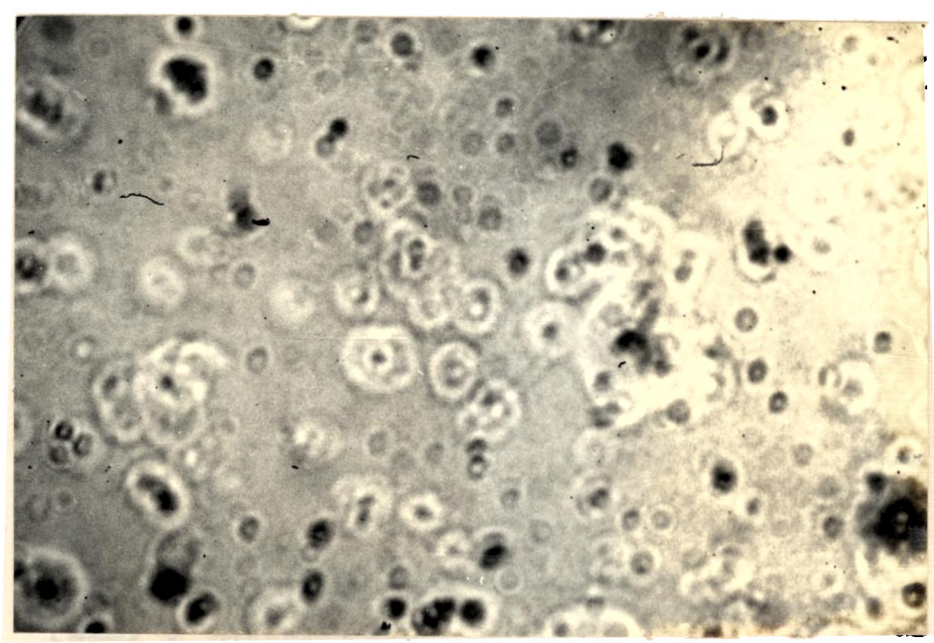

Figure 7.41 Surface features on room temperature annealed bilayer film, after 25 days (360 x).

have very good adherence to glass substrates. Their adhesive force was more than that of a freshly prepared film and that of a film annealed at higher temperature immediately after its preparation.

(iv) X-ray analysis

The powder pattern of the material of the films scraped from their substrate, immediately after their preparation, showed rather sharp low-angle and back-reflection lines (figure 7.42). But the back-reflection lines were found to disappear and certain low-angle lines became broader in the case of the semitransparent film material (figure 7.43).

7.2 Discussion

The resistance of a film, by Matthiessen's rule, as discussed in section 1.2, consists of

(i) an ideal part which is strongly dependent on the amplitude of the thermal motions of the ions, ρ_g

(ii) a residual part which is strongly dependent on lattice defects, ρ_i and

(iii) a thickness-dependent part due to the scattering of conduction electrons by the boundaries of the metal film, ρ_t

Figure 7.42 Debye-Scherrer pattern of bilayer film material, immediately after film preparation.

Figure 7.43 Debye-Scherrer pattern of the semi-transparent film material.

Therefore, $\rho_{film} = \rho_s + \rho_i + \rho_t$

The change occuring in these three resistance contributing components control the resistance of a film. Therefore, various factors like annealing, alloying, compound formation, structural changes, thickness variation etc. make changes in the resistance of a film. Factors like these have to be examined to understand the change of resistance occuring in various films.

A. Electrode-film combinations

In thin films there are imperfections like dislocation lines, stacking faults, microtwins etc.[186] Annealing out these defects at higher temperatures normally produces a reduction in resistance. But, since the electrode films used in the experiments are thick ($\sim$ 3000 Å) and their dimensions are kept small compared to those of the films under study, the reduction in resistance in the annealed electrodes due to the annealing out of defects during annealing at higher temperature can be considered to be small. Similarly the small possible reduction in resistance in the unannealed electrodes due to time annealing also need not be taken into consideration.

The films on annealed electrodes and those on unannealed electrodes were kept under identical conditions. Therefore the resistance changes occured in the specimen films as such should be identical. Hence, it is reasonable to infer that the difference in the variation of resistance between the films having annealed electrodes and those having unannealed electrodes is due to the changes occuring at the electrode-film junctions. In fact several investigaters have observed various[51,90,95,96,187-193] interfacial structural effects like intergranular strain, intermixing, alloying, compound formation etc. in bilayer films of various metal combinations.

In vacuum deposited films, diffusion of one metal into another and the consequent formation of alloys and compounds can take place. This formation is one or two orders of magnitude greater than that in bulk materials,[186] particularly if a metal with a high evaporation temperature is deposited on a low melting material.[194] During the film preparation, if the material first deposited is of low melting point, the kinetic energy of the impinging atoms of the higher melting point material is sufficient to make them penetrate through two or three atomic layers of the base layer material.

This alloying in thin films is confined to the first 5 Å of the deposit.[92,195] Therefore, in depositing films on indium electrode films, interfacial alloying is likely to happen.

An oxide layer may spatially separate two films and thereby reduce the proximity effect of diffusion.[196] These oxide layers, in general, are bad electrical conductors. But oxides like In_2O_3, SnO_2 and TiO_2 give good ohmic contact.[197]

a) Aluminium films with gold electrodes

Campisano et al.[198] have observed that, in polycrystalline aluminium-gold layered films, heat treatment at $\sim 100^{\circ}C$ produce a layer of Au_2Al via a brief intermediate stage of Au_5Al_2. This process dominates until all the aluminium or gold has been used upto form Au_2Al. If there remains any unconsumed aluminium, further heating at $125^{\circ}C$, causes conversion of Au_2Al into Au_5Al_2. Annealing at $175^{\circ}C$ forms Au_4Al. If after the production of Au_2Al layer, an excess of Au remains unconsumed, a heating at $230^{\circ}C$ causes conversion to $Au Al_2$. In all these cases the thickness of a compound layer developing is proportional to $t^{\frac{1}{2}}$,

where t is the time of reaction. The $t^{\frac{1}{2}}$ dependence indicates that diffusion rates limit the reaction of aluminium with gold. As the intermetallic compounds are formed, the resistance of the film also increases.[45]

Allen et al.[199] have shown that annealing of a surface reduces the area of a film. Therefore, a film deposited on annealed electrodes have a lesser area of contact compared to that of unannealed electrodes. As the contact area is small for an annealed electrode, there is larger resistance at the junction. Therefore the intermittent passage of a current, even though only of magnitude $\sim$650 pA, will produce more heating at the junction sufficient to produce an intermetallic compound. This heating may also produce microdiscontinuities at the junction region as shown in figure 7.2. The intermetallic compound formation consequent on diffusion at higher temperatures produced due to the passage of current through it and the production of microdiscontinuities make the resistance of the films with annealed electrodes rise as in figure 7.1. Since the temperature rise at the film-electrode junction in films with unannealed electrodes remains to be small, the resistance rise of these films is not very large.

Tareev and Lerner,[200] and Roy Bardhan et al.[201] have shown unidirectional flow of current in MIM structures. In Al/Au system it is reasonable to assume that a very thin layer of Al_2O_3 may be formed between the electrode and the film owing to the adsorbed oxygen on the electrode surface. This thin Al_2O_3 layer on the aluminium forms an MIM structure with the electrode. Due to the unidirectional flow of current, heating occurs more at one junction and microdiscontinuities are produced in this particular junction.

b) Aluminium films with silver electrodes

The nature of the resistance variation in the aluminium films with silver electrodes is similar to that in aluminium films with gold electrodes. The intermetallic compound formation and the production of microdiscontinuities, as in the case of aluminium films with gold electrodes, increase the resistance of the films with annealed electrodes as in figure 7.3. However, in Ag/Al combination the diffusion and the phase formation occur at a higher temperature. Weaver and Brown,[92] using optical reflection and TEM techniques, observed formation of Ag_2Al phase in Ag/Al films annealed

upto 240°C. Their results indicate a rapid initial diffusion occuring over a limited distance without forming an intermetallic compound. Pioreux[202] has also observed the parabolic growth of Ag_2Al phase in an Ag/Al system and noticed effects of substantial grain boundary diffusion. The higher temperature required for diffusion and phase formation in Al/Ag system appears to account for the low rate of resistance variation observed in Al films with unannealed silver electrodes.

The formation of an Al_2O_3 thin layer between the electrode and the film due to the presence of adsorbed oxygen on the electrode film surface makes an MIM structure at the film-electrode junction. The unidirectional flow of current in the MIM structure[200,201] causes microdiscontinuities at one junction as in the aluminium films with gold electrodes.

c) Aluminium films with aluminium electrodes

An oxide layer forms on the aluminium electrode film surface when exposed to atmosphere. On annealing at higher temperature, as the vacuum of the annealing atmosphere is not high, the thickness of the oxide layer on these electrode films increases. Therefore the oxide layer is thicker on annealed electrodes

compared to that on unannealed electrodes. On deposition of the specimen film the oxide layer produces an $Al-Al_2O_3-Al$ sandwich structure at the film-electrode junctions. Since the thickness of the oxide layer is less than 50 Å in both the cases, conduction of electrons is possible by tunnelling.[203]

When current passes through the films, heating occurs at the junction and, as a consequence, the thickness of the oxide layer increases using the adsorbed oxygen at the junction. However, in films with unannealed electrodes this increase is more likely to vary according to the logarithmic law of oxidation.[204] Hence there is an initial increase in the variation of resistance in films with unannealed electrodes as in figure 7.4.

The figure shows also fluctuations in the values of resistance. These fluctuations are probably due to thermal variations during the day.

d) Aluminium films with copper electrodes

Pashley,[195] and Hauser et al.[196] have shown that layered films of metal pairs having very large mutual solubility can have appreciable alloying at overlapping

regions even at room temperature. Therefore good alloying of these metals can be expected if there is no diffusion barrier. Hence in aluminium films with unannealed copper electrodes an alloy film may form between the electrode film and the aluminium specimen film. Since the electrode potential of the alloy is different from that of pure metal and is more cathodic than that of aluminium,[205] a higher resistance can exist at the positive junction. Heat produced during the passage of electric current may increase the rate of alloy formation. This increasing alloy layer thickness, in turn, may cause a rapid increase in the resistance of the films. The striations observed at the positive junction also indicates the changes occuring in that region. These changes occuring at the film-electrode junctions account for the rapid resistance changes happening in films with unannealed electrodes.

In films with annealed electrodes there is an oxide layer which acts as a barrier reducing the proximity effect of diffusion.[196] Therefore the rapid changes occuring in films with unannealed electrodes does not happen in films with annealed electrodes.

e) Gold films with indium electrodes

Unlike aluminium films on various electrodes, gold films on indium electrodes have a decrease of resistance with time. This decrease in films with annealed and unannealed electrodes appears to be due to the annealing out of defects in the gold film and the release of the intergranular strain.

When gold is deposited on indium electrodes, interdiffusion can occur even at room temperature and, as Simić and Marinković[206] have shown, intermetallic compounds $AuIn_2$, AuIn, Au_7In_3 or Au_4In can form depending on the Au : In ratio in the layer and the diffusion time. This alloying makes very good ohmic contact between the two metals. The penetration of energetic gold atoms into the indium electrode during the deposition of the films also helps the alloy formation.

In annealed electrodes an oxide layer separates the two metals and acts as a diffusion barrier between the two. This accounts for the observed difference in the percentage variation of resistance in gold films on annealed electrodes and those on unannealed electrodes.

f) Silver films with indium electrodes

As in the case of gold films with indium electrodes, the decrease in resistance observed in films with annealed and unannealed electrodes is due to the annealing out of defects and the release of intergranular strain.

Indium will absorb silver unless it already contains a small amount of silver (about 5 %) as impurity.[207] Therefore, as no impurity of silver is present in the indium electrode, the absorption of silver film by the electrode material takes place in the electrode-film overlapping region of the films with unannealed electrodes, forming alloys. But in the films with annealed electrodes, the oxide layer on the electrode prevents the alloy formation. This difference in behaviour appears to be the reason for the initial difference observed in films with annealed electrodes and those with unannealed electrodes.

The cluster formation observed on silver films with unannealed electrodes (figure 7.10), separated from the electrode edge, can be due to the electromigration of indium atoms and subsequent alloy

formation with silver. Electromigration of gold films on molybdenum surfaces in the direction of electron flow has been observed by Bleeh and Kinsbron.[208] Similarly several cases of electromigration through the grain boundaries of metals, especially of noble metals have been reported.[139,151-153] In the present case, the passage of current is intermittent and the duration of passage of current is short. During the passage of current indium atoms move from the electrode into the silver film through a small distance. When the flow of current is stopped, the atoms which have already moved into the silver film form an alloy with silver. This process of electromigration of indium atoms and the subsequent alloy formation is repeated during the intermittent measurement of resistance and results in the cluster formation.

g) Copper films with indium electrodes

The microscopic observation of the electrode-film junction of both the annealed and the unannealed electrodes shows identical features. Therefore the same process of diffusion seems to occur in both the cases. This may account for the fact that the resistance variation is the same in both the films.

The observed small increase in resistance with time is due to the oxidation of copper films when exposed to atmosphere.

h) Aluminium films with indium electrodes

Unlike In/Au, In/Ag and In/Cu systems, in the In/Al system no diffusion takes place on account of the very small solid solubility and the non-existence of intermetallic compounds.[209] The resistance of the films increases due to the oxide formation on aluminium films. The initial lower resistance of aluminium films with unannealed electrodes shows that there is better initial contact between the film and the electrode. This may be due to the larger surface area of the unannealed electrode film. The large and non-uniform increase in resistance observed in films with unannealed electrodes (figure 7.13) may possibly be due to the bubble formation between the aluminium film and the indium electrode. Even though the film is in controlled contact with the atmosphere, water vapour oxidises the top surface of aluminium film and releases hydrogen. A small part of this hydrogen diffuses into the aluminium film and recombines at the indium-aluminium interface. Since

the molecular hydrogen formed at this interface is unable to diffuse away, forms bubbles at the interface as reported by Miles and Smith.[210] The formation and the growth of bubbles increase with time and accordingly the junction resistance also increases. The heating effect during the resistance measurement may also affect the growth of bubbles.

In films with annealed electrodes such bubble formation is not likely to happen on account of the presence of In_2O_3 layer. Therefore these films have a rather uniform increase of resistance.

i) General remarks

The Fermi surface of the alloys of noble metals are highly distorted.[211] As Kinbara and coworkers[9] have pointed out there is a change in the electronic structure like increment in the degree of distortion of the Fermi surface in unannealed films. Therefore, the difference in the distortion of the Fermi surface can account for the observed difference in the variation of resistance between films with annealed electrodes and those with unannealed electrodes.

B. Bilayer films

B-1 Bismuth films having a very thin ($\sim$ 50 Å) silver overlayer

Comparing figure 7.19 with figures 7.18 and 7.20 to 7.26, it can be seen that the behaviour of a bismuth film with a silver overlayer $\sim$ 50 Å is similar to that of a pure bismuth film. This may be due to the fact that the silver overlayer is not forming a continuous overlayer on bismuth and, is not contributing directly to the conduction. Further, the TCR at room temperature for different silver layer thickness given in Table 7-3 and the variation of sheet resistance before annealing Vs. silver layer thickness shown in figure 7.28 indicate that the behaviour of a film having a 50 Å silver overlayer is different from that of films with larger silver layer thickness.

The variation of resistance with temperature, the resistance showing a minimum at a particular temperature and increasing with further heating or cooling, observed in bismuth films having a thin Ag overlayer can be explained as a consequence of the limiting of the mean free path and the changes in the number of

charge carriers as suggested by Hoffman et al.[212] and Block et al.[181] in the case bismuth films using the model proposed by Kaidanov and Regal.[213] According to the model the semimetal bismuth acts as a metal above the resistivity minimum temperature, having a characteristic positive temperature coefficient of resistance. At these temperatures, the mean free path of charge carriers is smaller than the crystallite size. As the temperature decreases the mean free path increases rapidly and the density of carriers decreases. But the increase of mean free path overrides the decrease in the density of carriers. So the overall resistance decreases. Once the mean free path becomes comparable to the crystallite size, it increases only very slowly with decrease of temperature. So, finally, a temperature is reached at which the rate of mean free path increase becomes slower than the charge carrier density decrease. On further decrease of temperature, the net effect of the two rates makes the resistance rise. Now the semimetal acts as a semiconductor with a negative temperature coefficient of resistance.

It has been suggested by Duggal and Rup[214] that the semiconductor-like behaviour observed in thin bismuth films is due to the uncrossing of the conduction and

valence bands predicted by the quantum size effect theory. But Hoffman and Frankl[212] point out that this behaviour is a consequence of the limiting of the carrier mean free path and the decrease in the number of carriers with decreasing temperature rather than the uncrossing of the bands.

Chopra[215] has shown that the deposition of an overlayer of one material modifies the surface of the underlayer of another material and, consequently, the electrical properties of that layer. This modification at the surface, which depends on the combination of the layers, influences the scattering of electrons and the effective number of free electrons near the interface. Depending on the nature of the change, an increase or decrease in the surface scattering may occur. The resistance of a bismuth film with a silver overlayer ~ 50 Å is found to be higher than that of a pure bismuth film of the same thickness (figure 7.14). So it may reasonably be said that the silver layer which is present on the bismuth base layer modifies the interface so as to increase the surface scattering of electrons and, consequently, the resistivity of the film.

The slower rate of variation of resistance and the shift of resistance minimum to lower temperature region observed as the thickness of bismuth and bismuth-silver bilayer films increases, are due to the increasing crystallite size with increasing film thickness as observed by Neuman and Ko[216] in bismuth films. But the shift of resistance minimum to a higher temperature in the case of bismuth films with a thin silver overlayer as compared to that of pure bismuth films of the same thickness may be due to the decrease in the mean free path consequent to the increase in the surface scattering of electrons resulting from the interface modified by the silver layer.

B.2. Bilayer films of varying layer thickness

a) Films annealed at higher temperature

The resistance of a thin metal film reflects to a remarkable degree the microstructure of the film.[121] So the variation of resistance in the bilayer films demonstrate the changes occuring in them.

(i) The change of resistance in the initial stage of heating

In the bilayer films, during the initial stages of heating, there is a slow decrease or gradual increase

of resistance depending on the thickness of the silver overlayer. This change may be partly due to the slight interdiffusion of the materials possible at this range of temperature. But the main factor for this appears to be the combined effect of the resistance changes occuring in the individual layers. Since silver has a positive temperature coefficient of resistance, as the thickness of silver layer increases the effective resistance variation turns to be a gradual increase.

(ii) The steep increase of resistance

The steep increase of resistance occuring in the films above 100°C appears to be due to increased interdiffusion at that temperature and aggregation of the overlayer.

Grain boundaries play a major role in the process of diffusion in polycrystalline films.[217] In layered films, the motion of materials is predominantly from a layer having smaller number of grains to that having larger number of grains.[46] If the melting point of a material is higher, the size of the grains in its polycrystalline film form is small and, consequently,

the number of grains is large.[68] Therefore, as the melting point of silver is higher than that of bismuth, the number of grains is large in the upper silver layer. Hence diffusion of bismuth into silver is possible. Such a diffusion of bismuth through gold has already been observed by Pariset and Chauvineau.[126] In pairs of materials like chromium-copper and gold-nickel which have very little mutual solubility (less than 0.1 %) and no compound formation, intermixing is observed at higher temperatures when the metals are in the form of polycrystalline double layers.[46,217] Similarly good intermixing is possible also in bismuth-silver polycrystalline bilayers in which the solid solubility of bismuth in silver is 3 at. % and that of silver in bismuth is negligible.[218] The diffusion of bismuth into the silver layer increases the resistance of the bilayer as in the case of chromium-gold bilayers where resistance has been observed to increase due to chromium diffusion into gold.[219]

The interdiffusion and intermixing in multilayer films are found to increase with rise of temperature. In bismuth-silver films the diffusion appears

to be rapid above 100°C which is a temperature of the order of $\frac{2}{3} T_m$ where T_m is the melting point of the metal. The increasing rate of diffusion with temperature is evident from the duration of time taken to reach the maximum value of resistance when the specimens are annealed at 100°C, 120°C and 140°C.

Belser[121] has shown that in two layer films there may be a sharp increase in resistance, which in many cases is due to a compound formation and in some cases is due to aggregation of one of the metals. Microscopic observation of annealed samples having thinner silver overlayer after H_2S treatment, seems to indicate the occurrence of aggregation of silver in these samples (figure 7.29). According to Weaver the aggregation generally occur at a high temperature and for silver it is about 300°C. Hollingsworth Smith and Gurev[220] have also shown the occurrence of severe agglomeration at temperatures greater than 200°C in the presence of oxygen. But Mohan and Jayarama Reddy's[221] study shows the occurrence of agglomeration in thin silver films around 160°C. In the case of bismuth-silver bilayers, diffusion of bismuth may have assisted the aggregation to occur at a lower temperature.

From the above considerations it is suggested that the steep rise of resistance observed above 100°C is due to the diffusion of bismuth into the silver overlayer and the aggregation of the overlayer film.

(iii) Further changes in resistance

The final slow decrease of resistance above 150°C is due to the gradual annealing out of defects. The behaviour of the film after the first annealing appears to depend on the bismuth silver ratio in the films.

The components of the bilayer films do not have a normal compound phase. Debye-Scherrer X-ray diffraction photographs of films having 200 Å silver overlayer annealed at various temperatures (figures 7.31 to 7.34) show that the pattern of lines remain the same in all the cases. So it appears that the components do not form any inter-metallic compound or alloy. Since the components retain their individual properties, as the quantity of silver increases the properties of the films are dominated more and more by silver. In films having a 600 Å silver layer after annealing, the decrease of resistance in bismuth is

balanced by the increase in silver. So the resistance of these films, after the first heating, remains almost steady during further heatings and coolings. But above 600 Å silver layer thickness, there is a slow increase of resistance with rise of temperature due to the positive temperature coefficient of resistance of the dominating silver part.

b) Films annealed at room temperature

When bismuth-silver bilayer films are annealed at room temperature, if the silver overlayer is thin (< 100 Å) the colour change is found to occur on the upper free surface. But as the silver layer thickness increases (> 300 Å) the change of colour is observed on the substrate side (Table 7-4). Besides, the regions where there is no overlapping of the two layers, remain unaffected (figure 7.35). From the observations it appears that the observed changes do not take place unless both the materials are present.

Interdiffusion is found to take place in bilayer films even at room temperature[222-224] and the initial diffusion zone is in a metastable state analogous to a

supersaturated solution. As Bauer and Jordan[125] have pointed out when two similar or dissimilar materials are joined, the resulting interfacial region is not generally in an equilibrium state. Concomitant properties may be affected by numerous variables like surface contamination, interfacial perfection and subsequent interfacial reactions in the solid state. So the interface may have different structure and different properties. The phase of the diffused interface may be different from that of the equilibrium phase diagram. Nakashima et al.[225] have detected by Auger electron spectroscopy a diffused interface in silicon-gold thin film system. In this system, although there is no equilibrium solid compound or solid phase, they have observed difference in the silicon spectra which strongly suggests that the electronic state of silicon in the diffuse interface is quite different from that of pure silicon. As a consequence, although silicon atoms are tightly bound to one another by covalent bonding the atoms in the diffuse state are able to break the weaker bond existing at the interface and migrate through gold to the surface. As the diffusion zone is in a metastable state, the pure metals are not in

equilibrium with each other. So diffusion is occurring under abnormal conditions.[92] In this stage defects, besides controlling interdiffusion, may also give rise to levels of diffused or reacted materials that are not interpretable in terms of equilibrium phase diagram.[217] In a similar manner, in bismuth-silver bilayer films annealed at room temperature a slow interfacial reaction between the metals seems to take place producing some interphase compound which is not explainable in terms of equilibrium phase diagram. This interfacial reaction appears to be the reason for the formation of the features (figures 7.37 to 7.41) observed in the films.

The reaction at the interface also appears to make the crystallite size of bismuth smaller. X-ray diffraction analysis of the material indicates this phenomenon. As Klug and Alexander[226] have pointed out, in the absence of lattice strains, well crystallized materials should give reasonably sharp lines at all angles if the crystallite dimension is larger than 0.1 μ. As the dimension falls below this level, the sharpness of the back-reflection lines is first affected. At sizes much less than 0.01 μ, the back-reflection

lines disappear entirely, and the low-angle lines become very wide and more diffuse. The Debye-Scherrer pattern of bismuth-silver bilayer films having 200 Å silver overlayer, immediately after their preparation, gives rather sharp low-angle and back-reflection lines (figure 7.42). But in films which have already become semitransparent and have changed their colour, the back-reflection lines are almost missing while certain low-angle lines became weak and other broadened (figure 7.43). This is naturally due to the reduction in size of the bismuth crystallites. The silver atoms during their interaction with bismuth reduces the size of the bismuth crystallites. The transparency of the film also appears to be due to this reduced crystallite size.

The increased adhesive force of the film may possibly be due to the formation of some compound phase in the film. Weaver and Hill[92], considering the difference in the adhesive force of a pure chromium film and of that having an aluminium overlayer, have shown that the ageing process for double layered films at room temperature normally consists of two stages occurring at different times. The two stages of the ageing

process are an interdiffusion of the two metals followed by a partial precipitation of an intermetallic compound. According to the theories of age hardening,[227] the interdiffusion would cause a hardening or increased resistance to deformation with no change in lattice parameters and this would be followed by a release of strain and precipitation of inter-metallic compound. In bismuth-silver bilayer films annealed at room temperature interdiffusion and compound precipitation seem to happen which account for the increased adhesive force.

CONCLUSION

If electrode films are used in measuring the resistance of metal films the variation of the film resistance with time is dependent on the material of the electrode. Further, this variation differs with annealed and unannealed electrodes. The difference in the rate of variation of resistance with time is due to various factors like interdiffusion of the materials at the film-electrode junction, oxide formation at the junction, alloying of the materials, electromigration, bubble formation etc.

In bilayer films, the overlayer is found to modify the electrical properties of the underlayer. In bismuth-silver bilayers, a thin overlayer of silver increases the resistivity of the bismuth films. It also makes the TCR at room temperature more negative and shifts the temperature corresponding to the resistance minimum of the bismuth films to a higher temperature.

When thickness of the bilayers remain constant, their electrical properties depend on the thickness of the individual layers. In bismuth-silver

bilayers, as the silver overlayer thickness increases, their sheet resistance decreases and TCR at room temperature changes from a negative to a positive value. When annealed at room temperature, their crystallite size diminishes and their surface feature change gradually. On heat treatment, their resistance variation with temperature can be understood on the basis of diffusion at the interface and aggregation of the silver overlayer. By controlling the thickness of the individual layers it is possible to keep the resistance variation with temperature to a minimum.

REFERENCES

1. N. Inoue, Y. Tanaki and H. Yagi, J. Appl. Phys., 45 (1974) 1562.
2. L. Ždanovics, A. Sas and B. Deidc, Thin Solid Films, 36 (1976) 269.
3. N. Adamov, B. Perović and T. Nenadović, Thin Solid Films, 24 (1974) 89.
4. H. Goebel, K. Dettmer and F.R. Kessler, Phys. Status Solidi A, 16 (1973) 61.
5. D.R. Goyal, O.S. Panwar, K.K. Srivastava, K.N. Lakshminarayan, Ashok Kumar and D.R.Ravikar, Indian J. Pure and Appl. Phys., 15 (1977) 10.
6. S. Baba, H. Sugawara and A. Kinbara, Thin Solid Films, 31 (1976) 329.
7. M.J. Capers and M. White, Thin Solid Films, 15 (1973) 5.
8. Ritu Suri, A.P. Thakoor and K.L. Chopra, J. Appl. Phys., 46 (1975) 2574.
9. H. Sugawara, T. Nagano, K. Uosumi and A. Kinbara, Thin Solid Films, 14 (1972) 349.
10. H. Sugawara, T. Nagano and A. Kinbara, Thin Solid Films, 21 (1974) 33.

11. Roland Gerber and Jean-Louis Mayeux, C.R.Acad. Sci., B 268(1969) 881.

12. A. Goswami and S.N. Ojha, Indian J. Phys., 49 (1975) 847.

13. P. Sen and A.K. Pal, Japanese J. Appl. Phys., 14 (1975) 1475.

14. R. Suhrmann, G. Wedler and E.A. Dieck, Proc. Intern. Conf. Brussels, 4 (1958) 942.

15. Fritsche Von L. and H. Seufert, Z. Naturforsch, 18(a) (1963) 1013.

16. R.D. Bhide, Ph.D. Thesis, Poona University (1972).

17. Reime Von.L, Z. Naturforsch, 12(a) (1957) 525.

18. Joy George, V. Unnikrishnan Nayar, E.C. Joy and N.K. Radhakrishnan, Thin Solid Films, 47 (1977) 121.

19. Joy George, E.C. Joy and N.K. Radhakrishnan, Thin Solid Films, 68 (1980) 289.

20. K.L. Chopra and N.R. Randlett, J. Appl. Phys., 38 (1967) 3144.

21. M.S.P. Lucas, Appl. Phys. Letters, 4 (1964) 73.

22. K. Yamanouchi, T. Kozuno and K. Shibayama, Proc. IEEE, 63 (1975) 726.

23. C. Pariset and J.P. Chauvineau, Surf. Sci., 47 (1975) 545.

24. H.A. Lorentz, Elektronentheorie der Metalle, Leipzig, 1909.

25. A.H. Wilson, The Theory of Metals, Cambridge University Press, Cambridge, 1954.

26. C. Kittel, Introduction to Solid State Physics, John Wiley and Sons, New York, 1956.

27. A.J. Dekker, Solid State Physics, Prentice-Hall, N.J., 1957.

28. J.C. Slater, H. Jones and A.E. Gerritsen, in S. Flügge (ed.), Handbuch der Physik, Vol XIX, Springer-Verlag, Berlin, 1956.

29. G.T. Meaden, Electrical Resistance of Metals, Plenum Publishing Corp., New York, 1965.

30. J.J. Thomson, Proc. Cambridge Phil. Soc., 11 (1901) 120.

31. K. Fuchs, Proc. Cambridge Phil. Soc., 34 (1938) 100.

32. E.H. Sondheimer, Advan. Phys., 1 (1952) 1.

33. E.H. Sondheimer, Phys. Rev., 80 (1950) 401.

34. D.K.C. Mac Donald and K. Sarginson, Proc. Roy. Soc. London, A203 (1950) 223.

35. V. Vand, Proc. Phys. Soc. London, 55 (1943) 222.

36. R.W. Hoffman, F.J. Anders and E.C. Crittenden, Jr., J. Appl. Phys., 24 (1953) 231.

37. C.A. Neugebauer, in G. Hass and R.P. Thun (eds.), Physics of Thin Films, Vol.2, Academic Press, New York, 1964, p.1.

38. J.P. Borel, Compt. Rend., 233 (1951) 296.

39. R.B. Belser, J. Appl. Phys., 28 (1957) 109.

40. A.E. Hanes, Brit. J. Appl. Phys., 8 (1957) 113.

41. H. Basseches, IRE Trans. Component Pts., CP8 (1961) 51.

42. M.S.P. Lucas, Thin Solid Films, 7 (1971) 455.

43. M.S.P. Lucas, Ph.D. Dissertation, Duke University, 1964.

44. J.W.M. Du Mond and P.J. Youtz, Phys. Rev., 48 (1935) 703.

45. C. Weaver, in M.H. Francombe and R.W. Hoffman (eds.) Physics of Thin Films, Vol 6, Academic Press, 1971, p.301.

46. M.A. Nicolet, Thin Solid Films, 52 (1978) 415.

47. R.W. Balluffi and M.J. Blakely, Thin Solid Films, 25 (1975) 363.

48. K.N. Tu and S.S. Lau, in J.M. Poate, K.N. Tu and J.W. Mayer (eds.), Thin Films—Interdiffusion and Reactions, Wiley-Interscience, 1978, p.81.

49. H.E. Cook and J.E. Hilliard, J. Appl.Phys., 40 (1969) 2191.

50. R.G. Kirsch, J.M.Poate and N. Kibschman, Appl. Phys. Letters, 29 (1976) 772.

51. P.M. Hall, J.M. Morabito and H.T. Panousis, Thin Solid Films, 41 (1977) 341.

52. K.L. Chopra, Thin Film Phenomena, McGraw-Hill, New York, 1969, p.182.

53. C.A. Neugebauer, in L.I. Maissel and R. Glang (eds.) Handbook of Thin Film Technology, McGraw-Hill, New York, 1970, p.8-3.

54. R.W. Balluffi, Phys. Status Solidi, 42 (1970) 11.

55. N.A. Gjostein, in Diffusion, Am. Soc. Metals, Metals Park, Ohio, 1973, p.241.

56. W.D. Kingery, J. Amer. Cer. Soc., 57 (1974) 1.74.

57. D. Shaw, in D. Shaw (ed.), Atomic Diffusion in Semiconductors, Plenum Press, New York, 1973, p.1.

58. L.G. Harrison, Trans. Faraday Soc., 57 (1961) 1191.

59. J. Unnam, J.A. Carpenter and C.R. Houska, J. Appl. Phys., 44 (1973) 1957.

60. K.N. Tu and R. Rosenberg, Thin Solid Films, 13 (1972) 165.

61. D.Gupta, D.R. Campbell and P.S. Ho, in J.M. Poate, K.N. Tu and J.W. Mayer (eds.), Thin Films-Interdiffusion and Reactions, Wiley-Interscience, 1978, p.161.

62. D. Gupta, Phys. Rev., 7 (1973) 586.

63. D. Gupta, J. Appl. Phys., 44 (1973) 4455.

64. D. Gupta, and K.V. Asai, Thin Solid Films, 22 (1974) 121.

65. S.U. Campisano, E. Costanzo and E. Rimini, Philos. Mag., 35 (1977) 1333.

66. J.B.B. Baglin and F.M. d'Heurle, in O. Meyer, G. Linker and F. Kappeler (eds.), Ion Beam Surface Layer Analysis, Plenum Press, New York, 1976, p.385.

67. J.M. Harris, E. Lugujje, S.U. Campisano, M.A.Nicolet and R. Shima, J.Vac. Sci. Technol., 12 (1975) 524.

68. J.P. Hirth and K.L. Moazed, in G.Haas and R.E.Thun (Eds.) Physics of Thin Films, Vol 4, Academic Press, 1967, p.97.

69. T. Nenadović, B. Perović, N. Adamov and B. Nenkel, Thin Solid Films, 25 (1975) 515.

70. H.G. Tompkins and M.R. Pinnel, J. Appl. Phys., 47 (1976) 3804.

71. J.A. Borders, Thin Solid Films, 19 (1973) 359.

72. F.M. d'Heurle and R.E. Horstmann, IBM J. Res. Dev., 14 (1970) 461.

73. D. Gupta and R. Rosenberg, Thin Solid Films, 25 (1975) 171.

74. T.C. Tisone and J. Drobek, J. Vac. Sci. Technol., 9 (1972) 271.

75. R. Davidge, Phys. Status Solidi, 3 (1963) 1851.

76. R.J. Schwenafeir and C. Elbaum, J. Phys. Chem. Solids, 28 (1967) 597.

77. K.R. Lawless, Rep. Progr. Phys., 37 (1974) 251.

78. T.D. Dzhafarov and G.S. Kulikov, Sov. Phys.— Solid State, 12 (1970) 1237.

79. K.L. Chopra, Thin Film Phenomena, McGraw-Hill, New York, 1969, p.266.

80. D.S. Campbell, in L.I. Maissel and R. Glang (eds.), Handbook of Thin Film Technology, McGraw-Hill, New York, 1970, p.12-3.

81. A. Ganguleo, Acta Met., 22 (1974) 177.

82. L.S. Castleman and L.L. Seigle, Trans AIME, 212 (1958) 589.

83. L.S. Castleman, Acta Met., 8 (1960) 137.

84. G. Dearnaley and N.E.W. Hartley, Phys. Letters, 46A (1974) 345.

85. O. Kubaschewski and B.E. Hopkins, Oxidation of Metals and Alloys, Butterworths, London, 1962, p.64.

86. D.L. Douglas, in Oxidation of Metals and Alloys, Am. Soc. Metals, Metals Park, Ohio, 1971, p.157.

87. G. Barreau, G. Brunel, G. Cizeron and P.Lacombe, C.R. Acad. Sci. C, 270 (1970) 516.

88. R. Rosenberg, J. Vac. Sci. Technol., 9 (1972) 263.

89. P.S. Dobson, Phil. Mag., 24 (1971) 567.

90. R.E. Thomas and G.A. Haas, J. Appl. Phys., 43 (1972) 4900.

91. F. Hasegawa, J. Appl. Phys., 45 (1974) 1944.

92. C. Weaver and L.C. Brown, Phil. Mag., 17 (1968) 881.

93. T.C. Tisone and S.S. Lau, J. Appl. Phys., 45 (1974) 1667.

94. M.H. Francombe, A.J. Noreika and W.J. Takei, Thin Solid Films, 1 (1967/68) 353.

95. K.N. Tu and R.S. Berry, J. Appl. Phys., 43 (1972) 3283.

96. K.N. Tu, Acta Met., 21 (1973) 347.

97. J.M. Poate and T.C. Tisone, Appl. Phys. Letters, 24 (1974) 391.

98. J.F. Ziegler, J.W. Mayer, C.J. Kircher and K.N.Tu, J. Appl. Phys., 44 (1973) 3851.

99. J.C.Phillips, in J.M. Poate, K.N. Tu and J.W. Mayer (eds.), Thin Films—Interdiffusion and Reactions, Wiley-Interscience, 1978, p.57.

100. G.V. Kidson, J. Nucl. Mater, 3 (1961) 21.

101. R.T.P. Whipple, Phil. Mag., 45 (1954) 1225.

102. J.D. Baird, J. Fuel. Energy, All (1960) 81.

103. J.W. Mayer and J.M. Poate, in J.M. Poate, K.N. Tu, and J.W. Mayer (eds.), Thin Films—Interdiffusion and Reactions, Wiley-Interscience, 1978, p.119.

104. B.J. Isherwood, GEC J. Sci. Technol., 43 (1977) 111.

105. K.S. Band, B.J. Isherwood, I.H. Seeley and R.C.C. Ward, J. Mat. Sci., 12(1977) 577.

106. J.W. Mayer and K.N. Tu, J.Vac. Sci. Technol., 11 (1974) 86.

107. S.S. Lau, W.K. Chu, J.W. Mayer and K.N. Tu, Thin Solid Films, 23 (1974) 205.

108. N.L. Read and D.H. Hemaker, Thin Solid Films, 10 (1972) 123.

109. R. Feder and B.S. Berry, J. Appl. Cryst., 3 (1970) 372.

110. L. Angely, G. Bronoel and G. Poulerbe, C.R. Acad. Sci., C 286 (1978) 307.

111. M. Palaniappan, M.Phil. Thesis, School of Physics, Madurai Kamaraj University, 1978.

112. L. Dumas, Thin Solid Films, 43 (1977) 285.

113. C.R. Houska, Thin Solid Films, 25 (1975) 451.

114. M. Murahami, D. De Fontaine and J. Feder, J. Appl. Phys., 47 (1976) 2050.

115. Y. Takano, H. Miyata and Y. Iwama, Japanese J. Appl. Phys., 16 (1977) 1153.

116. V.A. Isveschikov and V.V. Laptev, Sov. Phys.— Solid State, 18 (1976) 2175.

117. K.N. Tu, J. Appl. Phys., 48 (1977) 3400.

118. C. Pariset, N. Galtier and M. Gaugnier, Thin Solid Films, 29 (1975) 325.

119. E. M. Hoxl and R.H. Rieder, J. Vac. Sci. Technol., 9 (1972) 276.

120. J.K. Howard, R.F. Lever, P.J. Smith and P.S. Ho, J. Vac. Sci. Technol., 13(1976)68.

121. R.B. Belser, Rep. No.7, Proj. No.163-176, U.S. Army Signal Corps Contr. DA-36-039-SC-42453 (1954).

122. C. Weaver and R.M. Hill, Advan. Phys., 8 (1959) 375.

123. W.D. Sylwestrowics, M.A. Elkholy and G.W. Kammlott, J. Mat. Sci., 14 (1979) 875.

124. R. Pecrschke and H. Wollenberger, Thin Solid Films, 25 (1975) 167.

125. C. Bauer and A.G. Jordan, Phys. Status Solidi A, 47 (1978) 321.

126. C. Pariset and J.P. Chauvineau, Surf. Sci., 57 (1976) 365.

127. N.V. Belous, L.O. Sverykin, E.V. Serdyukova and I. Ya. Khandros, Metallofizika, no.7 (1978) 73.

128. K. Narayanadas, M. Radhakrishnan, C. Balasubramanian, Phys. Status Solidi A, 49 (1978) K.213.

129. H.S. Coleman and H.L. Yeagley, Trans. Amer. Soc. Metals, 31 (1943) 105.

130. H. Schopper, Z. Phys., 143 (1955) 93.

131. C. Weaver and R.M. Hill, Phil. Mag., [8] 3 (1958) 1402.

132. P. Nielsen and J.J. Ritsko, J. Appl. Phys., 49 (1978) 632.

133. W.J. De Bonte, J.M. Poate, C.M. Melliar-Smith and R.A. Levesque, J. Appl. Phys., 46 (1975) 4284.

134. A.K. Sinha, T.E. Smith and T.T. Sheng, Thin Solid Films, 22 (1974) 1.

135. R.F. Broom and TH.O. Mohr, Thin Solid Films, 47 (1977) 249.

136. J.N. Pratt and R.G.R. Sellors, Electrontransport in Metals and Alloys, 2 in Diffusion and Defect Monograph Series, Trans. Tech. SA, Riehen, Switzerland, 1973.

137. H.B. Huntington, in H.I. Aaronson (ed.), ASM Seminar Book on Diffusion, Am. Soc. Metals, Metals Park, Ohio, 1974.

138. H.B. Huntington, in A.S. Nowick and J.J. Burton (eds.), Diffusion in Solids : Recent Developments, Academic Press, New York, 1974, Ch.6.

139. F.M. d'Heurle and R. Rosenberg, in G.Haas (ed.), Physics of Thin Films, Vol 7, Academic Press, 1974, p.257.

140. P.S. Ho and H.B. Huntington, J. Phys. Chem. Solids, 27 (1965) 1319.

141. H.B. Huntington, Thin Solid Films, 25(1975) 265.

142. P. Kumar and R.S. Sorbello, Thin Solid Films, 25 (1975) 25.

143. W.L. Schaich,Phys. Rev. B.13 (1976) 3350.

144. W.L. Schaich,Phys. Rev. B.13 (1976) 3360.

145. F.M. D'Heurle and A. Gangulee, Thin Solid Films, 25 (1975) 531.

146. H.B. Huntington and A.R. Grone, J.Phys. Chem. Solids, 20 (1961) 76.

147. M. Revitz and P. Tetta, Extended Abstracts, Fall Meeting, Electrochemical Society, 1972, p.631.

148. R.E. Hummel and R. Breitling, Appl. Phys. Letters, 18 (1971) 373.

149. S.M. Klotsman, A.N. Timofeev and I.Sh. Trakhtenberg, Fis. Met. Metalloved., 16 (1964) 611.

150. K. Kenmochi and K. Hirano, Thin Solid Films, 25 (1975) 353.

151. I.A. Bloch and R.S. Nademan, J. Appl. Phys., 40 (1969) 485.

152. R. Rosenberg, Appl. Phys. Letters, 16(1970) 27.

153. J.C. Pieri, J. Bagnol and B. Berger, C.R. Acad. Sci. C, 273 (1971) 946.

154. S.M. Klotsman, A.N. Temofeev and I.S.H. Trakhtenberg, Phys. Met. Metallogr., 14(1962) 140.

155. A. Ganguloe and P.M. d'Heurle, J. Phys. Chem. Solids, 35 (1974) 295.

156. K.L. Chopra, Thin Film Phenomena, McGraw-Hill, New York, 1969, p.10.

157. L. Holland, Vacuum Deposition of Thin Films, John Wiley and Sons, New York, 1961.

158. R.W. Berry, P.M. Hall and M.T. Harris, Thin Film Technology, Van Nostrand Reinhold, New York, 1968.

159. R. Glang, in L.I. Maissel and R. Glang (eds.), Handbook of Thin Film Technology, McGraw-Hill, New York, 1970, p.1-3.

160. D.S. Campbell, in J.C. Anderson (ed.), The use of Thin Films in Physical Investigations, Academic Press, London, 1966, p.11.

161. D.S. Campbell, in C.H.S. Dupuy and A. Cachard (eds.), Physics of Nonmetallic Thin Films, Plenum Press, New York, 1976, p.9.

162. I. Langmuir, Physik. Z., 14 (1913) 1273.

163. M. Knudsen, Ann. Physik, 47 (1915) 697.

164. K.G. Günther, in J.C. Anderson, The Use of Thin Films in Physical Investigations, Academic Press, London, 1966, p.213.

165. J.P. Hirth and G.M. Pound, Condensation and Evaporation, The Macmillan Co., New York, 1963.

166. R.A. Sigsbee and G.M. Pound, Advan. Coll. Interf. Sci., 1 (1967) 335.

167. M. Volmer and A. Weber, Z. Phys. Chem., 119 (1925) 277.

168. R. Becker and W. Doering, Ann. Physik, 24(1935)719.

169. T. Rhodin and D. Walton, Trans. 9th Natl. Vacuum Symp., The Macmillan Co., New York, 1962,p.3.

170. T. Rhodin and D. Walton, in M.H. Francombe and H. Sato (eds.) Single Crystal Films, Pergamon Press, New York, 1964, p.31.

171. D.W. Pashley, M.J. Stowell, M.H. Jacobs and T.J. Law, Phil. Mag., 10 (1964) 127.

172. M. Levinstein, J. Appl. Phys., 20 (1949) 306.

173. H.A. Stahl, J. Appl. Phys., 20 (1949) 1.

174. K.L. Chopra, J. Appl. Phys., 37 (1966) 2249.

175. L. Holland, The Properties of Glass Surfaces, Chapman and Hall, London, 1964.

176. L. Holland, Brit. J. Appl. Phys., 9 (1958) 410.

177. T. Putner, Brit. J. Appl. Phys., 10 (1959) 332.

178. H.E. Bennet and J.M. Bennet, in G. Hass and R.E. Thun (eds.), Physics of Thin Films, Vol 4, Academic Press, New York, 1967, p.1.

179. R. Brown, in L.I. Maissel and R. Glang (eds.), Handbook of Thin Film Technology, McGraw-Hill, New York, 1970, p.6-1.

180. S. Tolansky, Surface Microtopography, Interscience Publishers, New York, 1960.

181. W.H. Block and C.L. Gaddy, IEEE Trans. Parts, Hybrids and Packag., PHP 9 (1973) 136.

182. Yu. F. Komnik, E.I. Bukhshtab, Yu. V. Nikitin and V.V. Andrievskii, Sov. Phys.—JETP, 33 (1971) 364.

183. P. Maet and A. Colombani, C.R. Acad. Sci., 244 (1957) 865.

184. P. Michon, Thin Solid Films, 16 (1973) 335.

185. Roland Gerber and Jean-Louis Mayeur, C.R.Acad. Sci., 268B (1969) 881.

186. D.P. Seraphim and A.S. Nowick, Acta Met., 9 (1961) 85.

187. C. Chieu and E. Klokholm, Acta Met., 12 (1964) 883.

188. K.N. Tu, J. Appl. Phys., 43 (1972) 1503.

189. A.W. Czanderna and R.S. Summermatter, J.Vac. Sci. Technol., 13 (1976) 586.

190. K.M. Meinel, M. Klaus and H. Bethge, Thin Solid Films, 34 (1976) 157.

191. S.P. Murarka, I.A. Blech and H.J. Levinstein, J. Appl. Phys., 47 (1976) 5175.

192. S.U. Campisano, G. Foti, P. Grasso and E. Rimini, Thin Solid Films, 25(1975) 451.

193. S.K. Lahiri, Thin Solid Films, 25 (1975) 279.

194. A. Boettcher, G. Haase and K. Thum, Z. Metall., 46 (1955) 586.

195. D.W. Pashley, Adv. Phys., 14 (1965) 327.

196. J.J. Hauser, H.C. Theuerer and N.R. Werthamer, Phys. Rev., 142 (1966) 118.

197. J. Morimoto, Memoirs of Defence Academy, Japan, 16 (1976) 117.

198. S.U. Campisano, G. Foti, E.Rimini, S.S. Lau and J.W. Mayer, Phil. Mag., 31 (1975) 903.

199. J.A. Allen, C.C. Evans and J.W. Mitchell, in C.A. Neugebauer, J.B. Newkirk and D.A. Vermilyea (eds.), Structure and Properties of Thin Films, Wiley, New York, 1959, p.46.

200. B.M. Tareev and M.M. Lerner, J. Sci. Ind. Res., 24 (1965) 516.

201. A. Roy Barthan, P.C. Srivastava and D.L. Bhattacharya, Thin Solid Films, 28(1975)257.

202. S.T. Pieraux, Proc.VI International Vac. Congress, Jap. J. Appl. Phys. Suppl., 2 (1974) 657.

203. N. Cabrera and N.F. Mott, Rep. Prog. Phys., 12 (1949) 163.

204. D.D. Eley and P.R. Wilkinson, in C.A. Neugebauer, J.B. Newkirk and D.A. Vermilyea (eds.), Structure and Properties of Thin Films, Wiley, New York, 1959, p.308.

205. Metals Handbook, Vol 1, American Society for Metals, Metals Park, Ohio, 1961, p.918.

206. V. Simić and Ž. Marinković, Thin Solid Films, 41 (1977) 57.

207. R.E. Belser, Rev. Sci. Instrum., 25 (1954) 180.

208. I.A. Bleeh and E. Kinsbron, Thin Solid Films, 25 (1975) 327.

209. G.J. Van Gurp, Phys. Letters, 5 (1963) 303.

210. John L. Miles and P.M. Smith, J. Appl. Phys., 34 (1963) 2109.

211. I.B. Bhattacharya and D.L. Bhattacharya, Int. J. Electronics, 41 (1976) 285.

212. R.A. Hoffman and D.R. Frankl, Phys. Rev., B3(1971) 1825.

213. V.I. Kaidanov and A.R. Regal, Sov. Phys.— Tech. Phys., 3 (1958) 376.

214. V.P. Duggal and R. Rup, J. Appl. Phys., 40 (1969) 492.

215. K.L. Chopra, Thin Film Phenomena, McGraw-Hill, New York, 1969, p.328.

216. M.R. Neuman and W.H. Ko, J. Appl. Phys., 37 (1966) 3327.

217. J.E.E. Baglin and J.M. Poate, in J.M. Poate, K.N. Tu and J.W. Mayer (eds.), Thin Films— Interdiffusion and Reactions, Wiley-Interscience, 1978, p.305.

218. M. Hansen, Constitution of Binary Alloys, McGraw-Hill, New York, 1956.

219. A. Munitz and Y. Komem, Thin Solid Films, 37 (1976) 171.

220. P. Hollingsworth Smith and H. Gurev, Thin Solid Films, 45 (1977) 159.

221. S. Mohan and P. Jayarama Reddy, Phys. Stat. Soli. A, 15 (1973) K1.

222. L. Dueme and S.T. Jacobsen, Phys. Scr., 18 (1978) 397.

223. V. Simić and Š. Marinković, Thin Solid Films, 34 (1976) 179.

224. A. Vagendristel, H. Bangert, K.H. Kaserouni and S.B. Dilmaghani, Appl. Phys., 17 (1978) 173.

225. K. Nakashima, M. Iwami and A. Hiraki, Thin Solid Films, 25 (1975) 423.

226. H.P. Klug and L.E. Alexander, X-ray Diffraction Procedures for Polycrystalline and Amorphous Materials, John Wiley, New York, 1974, p.419.

227. M.E. Ertl, P. Marchant and H.L. Johnson, J. Mat. Sci., 4 (1969) 1114.

PUBLICATIONS

1. The Effect of the Annealing of Electrode Films on the Electrical Resistivity of Thin Aluminium Films.

   Thin Solid Films, 47 (1977) 121.

2. The Effect of the Annealing of Indium Electrode Films in the Electrical Resistivity of Thin Metal Films.

   Thin Solid Films, 68 (1980) 289.

3. The Variation of Electrical Resistance with Temperature in Bismuth-Silver Bilayer Films.

   Thin Solid Films (accepted for publication).

ACKNOWLEDGEMENTS

I should like to express my sincere thanks to Dr. Joy George, Professor in Industrial Physics for his able guidance and continual assistance on all stages of my research work.

My sincere thanks are due to Professor K. Sathianandan, Head of the Department of Physics for providing laboratory and library facilities.

An acknowledgement is also due to Dr. V. Unnikrishnan Nayar, Reader, Department of Physics, University of Kerala for his cooperation during the early stages of the work.

I am also grateful to all the members of the faculty, the office staff and the technical personnel of the Department for their assistance during the course of my research work.

I acknowledge the cooperative and helpful attitude of all my fellow research students, especially Mr. P.K. Sarangadharan, Mr. S.K. Premachandran, Mr. M.K. Radhakrishnan, Mr. A.V. Alex and Mr.K.S.Joseph.

My thanks are due to the U.G.C., New Delhi for the award of a Teacher Fellowship from November 1976 to October 1979.